HYBRID HYDROGEL TEMPLATES FOR CARDIAC TISSUE ENGINEERING

Thesis submitted in partial fulfilment of the requirements for the Degree of
DOCTOR OF PHILOSOPHY IN ZOOLOGY

Under the Faculty of Science

UNIVERSITY OF CALICUT

by

SOUMYA K. C.

Under the supervision of

Dr. JOSHI C. O.
Associate Professor, Department of Zoology,
Christ College (Autonomous),
Irinjalakuda, Kerala, India - 680125

AUGUST 2024

DECLARATION

I, **SOUMYA K. C.**, hereby declare that the work presented in the thesis entitled **"HYBRID HYDROGEL TEMPLATES FOR CARDIAC TISSUE ENGINEERING"** is based on the original work done by me under the guidance of **Dr. JOSHI C.O**., Associate Professor (Retd.), Department of Zoology, Christ College (Autonomous), Irinjalakuda and has not been included in any other thesis submitted previously for the award of any degree. The contents of the thesis have undergone plagiarism check using iThenticate software at C.H.M.K. Library, University of Calicut, and the similarity index found within the permissible limit. I also declare that the thesis is free from AI generated contents**.**

Irinjalakkuda **Soumya K. C.**

18-08-2024

Dr. Joshi C.O.
Associate Professor Retd. &
Former Head of the Department

P.G. & Research Department of Zoology,
Christ College (Autonomous)
Irinjalakuda, Kerala, India – 680125
Mob: 9847908357, 9037167989
Email: profdrjco@gmail.com
drcojoshi@gmail.com

CERTIFICATE

This is to certify that the thesis entitled "**HYBRID HYDROGEL TEMPLATES FOR CARDIAC TISSUE ENGINEERING**" submitted to the University of Calicut in partial fulfilment of the requirements for the Degree of Doctor of Philosophy in Zoology is an authentic record of the work carried out by **Ms. SOUMYA K. C.** under my supervision at Department of Zoology, Christ College (Autonomous), Irinjalakuda, affiliated to University of Calicut and no part of the thesis has formed the basis for the award of any degree, diploma or other similar titles of any University. It is further certified that the corrections/suggestions recommended by the adjudicators have been incorporated in the thesis and that the contents in the thesis and the soft copy are one and the same.

Dr. JOSHI C. O. (Guide)

CHRIST COLLEGE (Autonomous),
IRINJALAKUDA, THRISSUR, KERALA,
INDIA. 680125

August 2024

CERTIFICATE

This is to certify that **Ms. SOUMYA K. C.** has completed the research work for the full period prescribed under the Ph.D. ordinance of the University of Calicut. This thesis "**HYBRID HYDROGEL TEMPLATES FOR CARDIAC TISSUE ENGINEERING**" embodies the results of her investigations conducted during the period at which she worked as a research scholar. I recommend the thesis to be submitted for the evaluation for the award of the degree of Doctor of Philosophy in Zoology of the University of Calicut.

PRINCIPAL

UNIVERSITY OF CALICUT

CERTIFICATE ON PLAGIARISM CHECK

1.	Name of the Research Scholar	SOUMYA K. C.	
2.	Title of thesis / dissertation	HYBRID HYDROGEL TEMPLATES FOR CARDIAC TISSUE ENGINEERING	
3.	Name of the Supervisor	Dr. C. O JOSHI	
4.	Department/Institution	PG & RESEARCH DEPARTMENT OF ZOOLOGY, CHRIST COLLEGE (AUTONOMOUS) IRINJALAKUDA	
5.	Similar content (%) identified	Non Core	Core
		Introduction/ Theoretical overview/Review of literature/ Materials & Methods/ Methodology	**Analysis/Result/Discussion/ Summary/Conclusion/ Recommendations**
		9	4
	Acceptable maximum limit (%)	10	10
6.	Software used	Ithenticate	
7.	Date of verification	31-07-2024	

**Report on plagiarism check, specifying included/excluded items with % of similarity to beattached.*

Dr. Nasirudheen. T
Assistant Librarian
University of Calicut, Kerala.

M. MUHAMMED KOYA LIBRARY * P.O. CALICUT UNIVERSITY * UNIVERSITY OF CALICUT

Checked by (with name , designation & signature)

Name and signature of the Researcher

Name and signature of the Supervisor.

The Doctoral Committee* has verified the report on plagiarism check with the contents of the thesis, as summarized above and appropriate measures have been taken to ensure originality of the Research accomplished herein.

Name & Signature of the HoD/HoI (Chairperson of the Doctoral Committee)

**In case of languages like Malayalam, Tamil etc..on which no software is available for plagiarismcheck, a manual check shall be made by the Doctoral Committee, for which an additional certificate has to be attached.*

ACKNOWLEDGEMENT

I would like to express my sincere gratitude and respect to my research supervisor, Dr. Joshi. C. O., Associate Professor (Retd.) and Former Head, PG and Research Department of Zoology, Christ College, Irinjalakuda. His knowledge, support, guidance, lively discussions, critical evaluations and encouragement helped in nurturing my passion for my research throughout the course of my study. I am grateful to him for the valuable support and guidance offered during my Ph.D programme.

I am grateful to Prof. Dr. Nasser M., Pro-Vice Chancellor and Dr. Binu R, Assistant Professor of Zoology, University of Calicut, for all the support provided during my work.

I am deeply indebted to Dr. Mathew Paul Ukken, former Principal and Rev. Dr. Jolly Andrews CMI, Principal, Christ College, Irinjalakuda for providing sufficient facilities for the successful completion of work.

I express my sincere gratitude to Dr. V. P. Joseph and Dr. V. T. Joy, former and present Research Co-ordinators, Christ College, Irinjalakuda for their support for the successful completion of work.

I am deeply indebted to teaching faculty of Department of Zoology, Christ College, Irinjalakuda for their co-operation and regular support during the period of my study.

I thank all administrative staffs at Christ College, Irinjalakkuda, for their constant support provided during my work. I remember with thanks, the library staff of Christ College, Irinjalakuda, for their assistance for reference works during the entire period of my research.

I am obliged to Ms. Dhilna Sunny, Research Scholar, Department of Zoology, Christ College, Irinjalakuda for her support.

I am very much grateful to research scholars of different research laboratories under Department of Zoology, Christ College, Irinjalakuda, for their assistance.

I express my gratitude to Department of Collegiate Education, Government of Kerala for the permission and support for completing my thesis.

I am truly grateful to the former and present principals of KKTM Government College for their unwavering support.

I am thankful to my colleagues Dr. Shaji E. M., Mr. Prasad N. K. and Dr. Seema Menon of Department of Zoology, KKTM Government College, Pullut, Kodungalloor for their uninterrupted motivation and encouragement.

Thanks to staff of various departments of KKTM Government College, Pullut, Kodungalloor and students in the campus for their lively companionship.

I am grateful to Dr. Anitha R., Oushadhi, Thrissur for her assistance during the evaluations.

I thank Dr. Rajesh Ramachandran and Dr. Smitha C., Directors, Biogenix Research Center, Thiruvananthapuram for extending their constant support and motivation.

Sincere gratitude to Ms. Renjitha C. S. for language edits and proofreading.

I am thankful to my parents, family, friends and teachers for their blessings, prayers, support and encouragements.

I further thank many who directly or indirectly helped me to prepare this thesis.

My immense gratefulness to the Lord Almighty for showering immeasurable blessings with ever loving family, caring supervisor, supporting friends and so on for the completion of this endeavour.

Soumya K. C.

ABSTRACT

ABSTRACT

Cardio-mimetic hydrogel-based biomaterials are inevitable in bioengineering cardiac tissue. The research focused to engineer and evaluate biologically favorable and cardiac compatible hydrogel scaffolds using the natural polysaccharides such as alginate, starch and carboxy methyl cellulose reinforced with synthetic polymers PVA and PEG for cardiac tissue engineering (CTE). Two panel of hydrogel scaffolds viz ACPV and ASPG were synthesized. ACPV hybrid hydrogel system was prepared by interpenetrating alginate and cellulose with the synthetic polymer PVA and the subsets ACPV1 and ACPV2 were prepared by varying the composition of the co-polymers. Similarly, PEG was used in ASPG system instead of PVA and the two subsets ASPG1 and ASPG2 were prepared by altering the constituent ratio of co-polymers. Divalent cation, Ca^{2+} was used as the crosslinking agent in both the preparations.

ATR-IR analysis, water profiling, surface morphometry studies, contact angle and tensile strength measurements and biostability studies evaluated the physicochemical and mechanical properties of the hydrogels. The findings showed that all the hydrogels exhibited appreciable properties with respect to the presence of surface functional groups, optimum pore architecture and water holding capacity. The hydrogels were amphiphilic and biodegradable with appreciable mechanical properties.

Cell material interaction was determined by direct contact assay, MTT assay and by evaluating the extent of cell adsorption and penetration onto hydrogel surfaces, using H9c2 cells. Direct contact assay demonstrated that the cells did not show any deviation from the normal morphology suggesting the biocompatibility of the hydrogels. Cytotoxicity studies of H9c2 cells cultured with hydrogel extract revealed viability of >80% in all subsets. Both ACPV and ASPG hydrogels displayed superior adhesion and spreading of H9c2 cells. Both ACPV and ASPG hydrogel systems promoted plasma

protein adsorption on their interstices where the major fraction of adsorbed protein was contributed by albumin.

The hydrogel surfaces were functionalized for antioxidant and antimicrobial activity by loading them with ascorbic acid and antibiotics viz, amikacin and vancomycin respectively. The antibiotic loaded ACPV and ASPG hydrogel subsets displayed significantly increased zone of inhibition against Gram-positive and Gram-negative bacteria. ACPV and ASPG hydrogels loaded with ascorbic acid displayed appreciable antioxidant response in vitro cell free system as evident from DPPH and nitric oxide scavenging assay. Interestingly, the hydrogels showed inherent antioxidant potential as they demonstrated significantly decreased level of oxidative stress in RAW267.4 cells upon direct contact with ACPV and ASPG hydrogels.

Immunocompatibility of ACPV and ASPG hydrogels were evaluated by studying the expression of inflammatory mediators such as IL6, NF-Kβ, IL-10, TGF-β, TNF-α and IKβ using RAW 264.7 cells. The activation of RAW cells upon contact with the hydrogels were minimal suggesting the immunocompatibility. Immunofluorescence revealed that ACPV hydrogels exhibited immunomodulatory effects when compared with ASPG system based on the expression status of IL6, NF-Kβ, IL-10, TGF-β, TNF-α and IKβ. The genes and regenerative pathways involving these genes were assessed by NetworkAnalyst program. The study concluded that the selected genes were intimately associated with 370 genes and 120 pathways related to inflammation and/or immunomodulation revealing their potential network.

Keywords: *Cardiac tissue engineering, Hydrogel scaffold, Biocompatibility, Cytotoxicity, Oxidative stress, Anti-microbial action, Immunomodulation.*

സംഗ്രഹം

ഹൃദയ കലകളുടെ നിർമാണ സാങ്കേതികവിദ്യയിൽ അനിവാര്യമായ ഒന്നാണ് കോശങ്ങളുടെ വളർച്ചയെയും വ്യാപനത്തെയും പിന്തുണയ്ക്കുന്ന പ്രതലങ്ങളായി പ്രവർത്തിക്കുന്ന സ്കഫോൾഡുകൾ. കൃത്രിമ പോളിമെറുകളും പ്രകൃതിദത്ത പോളിമെറുകളും സ്കഫൊൾഡുകളുടെ നിർമാണത്തിനായി ഉപയോഗിച്ച് പോരുന്നു. പ്രകൃതിദത്ത പോളിമെറുകൾ ആയ ആൽജിനേറ്റ്, കാർബോക്സി മീതൈൽ സെല്ലുലോസ്, സ്റ്റാർച്, എന്നിവയെ പോളി വിനയിൽ ആൽക്കഹോൾ, പോളി ഇതിലെൻ ഗ്ലൈക്കോൾ എന്നീ കൃതിമ പോളിമെറുകളുമായി സംയോജിപ്പിച്ചു ജൈവശാസ്ത്രപരമായി അനുകൂലവും ഹൃദയവുമായി പൊരുത്തപ്പെടുന്നതുമായ ഹൈഡ്രോജൽ സ്കഫോൾഡുകൾ നിർമ്മിക്കുകയും അവയുടെ കാര്യക്ഷമത വിലയിരുത്തുകയും ചെയ്യുക എന്നതായിരുന്നു ഗവേഷണത്തിൻറെ പ്രധാന ലക്ഷ്യം. ആൽജിനേറ്റ്, കാർബോക്സി മീതൈൽ സെല്ലുലോസ്, പോളി വിനയിൽ ആൽക്കഹോൾ എന്നിവ ഉപയോഗിച്ച് എസിപിവി, ആൽജിനേറ്റ്, സ്റ്റാർച്, പോളി ഇതിലെൻ ഗ്ലൈക്കോൾ ഉപയോഗിച്ച് എഎസ്പിജി എന്നീ രണ്ടു ഹൈഡ്രോജൽ സ്കഫൊൽഡുകൾ ആണ് നിർമ്മിച്ചത്. പോളിമറുകളുടെ അനുപാതത്തിൽ വ്യത്യാസം വരുത്തി എസിപിവി1, എസിപിവി2 എന്നീ ഉപവിഭാഗങ്ങൾ എസിപിവി സിസ്റ്റത്തിലും എഎസ്പിജി1, എഎസ്പിജി2 എന്നീ ഉപവിഭാഗങ്ങൾ എഎസ്പിജി സിസ്റ്റത്തിലും തയ്യാറാക്കി.

എ ടി ആർ-ഐ ആർ വിശകലനങ്ങൾ, വാട്ടർ പ്രൊഫൈലിംഗ്, സർഫേസ് മൊർഫോമെട്രി പഠനങ്ങൾ, കോൺടാക്റ്റ് ആംഗിൾ, ടെൻസൈൽ സ്ട്രെന്ത് അളവുകൾ, ജൈവസ്ഥിരത പഠനങ്ങൾ എന്നിവ ഉപയോഗിച്ച് ഹൈഡ്രോജൽ സ്കഫൊൾഡുകളുടെ ഭൗതിക-രാസ ഗുണങ്ങൾ വിലയിരുത്തി. ഇതിൽ നിന്നും എല്ലാ സ്കഫൊൾഡുകളും ഹൃദയകോശങ്ങളുടെ വളർച്ചയെയും വ്യാപനത്തെയും പ്രോത്സാഹിപ്പിക്കത്തക്ക വിധത്തിലുള്ള ആംഫിഫിലിക് ഗുണങ്ങളും, മെക്കാനിക്കൽ ഗുണങ്ങളും, ജൈവവിഘടനപരതയും പ്രദർശിപ്പിക്കുന്നതായായി കണ്ടു.

എച്9സി2 സെല്ലുകൾ ഉപയോഗിച്ച് നേരിട്ടുള്ള സമ്പർക്ക പരിശോധന, എം. ടി. ടി. പരിശോധന, ഹൈഡ്രോജൽ പ്രതലങ്ങളിലേക്കുള്ള എച്9സി2 കോശങ്ങളുടെ അധിശോഷണത്തിന്റെയും പെനെട്രേഷന്റെയും വ്യാപ്തി എന്നിവ വിലയിരുത്തിയാണ് കോശങ്ങളുടെയും സ്കഫൊൾഡുകളുടെയും പരസ്പര പ്രവർത്തനം നിർണയിച്ചത്. സാധാരണ ത്രിഘടനയിൽ നിന്ന് കോശങ്ങൾ ഒരു വ്യതിയാനവും കാണിക്കുന്നില്ലെന്ന് നേരിട്ടുള്ള സമ്പർക്ക പരിശോധന തെളിയിച്ചു. ഹൈഡ്രോജൽ എക്സ്ട്രാക്റ്റ് ഉള്ള മീഡിയത്തിൽ വളർത്തിയ എച്9സി2 കോശങ്ങളുടെ എം. ടി. ടി. പരിശോധന ഫലങ്ങൾ എല്ലാ ഉപവിഭാഗങ്ങളിലും >80% എന്ന നിലയിലാണെന്ന് കണ്ടെത്തി. കൂടാതെ എച്9സി2 കോശങ്ങൾ ഹൈഡ്രോജൽ പ്രതലങ്ങളിൽ മികച്ച

അധിശോഷണവും പെനെട്രേഷനും പ്രദർശിപ്പിച്ചു. ഇത് ഹൈഡ്രോജല്ലുകളുടെ ബയോകോംപാറ്റിബിലിറ്റിയെ സൂചിപ്പിക്കുന്നു. സ്കാഫ്ഫോൾഡ് പ്രതലങ്ങളിലെ പ്രോട്ടീൻ അധിശോഷണത്തിൻറെ വ്യാപ്തി നിർണയിച്ചതിൽ നിന്നും, എസിപിവി, എഎസ്പിജി ഹൈഡ്രോജൽ സംവിധാനങ്ങൾ അൽബുമിൻ അധിശോഷണത്തെ പ്രോത്സാഹിപ്പിക്കുന്നതായി കണ്ടെത്തി.

ആൻറിബയോട്ടിക് ഉൾക്കൊള്ളിച്ച എസിപിവി, എഎസ്പിജി ഹൈഡ്രോജൽ ഉപസെറ്റുകൾ ഗ്രാം പോസിറ്റീവ്, ഗ്രാം നെഗറ്റീവ് ബാക്ടീരിയകളുടെ വളർച്ചയെ തടയുന്നതായി കണ്ടെത്തി. ഡി പി പി എച്ച്, നൈട്രിക് ഓക്സൈഡ് സ്കാവഞ്ചിംഗ് പരിശോധന എന്നിവയിൽ അസ്കോർബിക് ആസിഡ് അടങ്ങിയ എസിപിവി, എഎസ്പിജി ഹൈഡ്രോജൽ ഉപസെറ്റുകൾ ഇൻ വിട്രോ സിസ്റ്റത്തിൽ മികച്ച ആൻറിഓക്സിഡൻറ് പ്രതികരണം പ്രദർശിപ്പിച്ചു. എസിപിവി, എഎസ്പിജി ഹൈഡ്രോജെല്ലുകളുമായി നേരിട്ടുള്ള സമ്പർക്കത്തിൽ ഹൈഡ്രജൻ പെറോക്സൈഡ് ഉപയോഗിച്ച് സംസ്കരിച്ച റോ267.4 കോശങ്ങളിലെ ഓക്സിഡേറ്റീവ് സമ്മർദ്ദം ഗണ്യമായി കുറഞ്ഞതായായി കണ്ടു. ഇത് ഈ ഹൈഡ്രോജൽ സ്കെഫൊൾഡുകളുടെ അന്തർലീനമായ ആൻറിഓക്സിഡൻറ് ഗുണം കൊണ്ടാണെന്ന നിഗമനത്തിൽ പഠനം എത്തിച്ചേർന്നു.

റോ267.4 കോശങ്ങൾ ഹൈഡ്രോജൽ സ്കെഫൊൾഡുകളുമായി സമ്പർക്കത്തിൽ വരുമ്പോൾ IL6, NF-Kβ, IL-10, TGF-β, TNF-α, IKβ തുടങ്ങിയ ഇൻഫ്ലമേറ്ററി മീഡിയേറ്റർമാരുടെ എക്സ്പ്രെഷൻ ലെവെലിനെ കുറിച്ച് പഠിച്ചുകൊണ്ട് എസിപിവി, എഎസ്പിജി ഹൈഡ്രോജല്ലുകളുടെ ഇമ്മ്യൂണോ കോംപാറ്റിബിലിറ്റി വിലയിരുത്തി. ഹൈഡ്രോജല്ലുകളുമായി സമ്പർക്കം പുലർത്തുമ്പോൾ റോ കോശങ്ങൾ അവയുടെ രൂപഘടനയിൽ ഒരു മാറ്റവും കാണിച്ചില്ല. മേല്പറഞ്ഞ ഇൻഫ്ലമേറ്ററി മീഡിയേറ്റർമാരുടെ എക്സ്പ്രഷൻ നിലയെ അടിസ്ഥാനമാക്കി എഎസ്പിജി സിസ്റ്റവുമായി താരതമ്യപ്പെടുത്തുമ്പോൾ എസിപിവി ഹൈഡ്രോജല്ലുകൾ ഇമ്മ്യൂണോമോഡുലേറ്ററി ഇഫക്റ്റുകൾ പ്രകടിപ്പിക്കുന്നതായി ഇമ്മ്യൂണോഫ്ലൂറസെൻസ് പഠനം വെളിപ്പെടുത്തി. ഈ ഇൻഫ്ളമേറ്ററി മീഡിയേറ്റർമാരുടെ ജീനുകൾ മറ്റ 370 ജീനുകളുമായും ഇമ്മുണോമോഡുലേഷനുമായി ബന്ധപ്പെട്ട 120 പാതകളുമായും ബന്ധപ്പെട്ടിരിക്കുന്നതായി നെറ്റ്വർക്ക് അനലിസ്റ്റ് പ്രോഗ്രാം വിലയിരുത്തി.

പ്രധാന പദങ്ങൾ: *ഹൃദയകലകൾ, സ്കഫോൾഡ്, ജൈവസ്ഥിരത, സൈറ്റോടോക്സിസിറ്റി, ഓക്സിഡേറ്റീവ് സ്ട്രസ്സ്, ആന്റി മൈക്രോബിയൽ ഗുണം, ഇമ്മ്യൂണോമോഡുലേഷൻ*

CONTENTS

LIST OF FIGURES

LIST OF TABLES

LIST OF ABBREVIATIONS

AHA	American Heart Association
ACPV	Alginate-CMC-PVA
ASPG	Alginate-starch-PEG
AuNPs	Gold Nano Particles
BADSCs	Brown Adipose-Derived Stem Cells
BP	Blood Pressure
BSA	Bovine Serum Albumin
CABG	Coronary Artery Bypass Graft
CF	Cardiac Fibroblasts
CMC	Carboxymethyl Cellulose
CNT	Carbon Nanotube
CTE	Cardiac Tissue Engineering
CVD	Cardiovascular Diseases
Cx43	Connexin 43
DAMPs	Damage Associated Molecular Patterns
dECM	decellularized ECM
DW	Distilled Water
ECM	Extracellular matrix
ESR	Equilibrium Swelling Ratio
EVs	Extracellular vesicles
EWC	Equilibrium Water Content
FBS	Fetal Bovine Serum
GelMa	Gelatin Methacrylate
HA	Hyaluronic Acid
HF	Heart Failure
ICD	Intercalated Discs
IHD	Ischemic Heart Diseases
IL	Interleukin
IPN	Inter Penetrating Network
LPS	Lipopolyscaccharide
LV	Left Ventricle
LVEF	Left Ventricle Ejection Fraction

MMPs	Matrix Metalloproteinases
MSC	Mesenchymal Stem Cells
NO	Nitric Oxide
NYHA	New York Heart Association
PCL	Polycaprolactone
PEG	Poly(ethylene glycol)
PEGDA	PEG diacrylate
PLA	Poly Lactic Acid
PRRs	Pattern Recognition Receptors
PU	Polyurethane
PVA	Poly(Vinyl Alcohol)
PVP	Polyvinyl Pyrrolidone
RGD	Arginine-Glycine-Aspartic acid
ROS	Reactive Oxygen Species
RT	Room Temperature
SR	Swelling Ratio
STEMI	ST-elevation myocardial infarction
TBA	Thiobarbituric acid
TCA	Trichloro Acetic acid
TIMPs	Tissue Inhibitors of Matrix Metalloproteinases
TLR	Toll Like Receptors
VEGF	Vascular Endothelial Growth Factor
VIC	Valvular Interstitial Cells
WHO	World Health Organization
YLD	Years Lost to Disability

CHAPTER 1
INTRODUCTION

Background

American Heart Association (AHA) reported that approximately 18 million global deaths were attributed to cardiovascular diseases (CVDs) with an increase of 28.5% when compared with the statistics of 2007 [1]. Also, CVDs account for one in every three deaths globally and have become a serious global economic concern. The global cost of CVDs is projected to increase to 1044 billion USDs in 2030 from 836 billion USDs of 2010 [2]. Heart failure (HF), a potential consequence of different CVDs is a major health concern causing severe morbidity and mortality among the global population. The prevalence of HF and the risk factors vary across the globe. The Global Health Data Registry shows that nearly 64 million people around the world suffer from HF and 8.2 of every 1000 inhabitant suffer mild, moderate, or severe form of HF accounting for an estimated years lost to disability (YLD) of 9.91 million. In addition, a 36% increase in the prevalence and YLD of HF from year the 1900 has been reported suggesting the increased prevalence [3]. Moreover, it is forecasted that the number of HF patients will increase by 2030 with a concomitant rise in diagnosis and therapy. Unfortunately, the current treatment strategies are insufficient and can offer only a five year survival rate of 50%, irrespective of HF phenotype [4].

Multiple factors including nutritional, physiological, behavioral, environmental and/or psychosocial contribute to the increased prevalence of CVDs. Clinical factors identified include high blood pressure (BP), diabetes, high cholesterol, smoking, high consumption of alcohol, poor diet, obesity and inadequate physical activity [5], [6]. Importantly, Ischemic heart disease (IHD), a type of CVD arises primarily due to the blockage of coronary arteries due to cholesterol deposition and plaque formation. Myocardial infarction (MI), the principal complication of IHD, occurs due to the obstruction to blood flow to heart muscles leading to hypoxia and necrotic/apoptotic

death of cell phenotypes of cardiac tissue. MI results in the permanent loss of cardiomyocytes, the beating elements of heart and cause structural and functional alterations of surviving heart tissue. Cardiomyocytes are terminally differentiated; which hurdles the regenerative mechanisms following MI and promotes fibrosis [7].

Conventional therapeutic approaches including thrombolytic agents, statins, beta-blockers, ACE inhibitors and drugs such as aspirin improved the cardiac symptoms following the MI, however, has failed to effectively manage MI due to several challenges inherent with them [8]. Interestingly, cardiac transplantation has been attempted for the potential treatment of end-stage cardiac failure; however, the dearth of transplantable heart offers significant challenges. For instance, the cardiac patients with class III NYHA (New York Heart Association) heart failure are reducing despite therapeutic interventions, but still have some cardiac reserve and increased survival rate.

Specifically, surgical approaches including CABG (Coronary Artery Bypass Graft) to treat pre and post infarcted heart have saved millions of sufferers globally; however, fails to replace the lost myocardium with normal cardiac function [9]. Hence, novel treatment strategies for the effective management of MI are the critical need of the hour. At this juncture, tissue engineering approaches are gaining promise as a novel and effective method for the treatment of post-MI myocardium.

Structure of Cardiomyocyte

Cardiomyocytes are the structural and functional units of the heart, exhibiting distinct structural adaptations for a peculiar functional role as the beating element of the heart. Though the cardiomyocytes of the auricles and ventricles have common structure and function, the contractile machinery of the latter is well organized to support pulmonary and systemic circulation [10]. In contrast to skeletal muscles, cardiomyocytes

are uninucleate and branched cells with regular striations. Each of these cells is connected to each other by junctions called intercalated discs. Each cardiomyocyte has an outer limiting membrane composed of phospholipids called sarcolemma enclosing the cytoplasm called as sarcoplasam. L-type calcium channels in the sarcoplasam facilitate the movement of extracellular calcium required for contraction. The sarcolemma extends deep into the sarcoplasam with the help of finger like projections called T tubules. A single nucleus, organelles such as sarcoplasmic reticulum, golgi complex, ribosomes and a well-organized cytoskeletal network are seen within the sarcoplasam. To ensure an uninterrupted supply of sufficient energy for a continuous and fatigue free contraction, the cells are also equipped with numerous mitochondria [11] [12] [13].

The cardiac myofibrils are constituted by alternating bundles of actin and myosin. The myofilaments of cardiac myofibrils are arranged separately in bundles in such a way that actin filaments alternate with myosin bundles giving it a striated appearance. The region constituted by actin is called I band or light band. An actin myofilament is a double stranded helical structure and each strand is formed by the polymerization of globular actin monomers. Other major proteins interacting with actin include troponin, tropomyosin and nebulin placed in the grooves of actin myofilament [14] [15] [16]. Tropomyosin prevents undesirable interactions between actin and myosin, whereas troponin belongs to calmodulin type of protein with three subunits viz troponin T which interacts with tropomyosin, troponin I, the inhibitory part and troponin C which binds to calcium. Binding of calcium ions to troponin C relieves this inhibitory effect through conformational changes in these proteins and allows actin and myosin filaments to interact during cross bridge cycle. Also, each I band is bisected by a narrow zone called Z disc/line [17] [18].

The region of myofilaments constituted by myosin myofilaments is called the dark band or A band. Even though I band is constituted exclusively by actin myofilaments, the I band located on either side of A band may overlap with myosin filaments of that A band. This occurs only at the ends of A band giving that region a much darker appearance. The middle region of A band is made exclusively of myosin and it is slightly lighter in appearance when compared with the ends. This zone is called H zone with M line in the middle. M line contains a special protein called myomesin that holds the thick filaments together. The region between two adjacent Z lines is called sarcomere which forms the basic unit of contraction. The proteins of the Z disc maintain the integrity of sarcomere. The major protein player in this region is α-actinin which binds to actin filaments of I band [19]. Nebulin is found throughout the length of actin filament in the sarcomere, with one end attached to the Z disc and other end pointing towards the end of actin filament and is expressed in low levels in cardiomyocytes functioning to regulate the length of thin filaments during contraction [20]. Another protein present is titin that extends from M-line to the Z-disc and provides a binding site for myosin.

Adjacent cardiomyocytes relate to each other through highly organized structures called intercalated discs (ICD) which are the specialized undulating regions in sarcolemma mediating electrochemical and mechanical coupling of cardiomyocytes. Major components of ICD are proteins and organized into three junction complexes viz gap junctions, adherens junctions and desmosomes [21]. Gap junctions are facilitators of direct chemical communication between cells composing of specialized channel formed of connexins. Both the participating myocardiocytes contributes to building a gap junction. Each of these cells assembles six connexin proteins to form a hemi-channel which is later assembled at the sarcolemma to from a functional gap junction. The

predominant connexion isoform contributing to gap junctions of cardiomyocytes is connexin 43. A gap junction offers a low resistant path for the propagation of electrical impulses between adjoining cardiac cells [22]. Coupling of contractile machinery between cardiomyocytes is accomplished through adherens junctions which includes N-cadherins and catenins. The extracellular domains of the transmembrane cadherins from adjacent myocytes associate to form homodimers in calcium dependent manner. The intra cellular domains, on the other hand, link with actin myofilaments through special cytosolic proteins belonging to catenin family [21].

Cardiac Extracellular Matrix (ECM)

The cardiac ECM is a complex consortium comprising structural and non-structural proteins which serve as a scaffold that mechanically support the intricate network of cardiomyocytes and preserve the tissue integrity. In addition, cardiac ECM facilitate signal transduction for cell-cell communication, distribution of contractile forces during cardiac cycle, cell proliferation, migration and adhesion essential for maintaining the proper anatomy and physiology of cardiac tissue. Also, the cardiac ECM acts as reservoir for growth factors, cytokines, matrikines and proteases such as MMPs (matrix metalloproteinases) and TIMPs (Tissue inhibitors of matrix metalloproteinases) which regulate the dynamic nature of ECM. The cell types that inhabit ECM other than cardiomyocytes include fibroblasts, endothelial cells and immune cells such as macrophages [8].

The most prevalent structural protein expressed in cardiac ECM includes the collagen isoforms, I and III constituting about 90% of total collagen of cardiac ECM and the rest is represented by other subtypes such as IV, V and VI. Collagen I exists as thick rod like fibres and is present predominantly in the epimysium and perimysium maintaining the rigidity and stability of ECM. Collagen III forms a fine network of fibres

mainly in the endomysium and imparts elasticity [23]**.** The main structural component of the basement membrane of cardiomyocytes is collagen subtype IV. In addition to its structural roles, the various subtypes of collagen are found to be involved in regulating cellular communications, proliferation and migration via FAK and P13K signalling [24]. The different collagen isoform content in ECM is tightly regulated by balancing the expression of collagen genes and cardiac collagenase activity. Any imbalance between collagen turn over and degradation aggravates the predisposition to cardiac pathologies [25]. Another structural protein prevalent in cardiac ECM is elastin. Elastin assembly is accomplished by the coacervation of monomeric tropoelastin secreted from elastogenic cells followed by organization into elastic fibres. Elastin fibres bestow the tissue with a reversible recoiling capacity after stretching and thus reduces mechanical load on cardiac musculature [26] [27]. Other macromolecular components that decorate ECM includes glycoproteins such as fibronectin, laminin, proteoglycans including syndecan, glypican, laminins, entactins, perlecanen and glycosaminoglycans such as chondroitin sulphate, hyaluronic acid and others. All these components are implicated to have both structural as well as non-structural functions.

Molecular Pathology of Myocardial Infarction

The myocardial ischemia induces a cascade of inflammatory responses to clear away dead cells and other debris from the zone of ischemia. Activation of complement cascade, reactive oxygen species, DAMPs (damage associated molecular patterns) and/or inflammasomes mediate the several events of proinflammatory response. The proteins of complement cascade such as C3b, C3a, C4a, C5a and C5b-9 promote the phagocytosis of the cellular debris by opsonisation and promotes further inflammation by activating the membrane attack complex. DAMPs such as HMGB1, S100A8/A9, S100A1,

Fibronectin-EDA, IL-1α, ATP and mitochondrial DNA released form ischemic cells bind with their receptors, PRRs (pattern recognition receptors), to activate cells of innate immune system [28]. Activation of TLRs triggers the release of pro-inflammatory cytokines IL-1β and IL18 aggravating the inflammation. In addition, the inflammasomes produced in response to DAMPs promote apoptosis of injured cardiomyocytes via various mechanisms including extracellular ATP release, K+ efflux, lysosomal destabilization and mitochondrial ROS generation [29]. Also, the battery of cytokines, IL-6, IL-1, MCP-1, CCL2, CCL5 and others, secreted by resident as well as migrant cells create a proinflammatory milieu and recruit additional immune cell sub-types to the infarct zone. Also, the combined action of cytokines and chemokines attract neutrophil, monocytes, macrophages and T and B lymphocytes. Interestingly, the pro-inflammatory phenotypes of cardiac fibroblast (CF) have been unveiled which upregulates cytokines, chemokines and MMPs in response to ischemic insult.

These cells work in conjunction to remove cellular remnants following the infarction and promotes ECM degradation by secreting various MMPs. Simultaneously, the MMPs secreted by fibroblast, immune cells and injured cardiomyocytes cause degradation of matrix components such as collagen, gelatin, laminin, elastin and fibronectin and the fragments thus generated are termed as matrikines which attract and activate immune cells such as neutrophils [30]. These responses facilitate the removal of damaged cellular and matrix components from infarct zone to activate the reparative responses [31]. The first step is the formation of a provisional matrix composed primarily of plasma derived fibrin which acts as a scaffold for cells including fibroblasts and endothelial cells and for the regenerative components such as PDGF, TGF, VEGF, FGF and other signals/growth factors. Such mediators are involved in the switching of leucocytes from a proinflammatory to anti-inflammatory phenotype.

The formation of the provisional matrix marks the transition from inflammatory phase accompanied by the disintegration of the provisional matrix by fibrinolytic enzymes and CCR2+ macrophages. This is replaced by a cell derived matrix composed mainly of hyaluronin, fibronectin and other matricellular proteins such as osteopondin and tenascin, while the anti-inflammatory signals triggered due to these profound changes in the infarct zone regulates the further infiltration of inflammatory cells. The uncontrolled production of these matrix components ultimately results in the formation of a scar tissue that is unable to contract and the mechanical stress generated due to the contraction of the heart causes deformation in the scar tissue resulting in an irreversible remodelling of myocardial tissue and reduced cardiac output [32]. The biochemical and molecular events associated with the scar tissue formation are depicted in **Figure 1**.

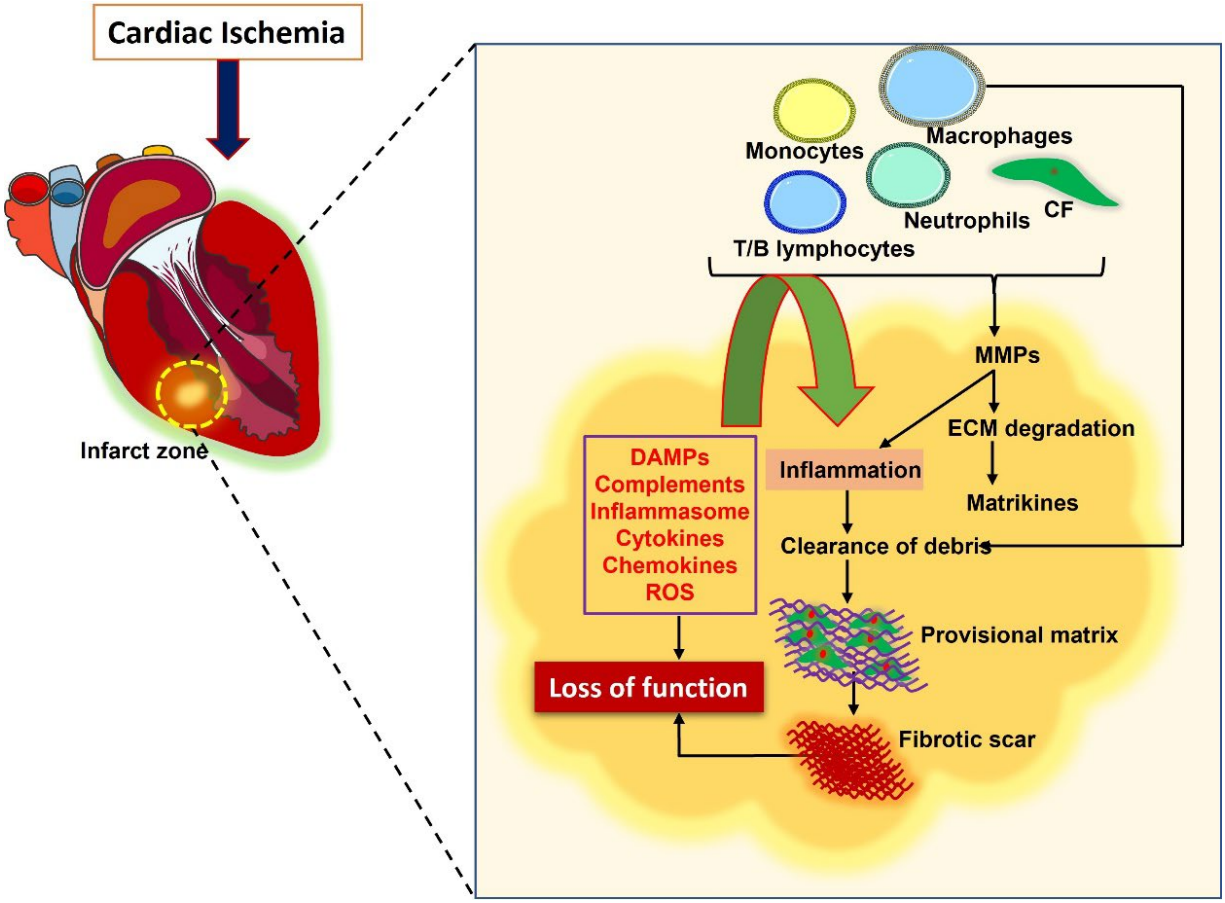

Figure 1: *Cellular and biochemical events associated with scar tissue formation.*

Tissue Engineering

Heart transplantation is considered as the most effective strategy for the management of MI. Dearth of donors, graft rejection, lifelong immune suppression and infections are the major shortcomings associated with this heart transplantation. Also, assistive devices used for cardiac management pose challenges including reduced life span, chances of infection and thrombosis [33] [34]. Thus, novel approaches for the successful management of MI and other cardiac ailments are urgently needed. An innovative treatment strategy emerged was to deliver cells such as stem cells or myoblast cells directly to the injury site for tissue repair; however, the injected cells failed to retain in the site of injection and/or underwent apoptosis. Hence, a supporting platform/scaffold to hold the cells at the injection addresses the challenges associated with cell retention [33]. The understanding that cell confinement and viability at site of injury effecting tissue repair catered with the support of a scaffold led to the evolution of a new branch of medicine, tissue engineering.

Tissue engineering, now-a-days, has gained immense attention as a novel and promising strategy for the reconstruction of damaged organs or tissues accelerating the inherent regenerative ability of the body. In this approach, specific cell phenotypes are grown on biodegradable scaffolds that physically and mechanically resembles the native ECM of the damaged tissue. The seeded cells proliferate, differentiate and form semi-tissue patches that are implanted onto the damaged sites of organs, which later secrete its their own ECM replacing the scaffold and integrate with the native tissue. Still in its infancy, developments in the field of cardiac tissue engineering (CTE), in the past 20 years have been astounding. Fundamentally, the CTE aims at constructing biomimetic 3D scaffolds having properties of native cardiac matrix for developing implantable/injectable cardiac patches for accelerating cardiac repair. Recent progress in

CTE research has witnessed the successful development of heart valves, cardiac muscles and blood vessels suggesting the growing potential [35]. The basic principles and approaches in CTE are given in **Figure 2**.

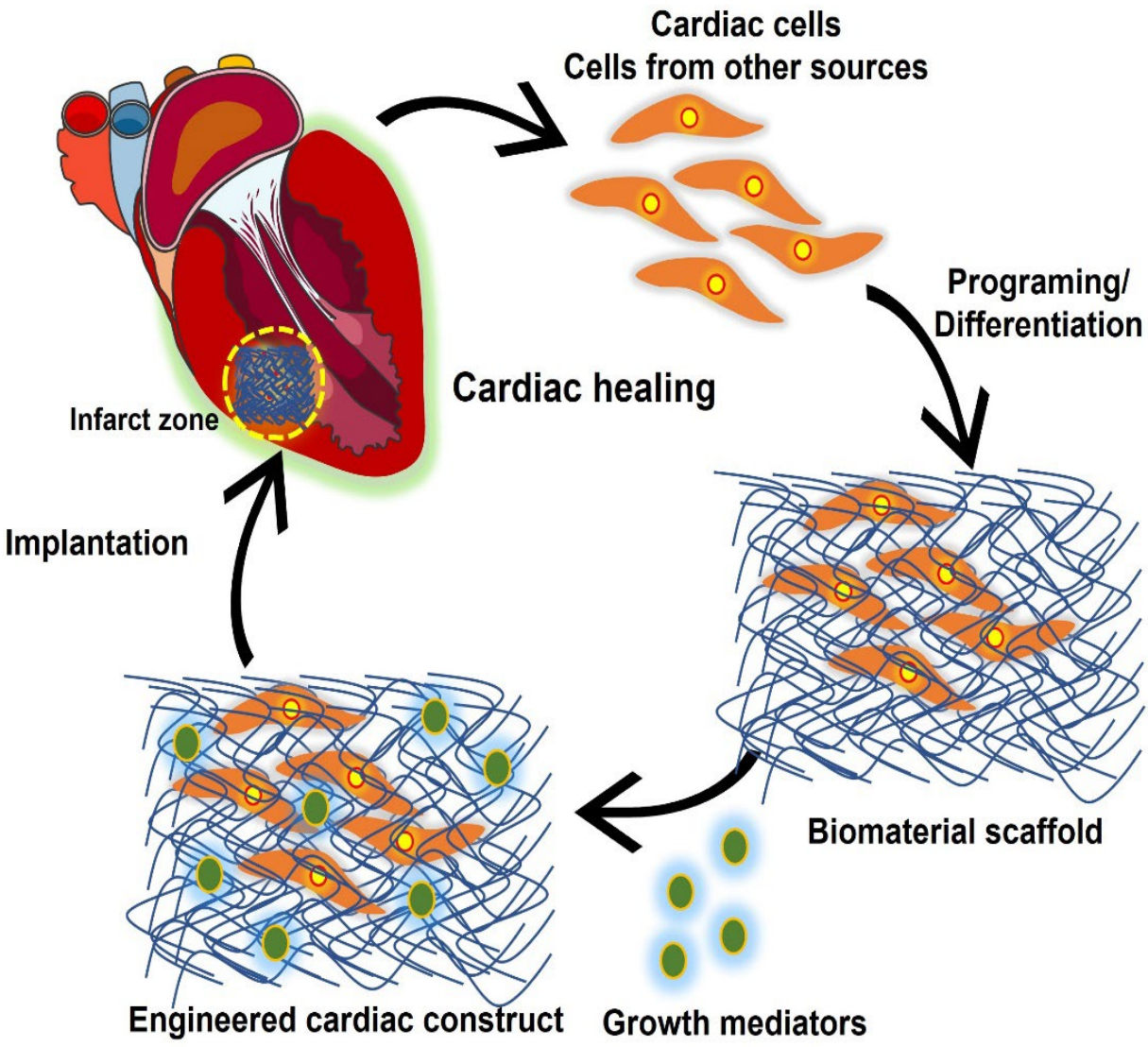

Figure 2: *Basic principles and approaches in CTE.*

Hydrogel Scaffolds

3D scaffolds are integral to the success of CTE approach and scaffolds should maintain the viability and support the growth of seeded cells until a functional ECM is formed, restoring normal tissue function. Biocompatibility and biodegradability are primary requirements for any scaffold to support cell growth. The scaffold or its degradation products prevents immunological insults at the implantation site. The presence of open and interconnected pores with optimum dimensions ensures the microenvironment required for cellular infiltration, adhesion, migration and proliferation. In addition, porosity ensures efficient trafficking of nutrients into and removal of metabolic by-products from the cells. Moreover, neovascularization has been reported to be triggered on the scaffold surface with optimum porosity [36]. The mechanical characteristics of the scaffold warrants compatibility with that of native myocardium in terms of contractility, elasticity, tensile strength, anisotropy and load bearing capacity. This is imperative for the scaffold to accommodate structural changes occurring in the heart during various phases of the cardiac cycle. Moreover, the mechanical properties of the scaffolds determine the phenotypic and contractile properties of seeded and host cardiomyocytes in the scaffold [37].

Several natural and synthetic polymers have been employed as scaffold materials in CTE. Among them, hydrogels are considered as an ideal candidate owing to their tuneable physical and chemical features that support cell adhesion, proliferation, migration, angiogenesis, ECM formation, neo-tissue formation and water content. Hydrogels are hydrophilic polymeric networks that swell rapidly by absorbing water. Both synthetic and natural hydrogels have proven to be promising for cardiac tissue engineering [38]. Alginate, chitin, fibrin, collagen, hyaluronic acid and decellularized matrix are some of the natural hydrogels generally used for CTE while synthetic

hydrogels include PVA, PEG, Poly(2-hydroxyethyl methacrylate), polyacrylamide and polyacrylate [39]. These materials are used either in combination with cells to form new tissue or functionalized with molecules such as growth factors to facilitate chemo attraction of circulating cells towards the scaffold which later gains more cues and assemble themselves into functional tissue.

Hydrogels based on natural polymers have been explored extensively for applications in three-dimensional cell cultures. Although promising results have been observed from cells cultured with these natural gels, complex, variable and ill-defined composition, poor mechanical properties and immune system activation by these materials often hurdle cardiac applications. In contrast, synthetic hydrogels with well-defined network and mechanical strength provide a regular three-dimensional platform for cell growth. However, uncontrolled degradation, toxicity of degradation products, lack of biological cues and immune reactivity limit the application of synthetic polymers in regenerative medicine.

Interestingly, the shortcomings of the individual applications of natural and synthetic hydrogels can be overcome by hybridizing together in specific proportions. Such hybrid hydrogels have been hailed to possess exceptional biocompatibility and appreciable mechanical strength for cardiac applications [40]. For instance, Grover et al. modified the decellularized myocardial matrix with the incorporation of synthetic polymer PEG. Their results demonstrated that PEG incorporation could enhance the mechanical characteristics of the myocardial matrix and decrease the rate of enzymatic degradation without affecting its natural properties [41]. In another study, gelatin methacrylate (GelMA) was reinforced by hybridizing with hyaluronic acid (HA) methacrylate (HAMA). HAMA-GelMA hydrogels exhibited better mechanical strength and promoted cell migration and growth when compared with GelMA or HAMA used

alone [38]. In a seminal study, PEG was hybridized with a natural insect protein, resilin and the resultant material displayed better mechanical characteristics and supported the growth of aortic adventitial fibroblasts [42].

Hydrogels are used in regenerative medicine as injectable hydrogels and implantable hydrogels. Injectable hydrogels transform to a gel phase when injected into cardiac muscles by extrinsic cues such as chemicals or manipulating the intrinsic cues such as temperature or pH. Some of the polymers that are generally used as injectable gels include alginate, chitosan, hyaluronic acid, copolymers based on PEG, pNIPAAM, PGS and self-assembling peptides. The main advantage of injectable gelling system is that its deployment into cardiac muscles can be done through intramuscular injections or through catheter delivery. Since the gels are injected directly to the site of injury, there are fewer chances that the cells or other molecules loaded in the gels are lost to untargeted sites. Also, the injected hydrogel acts as a flexible support essential for the contracting cardiac muscles [34]. However, difficulties in fine tuning the hydrogel characteristics such as toxicity, viscosity and gelation properties pose challenges in the clinical translation of this strategy [33].

Another concern is to fabricate gels that rapidly integrate into cardiac muscles as heart is undergoing cyclic contractions and relaxations [43]. In a clinical trial, alginate hydrogel was injected into the myocardium of left ventricle of patients with advanced HF demonstrating that the exercise profile and symptoms improved with the treatment with only 8.6% mortality. The study concluded that the hydrogels have an acceptable safety profile to be used as an injectable system [44]. In another study, therapeutic effects of injectable silk sericin hydrogel in mitigating MI complications were evaluated in a mouse model revealing that silk sericin hydrogel reduced scar formation and

inflammatory responses with a concomitant stimulation of cell survival, wall thickness and neovascularization [45].

Implantable hydrogels, on the other hand, are porous solid or semi-solid scaffolds fabricated ex situ for tailoring onto injured cardiac muscles. CTE hydrogels, designed for creating appropriate micro niche scaffoldings for 3D cardiac cell growth, primarily focus on the cell biology concerning the patency of the scaffolds [46]. Generally, the biochemical and physiological functions of a tissue is operated by the coordinated interactions between the respective cells and native ECM. Therefore, understanding the nature, chemistry and biology of the ECM is crucial for the *ex-vivo* design of hydrogel-based implantable systems that mimic cardiac ECM [47]. The cells or regenerative mediators loaded onto such hydrogels initiate communications with the hostile microenvironment of the surviving myocardium and trigger regenerative responses. However, the success of this approach depends on the physical and mechanical properties of the scaffolds such as biocompatibility, degradability, non-toxicity, pore size, pore density, contractility and electrophysiological stability.

The technological advancement in the field of biomaterials has led to the discovery of '*smart-hydrogels*' that respond to the environmental triggers (temperature, pH, ionic strength and others) and exhibit marked changes in their physiochemical properties such as swelling behaviour, mechanical properties, sol-gel transition, network structure and ionic balance. Smart hydrogels find a multitude of applications in CTE such as for controlled drug delivery, as biosensors or as surfaces with controlled cell adhesion [48]. In the current era of CTE, there is a significant focus on smart hydrogels to ensure the improved healing responses by targeting multiple aspects of MI pathology.

The deliverables paired with injectable or implantable hydrogels are cells or other bioactive leads that aid in regeneration [43]. The different cell types used for cardiac

tissue engineering include cardiomyocytes of adult foetal or neonatal origin, skeletal myoblast cells, bone marrow derived stem cells such as mesenchymal, endothelial or hematopoietic stem cells, embryonic stem cells, smooth muscle cells, adipose tissue derived stem cells, cardiac stem cells and induced pluripotent stem cells (iPS cells). Fundamentally, the selection of cells for CTE is crucial for the translational applications considering availability, convenience, proliferation capacity, phenotypic switch and healing responses [49].

Fabrication of CTE Scaffolds

Diverse approaches have been employed in the preparation of CTE scaffolds. The conventional techniques include solvent casting, phase separation, gas foaming, porogen leaching and freeze drying while the advanced methods employed include electospinning, bioprinting and computer assisted designing [50]. In solvent casting method, the polymer/s is dissolved into a uniform solution and is crosslinked into an interconnected fibrous scaffold with the addition of a crosslinking agents. The polymer matrix is dried to remove the solvent and washed in water to leach out the unreacted cross-linking agent. Gas foaming technique relies on subjecting polymers to high pressure with gas foaming agents such as CO_2 and/or nitrogen resulting in the formation of tiny gas bubbles within the scaffold which are degassed to develop into pores. Scaffolds with approximately 100 mm pore diameter and 90% porosity can be obtained by this method with an advantage of absence of toxic solvents that interfere with cell viability [51]. Porogen leaching employs a porogen, such as paraffin beads, NaCl or sucrose dispersed in the polymeric solution, prior to cross linking. Dissolution of porogenic material with appropriate solvent after fabrication generates highly porous scaffolds with well-defined pores. The processing time for such scaffolds is high and any

failure to completely remove the dissolution solvents affects the viability of the cells [52] [53].

Freeze drying method relies on the principle of sublimation wherein the solvent molecules are solidified and removed as gas. In freeze drying, the polymer is dissolved in a solvent with which it is miscible. The polymer solution is then freeze dried to remove the solvent molecules, resulting in a highly porous polymeric scaffold [54]. Electrospinning is used to create scaffolds with nano and micro scale architecture employing the electrostatic forces to pull out polymeric solutions into fine fibres. The equipment set up for this technique include a polymeric solution source, a high voltage supply and a collector. From the high voltage DC source, optimal charge to overcome the surface tension of the polymeric solution is supplied resulting in the emission of a fibre jet which is instantly collected on to a rotating or translating collector [55] [56]. 3D printing technology is a recently emerged technique used to create 3D tissue constructs with specified geometry and architecture [57]. 3D bioprinting is promising to address the issues such as organ scarcity or the challenges with conventional tissue engineering strategies. In 3D bioprinting, a robotic 3D bioprinter deposits biomaterials, contextually referred to as bioink, suspended with cells in a layer-by-layer fashion in accordance to a computer aided design of the original 3D functional tissue. Bioinks provide structural support and a microenvironment for the cells to adhere, migrate and proliferate. The 3D constructs are transferred into bioreactors with physiological environment to promote maturation. In this step, the cells in the construct proliferate to occupy the spaces of the gradually degenerating bioink and take the form of the predesigned tissue structure [58].

Application of decellularized ECM (dECM) as CTE scaffold has recently gained appreciable momentum. Decellularization refers to the careful removal of cellular components from a tissue through enzymatic and/or chemical treatments to harvest the

intact ECM. The dECM is later cellularized with cardiac cell phenotypes to develop a functional cardiac tissue construct [59]. The most promising tissue source of dECM for cardiac tissue engineering is myocardium owing to retention of specific biochemical and mechanical cues as well as tissue microenvironment essential for cardiac regeneration in myocardial dECM. This promotes proper and faster cell attachment, migration, proliferation and differentiation with minimal risk of immunological rejection, if the tissue source is allogeneic. Several investigations have reported that matrix bound growth factors that are involved in angiogenesis, cardiac homeostasis and cell growth are retained in the myocardial dECM [60] [61].

The emerging trends in CTE are beneficial to the patients waiting for heart transplants and those needing tissue entities, myocardium, valves or blood vessels. For successful CTE, biomechanically stable and biodegradable templates are the key to promote and maintain optimal numbers of cells for accelerating the specific biological functions. Therefore, it is highly relevant to develop biomimetic scaffold materials using biocompatible hybrid polymeric systems for successful CTE.

Objectives

CTE demands an ideal scaffold matrix such as hydrogel that mimic the native cardiac ECM. The swelling behaviour of hydrogels simulates tissue-like elastic properties and permeability to biological fluids. Interestingly, the hydrogel scaffolds from both natural polymers and synthetic biomaterials possess several demerits challenging their long-term application in CTE. Hence, hydrogels derived from either natural or synthetic origins fail to replicate the mechanical and viscoelastic characteristics of native myocardium as the hydrogel-based tissue constructs are mechanically weaker than their native tissue counterparts. However, these drawbacks can be addressed by chemically crosslinked hybrid biosynthetic hydrogel scaffolds which provide favourable physicochemical, mechanical properties and biocompatibility for CTE. Furthermore, the cells grown on the scaffolds fail to perform the intended function owing to the limited availability of metabolites from the surrounding medium, despite the extensive porous network. Also, the influence of physiochemical properties on the cell infiltration and their performance in the hydrogels in the absence of specific signals are yet to be determined.

The increased ROS production and subsequent oxidative stress during MI aggravates the pathology and antioxidant therapy for the management of reperfusion injury has been attempted. For instance, the polymeric materials immobilized with antioxidant mediators/enzymes for the management of ischemic injury has been successfully attempted. However, reports on ROS scavenging hydrogels for CTE are unavailable demanding the hydrogels with inherent ROS scavenging activities for the regeneration/repair of myocardium to restore the functional heart. The successful design of CTE strategies rely on judicious selection of biodegradable hydrogels with superior mechanical strength, non-toxic degradation products, interconnected pore architecture for nutrient trafficking, cues for cellular viability and differentiation, controlled

degradation along with excellent performance and survival complying with the contractile function of the injured heart. Importantly, the release of toxic by-products induces hyperinflammatory response which may contribute to fibrotic responses that prevent tissue remodelling, the transport of nutrient and angiogenesis. Similarly, the infection associated with MI pathology and implantation/intervention is challenging which warrants the hydrogels with antibiotic potential.

At this juncture, the present research focuses on the synthesis of biomechanically favourable and biodegradable hybrid hydrogel scaffolds involving sodium alginate, CMC, starch, PEG and PVA which favours cellular responses for CTE. The specific objectives of the study are as follows.

1. **Synthesis and characterization of novel biodegradable hybrid hydrogel scaffolds using the copolymers sodium alginate, CMC, starch, PEG and PVA.**
2. **Examinations on cell-material interaction and compatibility of the hybrid hydrogels.**
3. **Investigations on the biological responses of biosynthetic hydrogels for cardiac tissue engineering.**
    i. **Studies on antimicrobial response**
    ii. **Studies on antioxidant response**
    iii. **Studies on immunocompatibility and gene interactions**

Organization of the Report

This thesis has been organized into six chapters as follows:

Chapter I – Introduction: This chapter focuses on the general background, current understanding, emerging approaches in CTE with emphasis on MI pathology, cardiac tissue engineering and regenerative medicine, hydrogel scaffolds, biomaterials such as alginate, CMC, starch, PEG and PVA along with the objectives of the study and organization of the thesis.

Chapter II – Review of literature: This chapter provides insights into the review of literature and published information significant to the present study which has been categorized into evolution of CTE, biomaterials scaffolds in CTE, alginate-based scaffolds in CTE, cellulose-based scaffolds in CTE, PEG-based scaffolds in CTE, PVA-based scaffolds in CTE and hybrid hydrogels in CTE.

Chapter III – Materials and Methods: This chapter describes the methodology, protocols and procedures adopted for generating the meaningful data in the present study.

Chapter IV – Results: This chapter provides details on the major findings based on the standard protocols used and figures out overall outcome of the present study.

Chapter V – Discussion: This chapter assesses the results of the present study on the basis of the interpretations using the generated data in the light of published literature.

Chapter VI – Summary and Conclusion: This chapter categorically sums up the overall findings from the study and derives a meaningful conclusion.

Chapter VII – Recommendations: The chapter on recommendations contains suggestions for further experimental exploration in the future studies.

References: The section on references contains the citations used for this research work.

Publications: Publications based on the current research work are enumerated here.

CHAPTER 2
REVIEW OF LITERATURE

Evolution of CTE

The early half of 20th century witnessed attempts to assemble the whole heart in vitro [62] suggesting the early concept of tissue engineering. Later, Moscona was successful in culturing freshly isolated cells from foetal chicken heart obtaining an aggregate of cells similar to the intact heart tissue [63]. Interestingly, investigations by McDonald et al. demonstrated that the isolated cells from immature hearts were potent in forming cardiac-like tissues under optimal culture conditions [64]. Simpson et al. found out that neonatal rat cardiac cells possess self-organization potential leading to the formation of heart-like tissues [65]. The introduction of computer-controlled instrumentation to study the biomechanics of cardiac tissue by Vandenburgh and Terracio in late 1980s throws further insights into the orientation and organization of multiple cell types [66] [67]. Subsequently, the findings from embryonic fibroblasts paved the way for an improved in vitro heart model with appreciable properties [68].

The interdisciplinary collaboration of material sciences to cardiac biology resulted in defining novel principles of CTE. For instance, Carrier et al. employed polyglycolic acid as a scaffold in bioreactor cultures [69] and Li et al. cultured embryonic rat ventricular cells onto gelatin scaffolds in vitro and post-implantation infarcted rat hearts displayed spontaneous contractile function [70]. Leor was the first to report cardiomyocytes in tissue engineering; however, failed to integrate with the host myocardium [71]. Radisic et al. combined collagen foam with neonatal rat heart cells in Matrigel to generate cardiac constructs with improved biological features [72]. Interestingly, the effective utilization of bioreactors resulted in the construct 3D multilayer cardiac tissue like constructs with superior electrophysiological features using polymeric scaffolds and cells of interest [69] [73]. The emergence of organ printing unveiled novel avenues in CTE, especially for the development of single cell layers and

cell aggregates [74] which are superior to cell technologies [69]. Importantly, intelligent hydrogel-based CTE ensuring the responsiveness to the alterations in cardiac physiology, superior biocompatibility and biomimetic nature emerged as a promising approach in CTE [75].

Biomaterial Scaffolds in CTE

Several 3D in vitro culture systems employing natural/synthetic/hybrid polymers components have shown to promote the attachment and proliferation of cardiac cells. Kallukalam et al. designed carboxyl terminated-poly(propylene fumarate)-co-ethylene glycol)-acrylamide and polyethylene glycol terminated poly(propylene fumarate)/acrylamide hydrogel scaffolds favouring adhesion and proliferation of cardiac fibroblast cells of new born rat (Wistar) due to the formation of synergistic hydrophilic–hydrophobic surface-by-surface reorganization [76]. Similarly, the growth of fetal rat cardiac cells in thermoresponsive poly (N-isopropyl acrylamide)-grafted gelatin (PNIPAM-gelatin) scaffold exhibited appreciable outcomes in vitro [77]. Sakai et al. have studied the growth of cardiomyocytes in vitro in gelatin sponge and observed potent inflammatory reaction after 4 weeks of implantation due to dissolution of the sponge [78]. Interestingly, spatial orientation of cardiomyocyte has been achieved using biodegradable, elastomeric polyurethane films micro-patterned with adhesion molecule laminin [79]. A seminal study reported the construction of heart valve leaflets using the synthetic biodegradable polymer polyglycolic acid seeded with fibroblast cells and endothelial cells to form an engineered heart valve tissue construct. The study demonstrated the feasibility of valve replacement using autograft tissue constructs instead of mechanical valves in lamb model [80].

Another study traced the seeded cells onto a biodegradable polymeric leaflet demonstrated that the cells on the leaflets had persisted and generated a proper matrix on the polymer scaffold 8 weeks post- implantation [81]. Ishii et al. demonstrated the survival of primary neonatal rat cardiomyocytes in the biodegradable electro spun nano fibrous poly (ε-caprolactone) meshes employing the cell-layering technique revealing a 3D cardiac construct with beating cardiomyocytes [82]. Electrically conductive polyurethane/siloxane networks, stabilized with castor oil demonstrated the increased attachment and proliferation of C2C12 myoblasts suggesting the potential application in CTE [83]. Poly(vinyl alcohol) (PVA) based scaffolds are excellent potential for CTE owing to the mechanical properties conferring an adaptive behaviour towards load bearing functions of the heart, retention of significant amount of water or biological fluids without dissolution [84]. RGD peptide immobilized poly(3-hydroxybutyrate-co-4-hydroxybutyrate) [P(3HB-co-4HB)] scaffolds demonstrated improved cell–scaffold interaction promoting the attachment and proliferation of H9C2 myoblast cells [85].

Alginate Based Hydrogels in CTE

Alginate is a biocompatible biomaterial with enormous biomedical applications including tissue engineering. The biologically favorable properties of alginate including the ease of gelation and water holding capacity hail it as attractive material for CTE. Alginate is a naturally occurring heteropolysaccharide extracted from brown seaweeds composed of two units: α-L-guluronic acid (G) and 1,4-linked β-D-mannuronic acid (M) [86]. Alginate hydrogels have been promising in improving cardiac functions as evident in diverse animal models of MI as injectable and implantable CTE hydrogels. Injectable alginate hydrogels revealed marked attenuation in LV dilation and dysfunction and prevented pathologic cardiac remodeling in small and large animal models of MI [87] [88]. In a seminal study, VEGF-loaded alginate microspheres implanted on the epicardial

surface of a MI-rat model maintained their biological activity enhancing the spontaneous angiogenesis and vasculogenesis alginate microspheres [89]. Another study reported that the alginate based injectable hydrogel promotes the transmission of electrical impulses maintaining stable cardiac rhythm by restoring the synchronous contractions and the relaxation [90].

Delivery of growth factors/cytokines to infarcted heart using alginate-based biomaterials to facilitate cardiac regeneration is promising in CTE. A study attempted to deliver vascular endothelial growth factor (VEGF) encapsulated MSCs were prepared by layer by layer self -assembly with alginate and gelatin polyelectrolytes in MI rats via tail vein demonstrated appreciable bioavailability and cardiac outcomes [91]. In addition, alginate-chitosan scaffolds favored the growth and proliferation of cardiomyocytes and spheroid formation and the incorporation of metal nanoparticles, especially gold-alginate nanoparticles upregulated cardiomyocyte specific proteins such as troponin I, tropomyosin and myosin [92]. Moreover, blending cardiac ECM with alginate and chitosan significantly improved the performance of ECM displaying excellent tensile strength, swelling properties, stability and pore morphology. Cytochemical and histological evaluations revealed significant growth and proliferation of hMSCs with increased expression of cardiac specific markers [93]. Interestingly, the oxidized alginate-cardiac ECM based in situ double network hydrogel functionalized with amine reduced graphene oxide revealed improved electrical conductivity, appropriate tensile strength, biodegradation profile, gelation time and cytocompatibility [94].

In another study, melanin nanoparticles (MNPs)/alginate were found to eliminate ROS and oxidative stress in cardiomyocytes with a concomitant upregulation of macrophage polarization to regenerative M2 phenotypes in MI rat model [95]. Importantly, the stress relaxing alginate hydrogels synthesized by ionic crosslinking due

to the unbinding and rebinding of ionic crosslinkers has been effectively employed for CTE [96]. Hao et al. reported fullerenol-nanoparticle/alginate hydrogel with antioxidant properties, facilitates survival and differentiation of brown adipose-derived stem cells (BADSCs) towards cardiomyogenic lineage in a MI rat model [97]. Lv et al. reported that MSC-derived EVs incorporated in alginate hydrogel as a sustained delivery system allowed retention of EVs in the heart maintaining the local concentration, promoting cardiac healing [98].

Interestingly, several clinical trials have been conducted using alginate for cardiac applications. Algisyl-LVRTM and IK-5001 has successfully completed the clinical trials for the treatment of heart failure [99]. The trial (SYM-08-001) evaluated the efficiency of Algisyl-LVR in alleviating left ventricular remodelling in patients with dilated cardiomyopathy. Algisyl-LVR was administered as an intramyocardial injection during the CABG procedure in 11 patients displaying zero mortality and improved cardiac functions in terms of LV systolic and diastolic end dimensions, myofiber stress and ejection fraction following one year follow up [99]. Subsequent trials (AUGMENT HF and AUGMENT HFII) evaluated the efficiency of injectable Algisyl-LVR hydrogel. AUGMENT HF recruited 78 participants over five different countries proved that Algisyl-LVR ameliorated cardiac and general health of all the treated subjects [99]. Importantly, AUGMENT HFII is expected to end by 2024 with an estimated participants of 240 and aims to evaluate the efficiency of Algisyl in LV augmentation in dilated cardiomyopathic patients [99]. Another trial named PRESERVATION-1 was to evaluate the efficiency of IK-5001 (bioabsorbable and implantable hydrogel, consisting of 1% sodium alginate and 0.3% calcium gluconate) in patients with acute MI using 303 subjects reported appreciable outcomes [99].

Cellulose Based Hydrogels in CTE

CMC is a natural-derived polymer containing hydroxyl groups replaced by carboxymethyl groups in C2, C3 and C6 of glucopyranose of cellulose. The higher negative charge density provided by ample -COO- and -O- functional groups in aqueous solution drive water imbibition creating a hydrated niche simulating the native ECM [100]. In addition, combining synthetic/natural hydrophilic polymers with CMC addresses the mechanical limitation and preserve biological properties for the improved performance in CTE [100]. Importantly, CMC has FDA approval for various biomedical applications including wound management, drug delivery and tissue engineering [101] [102]. Interestingly, Sharona et al. recently reported a panel of carboxymethyl cellulose–alginate interpenetrating hydroxy ethyl methacrylate crosslinked polyvinyl alcohol reinforced hybrid hydrogels synthesized using IPN chemistry exhibiting promising translational potential for the engineering and regeneration of cardiac tissue [103]. A study by He et al. demonstrated a panel of two cellulose hydrogels from the tunic of sea squirts following a combined acid hydrolysis-Kraft cooking method and subsequent treatment with pyrrole. Both the hydrogels exhibited cardiac repair by upregulating the regenerative mediators in vivo MI-rats [104].

Simeoni et al. used bacterial cellulose membrane patches cocultured with skeletal myoblast cells and human MSCs to reduce post MI pathology in rat models demonstrating that the cellulose patches supported the adherence and proliferation of seeded cardiac cells. Post-implantation LV displayed protection against remodeling suggesting the translational significance [105]. Entcheva et al. demonstrated the application of cellulose acetate and regenerated cellulose scaffolds for developing structurally mature and functionally competent cardiac cell networks which promoted the growth of cardiac cells forming tissue-like cardiac constructs [106]. Chen et al. reported,

electro-spun scaffolds based on polyurethane (PU) and ethyl cellulose displayed high tensile strength (1-90MPa) and appreciable elastomeric properties for designing ultrathin patches compatible with myocardial tissue at cellular and protein level [107]. In another study, cellulose scaffolds made of cotton linters stabilized with gelatine were used to generate the origami crease pattern facilitating coordinated cell contractions in a 3D environment suitable for CTE applications [108].

Chainoglou et al. fabricated biofunctionalized cellulose acetate nano scaffolds for surface coating in artificial aortic valves made of pyrolytic carbon for enhancing the biocompatibility. The scaffolds were synthesized by electrospinning technique and biofunctionalization was achieved by immobilizing RGD peptides and YIGSRG laminins on scaffold surfaces displaying excellent proliferation ensuring the biocompatibility of cellulose based scaffolds [109]. A seminal study reported the application of bacterial cellulose to generate cardio-protective soluble factors unveiling significant post-implantation improvements in healing responses of carotid arteries in small and large animal models [110]. Similarly Andrade et al. reported chimeric proteins having cellulose-binding module and an adhesion peptide accelerating the adhesion and proliferation of human microvascular endothelial cells into bacterial cellulose [111]. Similarly, tissue-engineered vascular grafts made from bacterial cellulose for endothelialization have been successfully tested in a translationally relevant swine model [112]. A hierarchical-structured bacterial cellulose and potato starch was reported by Liu and co-workers demonstrating excellent in vitro outcomes [113]. Novotna et al. prepared 6-carboxycellulose based material displaying the adhesion and sustenance of vascular smooth muscle cells for the successful engineering of vascular tissue for regenerative applications [114]. Su et al. blended polyurethane with 10% cellulose and electro spun the mixture into a 3D scaffold exhibiting appreciable biocompatibility and mechanical

properties and displayed anisotropy essential for the growth and repair of damaged cardiac tissue [115]

PEG Based Hydrogels in CTE

PEG hydrogels are common in CTE and an important study reported the encapsulation of cardiomyocytes Arginine-Glycine-Aspartic acid (RGD)-modified PEG hydrogels affording greater cell density [116]. In another study, PEG coupled with thiol-modified hyaluronic acid hydrogels facilitated the differentiation of pre-cardiac cells from chicken embryo upregulating cardiac-specific markers compared with the control gels [117]. In another approach, Grover et al. incorporated PEG into cardiac dECM network by interacting the ECM proteins with an PEG and PEG-acrylates. The findings revealed that PEG incorporation into ECM-based hydrogels upgraded the scaffold properties which can find translational opportunities in regenerative cardiology [118]. Another seminal study utilized PEG–PCL–PEG triblock copolymer blended with α-cyclodextrin for encapsulating bone marrow MSCs and post-implantation rabbit MI model displayed significant retention and survival rate and significant reduction in the infarct area [119]. Zhang et al. obtained anisotropic mechanical properties using PEG hydrogels by crosslinking with PEG diacrylate (PEGDA) employing photolithographic patterning. This hydrogel was decorated with RGD peptide influenced the elongation and ECM deposition by valvular interstitial cells (VICs) for heart valve tissue engineering [120].

PEG hydrogel with a definite nanopillar design has been constructed by ultraviolet (UV) assisted capillary lithography which demonstrated that the nanopillars enhanced the formation of self-assembled aggregates of cardiomyocytes. Importantly, the cardiomyocytes exhibited spontaneous beating and generation of action potentials

revealing excellent contractile and conductive properties which are inevitable for CTE [121]. Somekava et al. synthesized PLA-PEG gel and evaluated its efficiency as an injectable system for preventing LV remodelling in MI rat models. The hydrogel showed a sol to gel transition at 37^{o}C and excellent biodegradation profile and reduced the infarct size and preserved cardiac function when injected to infarct zone of MI rat model [122]. Another recent approach demonstrated EVs incorporated PEG-ECM hydrogels displaying improved gelation time, robust mechanical properties, increased rate of retention and sustained bioactivity suitable for CTE applications [123].

PVA Based Hydrogels in CTE

Owing to the great capacity to retain a bulk amount of water, appreciable swelling without dissolving, tuneable mechanical properties and biocompatibility makes PVA as an excellent choice for biomedical applications. Dattola et al. fabricated a highly porous PVA hydrogel revealing the mechanical properties similar to cardiac ECM supporting the growth and differentiation of human induced pluripotent stem cells into cardiomyocytes for CTE [124]. In another study, biodegradable PVA/silk fibroin scaffold fabricated by an electrospinning technique using water as solvent and the scaffold displayed mechanocompatibility similar to native cardiac tissue and supported the growth and performance of human cardiac fibroblast cells [125]. A seminal study by Mombini et al. demonstrated nanofiber scaffolds based on PVA, chitosan and carbon nanotube (CNT) resulted in the differentiation of rat MSCs to cardiomyocytes and was electrically conductive suitable for CTE [126].

An important study by Pusph et al. examined PVA-PVP-based patches, plasticized with glycerol or propylene glycol which maintained neonatal mouse CMs and the transplantation into the rat MI models revealed their safer CTE applications [127]. Hu et al. reported a novel trilaminar membrane is composed of PVA and CMC which

effectively reduced postoperative pericardial adhesions following the implantation in a pericardial adhesion rabbit model suggesting the potential for CTE [128]. Thankam et al. reported PVA-alginate semi-IPN and IPN hydrogels for CTE where the IPN displayed increased structured and free water content, excellent hemo and biocompatibility and promoted the growth and survival of L929 fibroblast and H9c2 cardiomyoblasts compared to semi-IPN hydrogel [129]. Mousa et al. developed three layered nanofiber patch composing of PVA-Silk fibroin in the middle which is surrounded by PCL and PLA supporting the growth and proliferation of human endothelial cell line, EA.hy926 suggesting the potential application in CTE [130]. A seminal study by Ravichandran et al. demonstrated a hybrid hydrogel BSA/PVA/Au for combining the electrical, mechanical and biological properties for successful CTE. The hydrogel elicited superior biological and functional performance accelerating infarcted myocardium regeneration as evident from the differentiation of MSCs by upregulating the cardiomyocyte biomarker connexin 43 (Cx43) [131]. Another approach utilized PVA-dextran elastic hydrogel patches to locally deliver the natural antioxidant molecule, astaxanthin for improved cardiac healing. Ex vivo and in vivo findings revealed appreciable mechanical strength and biocompatibility along with superior antioxidant responses; which is highly beneficial for CTE applications [132].

Hybrid Hydrogels in CTE

Hybrid hydrogels comprising natural and synthetic polymers are the promising materials for CTE due to their structural, physiochemical, mechanical and biological functionalities along with the controlled degradation profile. Several hybrid hydrogels with diverse combinations of natural and synthetic biomaterials [133] [134] [135] [136] have been reported for versatile biomedical applications such as CTE [137] [138] [139]. The outstanding properties of alginate, especially the biocompatibility, biodegradability,

non-immunogenicity, non-thrombogenity and chelating power as well as FDA approval pave multiple ways for its use in versatile biomedical applications as in CTE [140] [141]. However, the relatively lower mechanical properties of alginate-based hydrogels result in structural and morphological deformities resulting in poor functional performance for CTE [142]. Translationally, the mechanical instability hinders the applications of alginate hydrogels for long-term and load bearing applications as in CTE. Similarly, the cellulose-based hydrogels have gained prior attention in CTE owing to the hydrophilicity, mechanical properties, biodegradability, biocompatibility, low cost and low toxicity, as well as the abundance of hydroxyl, carboxyl and aldehyde groups allowing the chemical modifications. However, the extreme higher density of inter and intramolecular hydrogen bonding in the cellulose impairs its solubility hurdling the biomedical applications [143]. Moreover, cellulose-based hydrogels lack inherent antibacterial, antioxidant and regenerative activities requiring tedious chemical reactions for functionalization to improve cardiac performance [143] [144] [145].

PEG-based hydrogels have been successful for biomedical applications owing to their tuneability especially surface modification, bioconjugation and hydrophilicity along with biocompatibility, mechanical strength non-immunogenity and resistance to protein adsorption. In addition, the terminal hydroxyl groups of PEG are available for functionalization into methyloxyl, carboxyl, amine, thiol, azide, vinyl sulfone, azide, acetylene and acrylate for CTE applications. However, PEG based hydrogels exhibit lower loading efficiency, risk of micelle formation acidic degradation products and extreme hydrophilicity challenge the CTE applications of PEG [146] [147]. Similarly, PVA-based hydrogels form colloidal dispersion network via crosslinking and swelling and are promising for CTE owing to the low toxicity, excellent water kinetics, tunable mechanical properties and exceptional biocompatibility [148]. However, uncontrolled

degradation pattern and poor cell adhesive properties offer significant hurdles for PVA-based hydrogels for CTE [148] [149] [150].

These demerits of alginate and cellulose can be resolved by co-polymerizing/grafting with synthetic polymers including PVA and PEG. Therefore, the design and fabrication of functionally active hybrid hydrogel scaffolds using the advantages of CMC, PVA, PEG and sodium alginate in optimal proportions is highly relevant for CTE; which is the central goal of this study.

CHAPTER 3
MATERIALS & METHODS

Synthesis and Characterization of Novel Biodegradable Hybrid Hydrogel Scaffolds Using the Copolymers Sodium Alginate, CMC, Starch, PEG and PVA

Four hydrogels based on the Alginate-CMC-PVA (ACPV) blend and Alginate-Starch-PEG (ASPG) blend were prepared by exploiting the interpenetration chemistry and ionic crosslinking [129]. All the chemicals and reagents used for the studies were of analytical/synthetic grade. The structures of sodium alginate, CMC, starch, PVA and PEG are given in **Figure 3** and overall schema for the methodology is given in **Figure 4**.

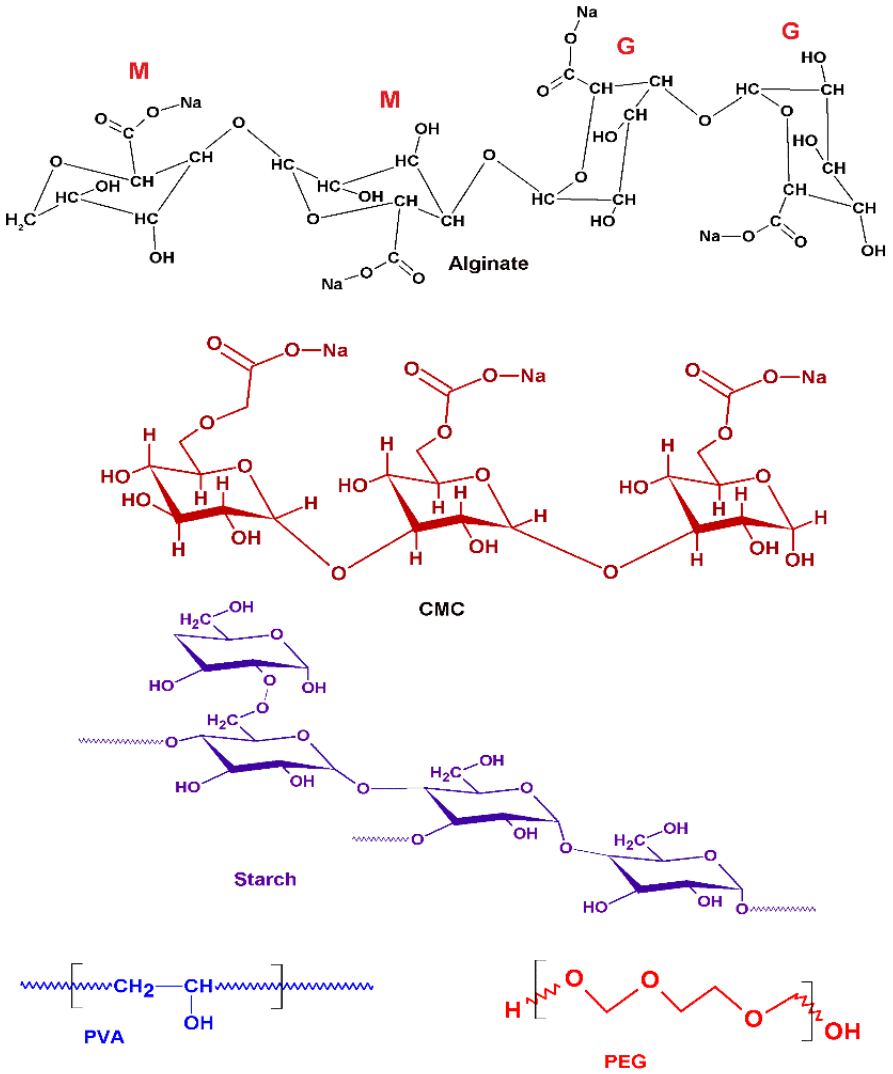

Figure 3: *Structures of sodium alginate, CMC, starch, PVA and PEG.*

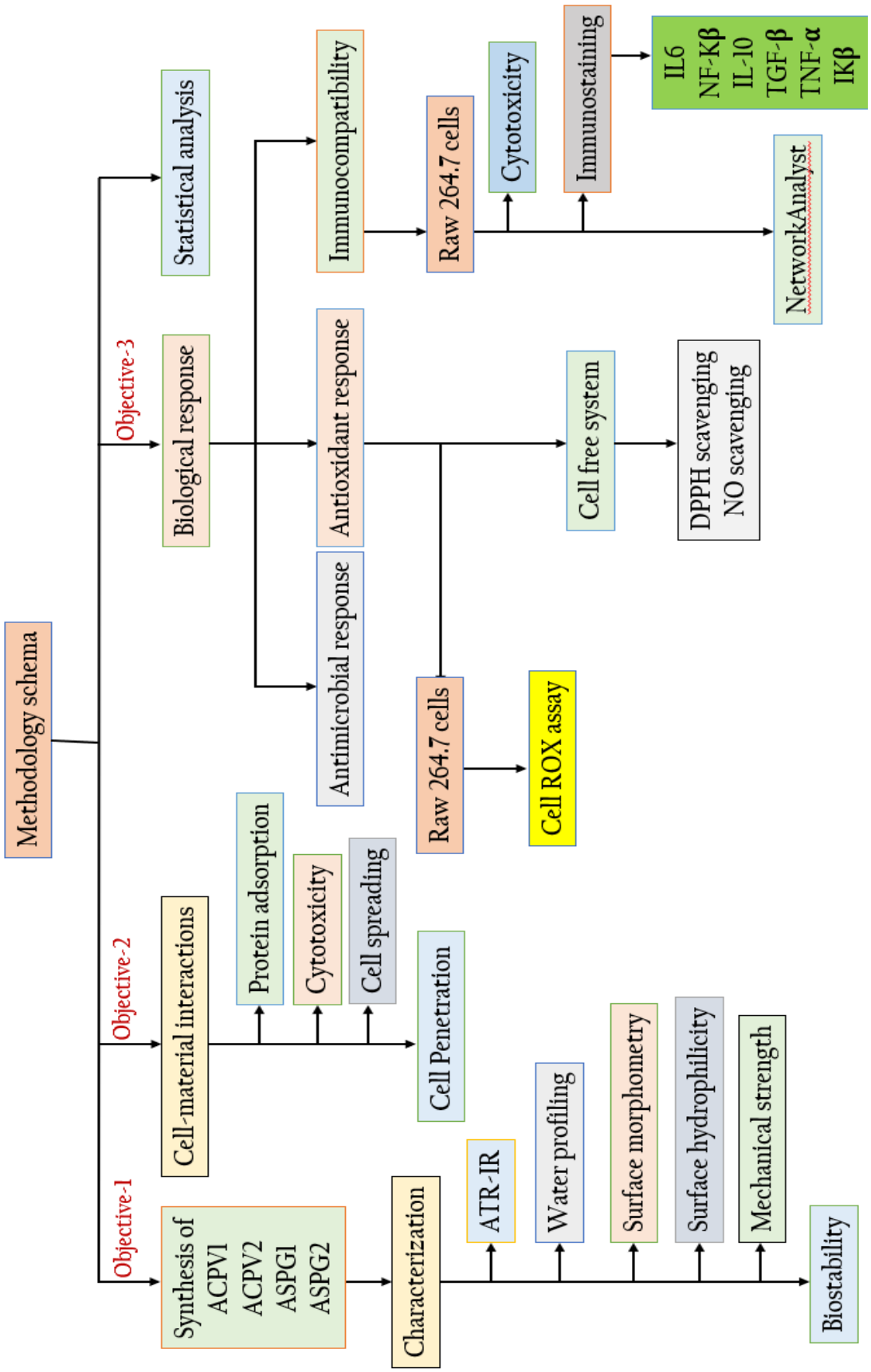

Figure 4: *Overall methodology schema of the study.*

Synthesis of ACPV Hydrogels

Alginate-CMC-PVA (ACPV) hydrogels were prepared by interpenetrating alginate, CMC and PVA. Briefly, 3% alginate (in water) was suspended in 5% Na_2HPO_4 which was mixed with 2% CMC (in water) and 5% PVA, followed by stirring with 1.5 % $CaCl_2$. The mixture was heated to 70^oC and casted in a plastic petri dish at 70^oC overnight. The dried hydrogels were carefully removed from the petri dish and incubated in 10% $CaCl_2$ for one hour for additional crosslinking. Two batches of ACPV hydrogels, ACPV1 and ACPV2 were prepared which differs in copolymer content. The percentage composition of alginate, cellulose and PVA were 30%, 20% and 50% respectively for ACPV1 and 46%, 15% and 39% respectively for ACPV2. The hydrogels were washed in warm water, freeze dried, sterilized under UV and stored aseptically in airtight containers at RT for further studies [129]. The overview of ACPV hydrogel synthesis is portrayed in **Figure 5**.

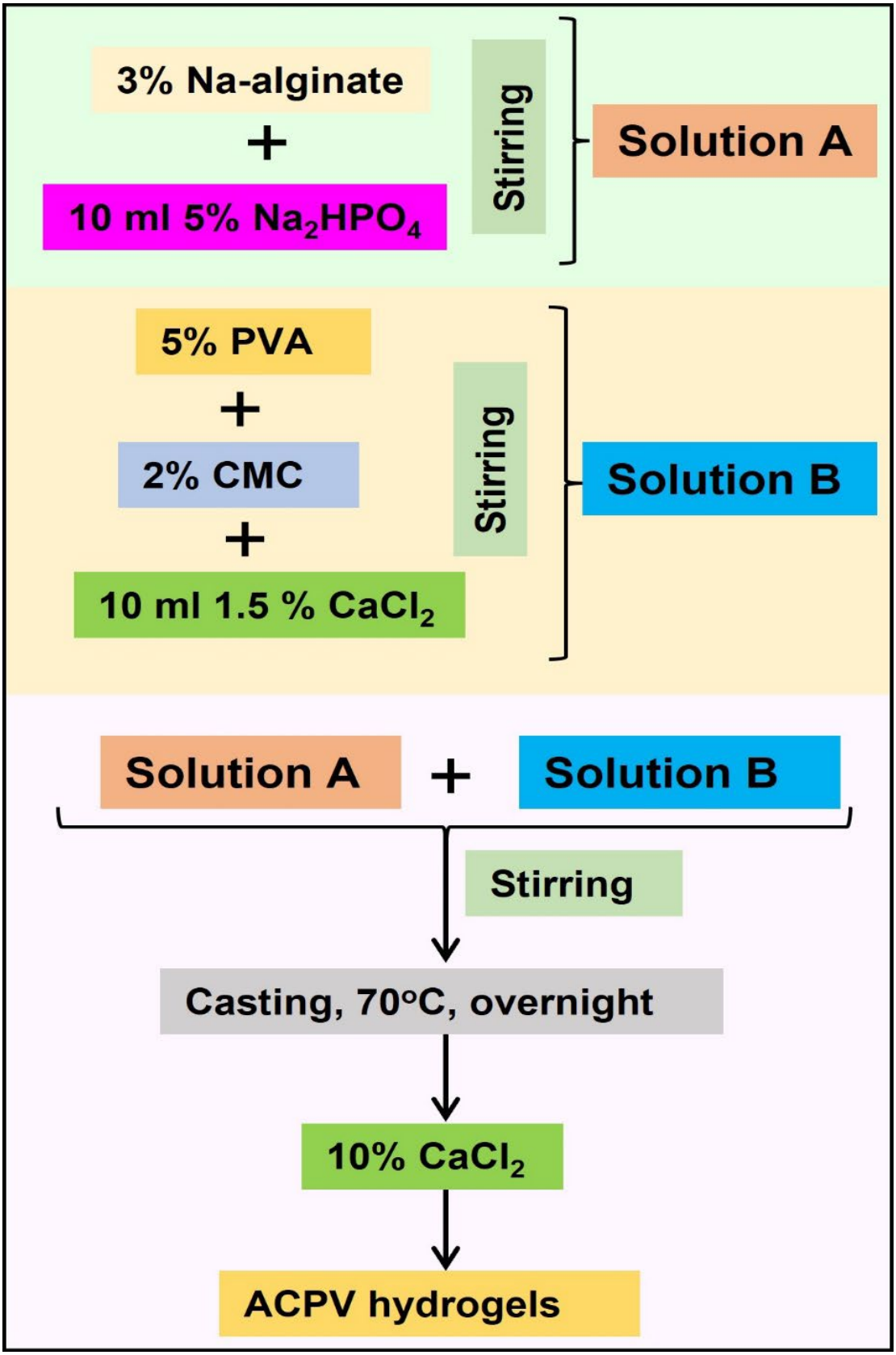

Figure 5: *The overview of the synthesis of ACPV hydrogels.*

Synthesis of ASPG Hydrogels

ASPG hydrogels were prepared by mixing 3% alginate (in water) was suspended in 5% Na_2HPO_4 and mixed with 2% PEG in 5% starch blend. This was followed by stirring with 1.5 % $CaCl_2$. The mixture was heated to 70^oC and casted at 70^oC overnight following the above procedure. The dried hydrogels were incubated in 10% $CaCl_2$ for one hour for additional crosslinking, washed in warm water, freeze dried, sterilized under UV and stored aseptically in airtight containers at RT for further studies. Two batches of ASPG hydrogels, ASPG1 and ASPG2 were prepared that differs in copolymer content. ASPG1 system contained 18%, 23% and 59% of alginate, PEG and starch respectively whereas ASPG2 contained 46%, 15% and 39% with respect to alginate, PEG and starch [129]. The overview of ASPG hydrogel synthesis is portrayed in **Figure 6**.

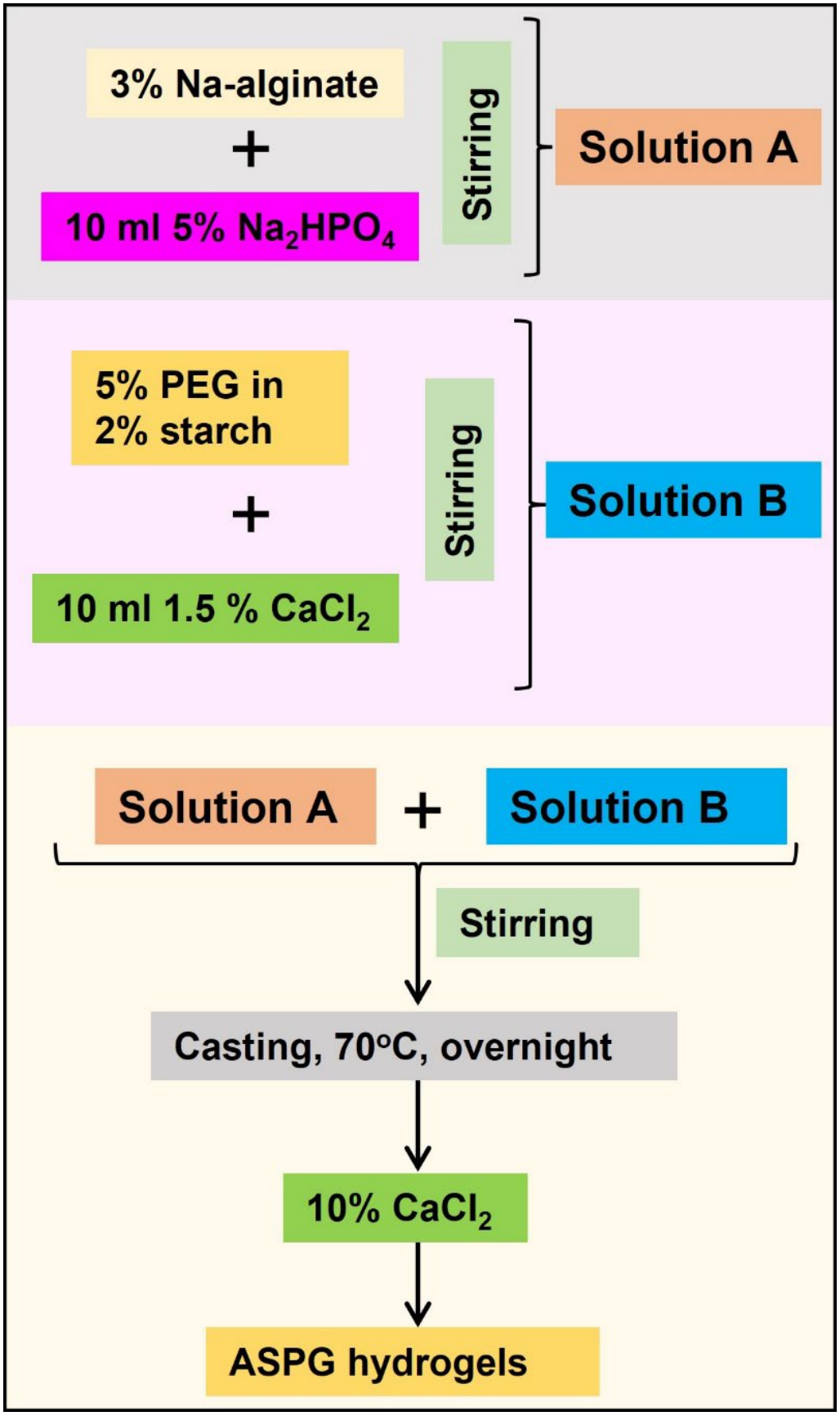

Figure 6: *The overview of the synthesis of ASPG hydrogels.*

Physiochemical Characterization

Analysis for surface functional groups

ATR spectrum, for assessing the surface functional groups, of ACPV and ASPG hybrid hydrogel subsets, was recorded by using Nicolet iS50 FTIR spectrometer using lyophilized samples following ASTME 1252-98 standards. The data were digitized and processed using Microsoft Excel and Origin software were used to plot the spectra [103].

Water profiling

Freeze dried ACPV and ASPG hydrogel samples (1 cm diameter discs) were used to determine the water content and swelling capacity. The samples were swelled in distilled water (DW) and allowed to attain equilibrium for 24 h at RT. The swollen samples were wiped carefully using blotting paper to remove the excess water prior to weighing. The equilibrium water content (EWC) and the swelling efficiency of the hydrogels were determined from the dry and wet weights following previously published reports [151]. Briefly, ACPV and ASPG hydrogels were imbibed in DW to determine swelling kinetics, swelling ratio (*S*), EWC and equilibrium swelling ratio (ESR) following the below equations.

$$Swelling\ ratio\ (S) = \frac{M_t - M_0}{M_0}$$

$$\%Swelling\ (\%S) = \frac{M_f - M_0}{M_0}$$

$$ESR\ (E) = \frac{M_f - M_0}{M_f}$$

$$EWC = \frac{M_f - M_0}{M_f} \times 100$$

Swelling kinetics reflected the swelling at regular time intervals of 15 minutes employing the following formula to define the diffusion of water molecules onto the interstices of the hydrogels [152].

$$\frac{S}{E} = Kt^n$$

M_t was the weight of the swollen hydrogel at time "*t*", M_0 was the dry weight and M_f represented the mass of the swollen hydrogel in equilibrium, "*E"* reflected ESR, '*S'* was the swelling ratio, '*K'* signified the swelling constant, '*n'* showed the diffusional exponent and '*t'* was the time interval for swelling measurements. *K* and *n* were obtained by the intercept and slope from the plot of log(S/E) vs log(time) respectively. For ACPV hydrogels, the equations were,

$$y = 0.1574 \ln(x) + 0.4336 \text{ (ACPV1)}$$

$$y = 0.1124 \ln(x) + 0.7165 \text{ (ACPV2)}$$

while the equations for ASPG hydrogels were

$$y = 0.2478 \ln(x) + 0.3169 \text{ (ASPG1)}$$

$$y = 0.4089 \ln(x) + 0.1562 \text{ (ASPG2)}$$

The total water absorption sites (TWAS) of the ACPV and ASPG hydrogels were determined by the following equation where 'm' is the molecular mass of one water molecule, which was determined as follows.

$$m = \frac{molar\ mass\ of\ water}{Avogadro's\ number} = \frac{18}{6.023\ X\ 10\text{^}23} = \sim 2.99\ X\ 10^{-23}$$

$$TWAS = \frac{M_f - M_0}{m}$$

Surface morphometry

The surface morphology and pore size of the ACPV and ASPG scaffolds were determined using a scanning electron microscope equipped with energy dispersive X-ray

spectroscope (SEMEDAX). Freeze dried hydrogel discs of 1 cm diameter were used. The average length and breadth of pores on scaffold surfaces were calculated from SEM images using ImageJ software with multi-measure plugin following previously published protocols [153]. Aspect ratio of the pores was calculated form length and breadth of each hydrogel.

Dynamic water contact angle

Four clean samples of ACPV and ASPG hydrogels of uniformly rectangular shape and known width (2mm) were swelled in DW and used for dynamic contact angle measurement for determining the surface hydrophilicity. Both advancing and receding contact angle were recorded following the Wilhelmy method (1863) in KSV sigma 701 tensiometer with DW as a solvent. The samples were immersed to a depth of 10 mm at a speed of 5 mm/min. The first 2 mm length was excluded for consistency. The contact angle values were processed automatically using the software associated with the instrument [153].

Tensile strength

Tensile strength of the water-swollen ACPV and ASPG hydrogels was determined using Shimadzu Universal Testing Machine (model AG-I) connected with long travel extensometer. Dumb bell-shaped specimens were punched out (ISO 527-2 type 5A) using a shear cutting die. Tensile strength was tested with a load cell of 100 N at 25^{o}C with a crosshead speed of 10 mm/min. The tensile properties were determined as reported elsewhere [154].

Biostability

The stability of ACPV and ASPG hydrogels was evaluated in the cell culture medium, DMEM, containing 10% FBS by aging at temperature 37^0C for 7 days. The long-term biostability and degradation of the ACPV and ASPG hydrogels were determined at pH 7.4 in the simulated biological fluid, PBS. Dried hydrogels of known weight were aged in 10 ml PBS at physiological pH and temperature. Then the relative loss of dry weight and changes in pH were monitored at regular intervals of 7 days for a total period of 30 days using a pH meter (cyber scan pc510). The aged hydrogels were oven-dried and the dry weight was used to calculate the weight loss to assess the extent of biodegradation [154].

Examinations on Cell-material Interaction and Compatibility of the Hybrid Hydrogels

Protein adsorption

The water swollen ACPV and ASPG hydrogels were incubated with commercially available fetal bovine serum (FBS) (1:10 dilution in PBS) at 37^0C on a shaker incubator overnight. Then the scaffolds were gently washed with PBS to remove the loose/unbound proteins and vortexed in minimum volume of PBS to extract the adhered proteins which were quantified by standard BCA method [103]. Then percentage of proteins adsorbed on to the hydrogels was quantified with respect to total serum protein content as control. SDS-PAGE was performed using the extracted proteins for assessing the extent of albumin adsorption using albumin (50μg/μl) as standard following the standard protocol. The relative adsorption of albumin was calculated using the image analysis ImageJ software from the bands obtained the SDS-PAGE gels [103].

Biocompatibility

Cell culture and maintenance

Rat cardiomyoblast cells H9c2 was used for the cytocompatibility evaluations of ACPV and ASPG hydrogels. The cells were grown in high glucose DMEM with 10% foetal bovine serum (FBS) at standard culture conditions of 5% CO_2, 95% humidity, 37°C and antibiotics (1%penicillin and 1%streptomycin). Upon 70-80% confluence the cells were split using standard trypizinization protocols [103].

Cytotoxicity test on extract

The ACPV and ASPG hydrogels were extracted in DMEM for 48 h and the cytotoxicity of hydrogel extract was determined by standard MTT assay using H9c2 cardiomyoblasts cell culture following previously reported protocol [155].

Direct contact assay

The toxicity of the ACPV and ASPG hydrogels under the direct influence of cell contact was determined by direct contact assay. The ACPV and ASPG hydrogel samples (10 mm diameter) were placed over the monolayer of H9c2 cells and allowed to proliferate for 24 h which were examined microscopically for alterations in their morphology compared to the control.

Cell adhesion assay

The healthy being of H9c2 cells in the ACPV and ASPG hydrogels was evaluated following 5 days of seeding by cell adhesion assay using FDA staining (100 µg/ml). The cells in the hydrogels were incubated with FDA and immediately viewed under an epifluorescence microscope using blue filter following previously published protocol [156].

Cell penetration

H9c2 cells were seeded onto ACPV and ASPG hydrogels as mentioned before and the migration was determined using the fluorescent microscope using Z-stack mode. The cells were stained with DAPI and 2.5 µm stacks were taken and penetration depth was calculated automatically using the software associated with the microscope following previously published protocols [103].

Investigations on the Biological Responses of Biosynthetic Hydrogels for CTE

Studies on Antimicrobial Response

The ACPV and ASPG hydrogels were loaded with antibiotics and the antibiotic releasing efficiency of the hydrogels was analyzed using disc diffusion method [8]. To prepare antibiotic incorporated scaffolds 10 mm discs were loaded with 5, 10, 20 µg respectively of amikacin and vancomycin by diffusion method. Both gram-positive (*Staphylococcus sps.*) and gram-negative bacteria (*Pseudomonas sps.*) used for the study were kindly donated by Polyclinic, Thrissur, Kerala, India. The bacteria were cultured on Muller Hinton agar plates, the antibiotic incorporated scaffolds were placed, incubated at 37^0C for 24 hours and the zone of inhibition was measured. Untreated discs were used as control. The zone of inhibition was measured and compared with that of the control.

Studies on Antioxidant Response

In cell free system

The natural antioxidant ascorbic acid (200 µg) was loaded into ACPV and ASPG hydrogels following the diffusion-controlled method and dried at sterile conditions and stored aseptically for further studies. The following tests were performed to determine the antioxidant activity.

DPPH radical scavenging activity

DPPH radical scavenging activity of ascorbic acid loaded ACPV and ASPG hydrogels was determined by following previously published protocols [157]**.** The hydrogels were incubated with the reaction mixture composing of 3 ml of absolute ethanol and 0.3 ml of DPPH radical solution (0.5 mM in ethanol) for 1 hr at RT. A mixture of 3.5 ml ethanol and 0.3 ml DPPH radical solution served as control. All the

tubes were read at 517 nm and DPPH radical scavenging potential of the test samples was determined by using the formula.

$$\%\, of scavenging = \frac{ODcontrol - ODtest}{ODcontrol} \times 100$$

Nitric oxide radical scavenging activity

Ascorbic acid loaded ACPV and ASPG hydrogels were incubated with 3 ml Sodium nitroprusside (5mM) in phosphate buffer at 25^0C for 30 min. 100 µM ascorbic acid was used as control. After incubation 1.5 ml Griess reagent (1% sulphanilamide, 2% H_3PO_4 and 0.1% napthyl ethylene diaminedihydrochloride) was added to all the tubes and the absorbance was read at 546nm using PBS as blank [158]. The percentage of scavenging was measured using the formula.

$$\%\, of scavenging = \frac{ODcontrol - ODtest}{ODcontrol} \times 100$$

In Cellular System

Culture, maintenance and treatment of RAW 264.7 cells

Mouse macrophage cell line RAW 264.7 was maintained in high glucose DMEM with 10% foetal bovine serum (FBS) (Cat# 30-2020, ATCC), under standard culture conditions (5% CO_2, 37°C and antibiotics). Upon 70-80% confluency the cells were split using cell scraper. The cells were treated 100 µM H_2O_2 and the scavenging effects were assessed by placing ACPV and ASPG hydrogels (swollen in serum-free media) overnight and the cells treated with 100 µM H_2O_2 and the untreated cells were used as treatment and comparison controls, respectively [103].

Direct contact oxidative stress

The ACPV and ASPG hydrogels treated RAW 264.7 macrophages were incubated with the Cell ROX Reagent (Invitrogen Waltham, MA), (5 µM) for 30 minutes

at 37°C, washed with sterile PBS, mounted with serum free media and the live cell imaging under fluorescence microscope at blue filter. The MFI was calculated using ImageJ program (N=10 images) as reported and the results were expressed as Log2FC normalized to the control [159]. The cells were treated 100 μM H_2O_2 and the untreated cells were treated in the same manner.

Studies on Immunocompatibility and Gene Interactions

Mouse macrophage cell line RAW 264.7 was maintained in high glucose DMEM with 10% fetal bovine serum (FBS) (Cat# 30-2020, ATCC), under standard culture conditions (5% CO_2, 37^{o}C and antibiotics). Upon 70-80% confluency the cells were split using cell scraper. The cells were treated with ACPV and ASPG hydrogels in serum-free media overnight and the cells treated with 100 μg/ml lipopolysaccharide (LPS) and the untreated cells were used as treatment and comparison controls, respectively [29].

Direct contact assay

The toxicity and the macrophage activation of the ACPV and ASPG hydrogels under the direct influence of cell contact was determined by direct contact assay. The ACPV and ASPG hydrogel samples (10 mm diameter) were placed over the monolayer of RAW 264.7 cells and allowed to proliferate for 24 h which were examined microscopically for alterations in their morphology compared to the control [40].

Immunofluorescence

The RAW 264.7 cells were cultured in contact with ACPV and ASPG hydrogels for 24 h and the expression of inflammatory mediators including IL6, NF-Kβ, IL-10, TGF-β, TNF-α and IKβ was determined using immunostaining following previously protocols [160]. Primary antibodies (1:400 dilution) against IL6, NF-Kβ, IL-10, TGF-β, TNF-α and IKβ were used for binding and respective fluorochrome conjugated secondary

antibodies (1:400) were used for detection. Nuclei were counterstained with 4′,6-diamidino-2-phenylindole (DAPI) and imaged under a fluorescent microscope (Leica Thunder, Germany). A negative control was used (without primary antibody) for fixing the exposure time and to minimize the background. MFI was calculated from the images using ImageJ program and were normalized with the number of nuclei to calculate the $\log_2$ fold-change (FC) following previously reported protocol [161].

Interconnecting genes and pathways

The genes and regenerative pathways involving IL6, NF-Kβ, IL-10, TGF-β, TNF-α and IKβ were assessed by NetworkAnalyst program following previous reports[162]. The input genes used for NetworkAnalyst program were IL6, NF-Kβ, IL-10, TGF-β, TNF-α and IKβ for human species specificity. Generic protein-protein interaction (PPI) based on IMex interactome and GO:BP were employed for assessing the genes interconnecting the input genes IL6, NF-Kβ, IL-10, TGF-β, TNF-α and IKβ along with the associated regenerative pathways. Similarly, the signaling associated with these genes was determined by ExpressAnalyst platform utilizing the enrichment network based on GO:BP [163], [164]. The PPI subnetworks were assessed separately.

Statistical analysis

The results were expressed as mean ± SEM/SD. ImageJ software was used for pore measurements, immunostaining and protein absorption. The statistical significance was determined by one-way ANOVA with two-stage linear step-up procedure of Benjamini, Krieger and Yekutieli test (2006) for multiple comparison using GraphPad Prism software. Statistical significance of $P<0.05$ was set for all experiments [103].

CHAPTER 4
RESULTS

Synthesis and Characterization of Novel Biodegradable Hybrid Hydrogel Scaffolds Using the Copolymers Sodium Alginate, CMC, Starch, PEG and PVA

Synthesis of Hybrid Hydrogels

ACPV hybrid hydrogel system was prepared by interpenetrating alginate and cellulose with the synthetic polymer PVA (**Figure 7**). ACPV1 and ACPV2 were prepared by varying the ratio of polymer constituents. The percentage composition of alginate, cellulose and PVA were 30%, 20% and 50% respectively for ACPV1 and 46%, 15% and 39% respectively for ACPV2 (**Figure 8**). The natural polymers used in ASPG system included alginate and starch along with the synthetic polymer PEG (**Figure 9**). The two subsets ASPG1 and ASPG2 were prepared by altering the constituent ratio. ASPG1 system contained 18%, 23% and 59% of alginate, PEG and starch respectively whereas ASPG2 contained 46%, 15% and 39% with respect to Alginate, PEG and starch (**Figure 10**). Divalent cation, Ca^{2+} was used as the crosslinking agent in all preparations.

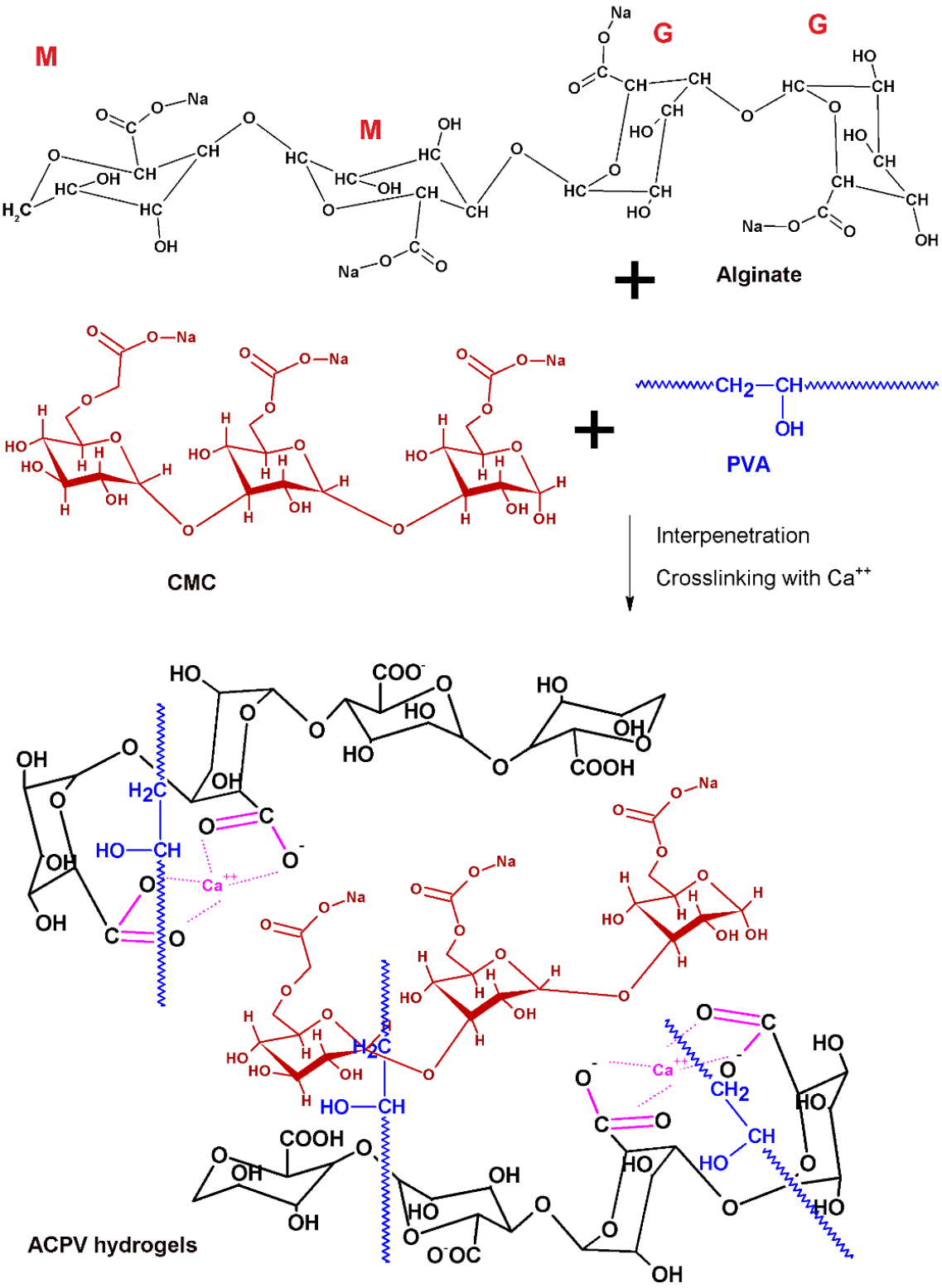

Figure 7: *Proposed structure of ACPV hydrogels.*

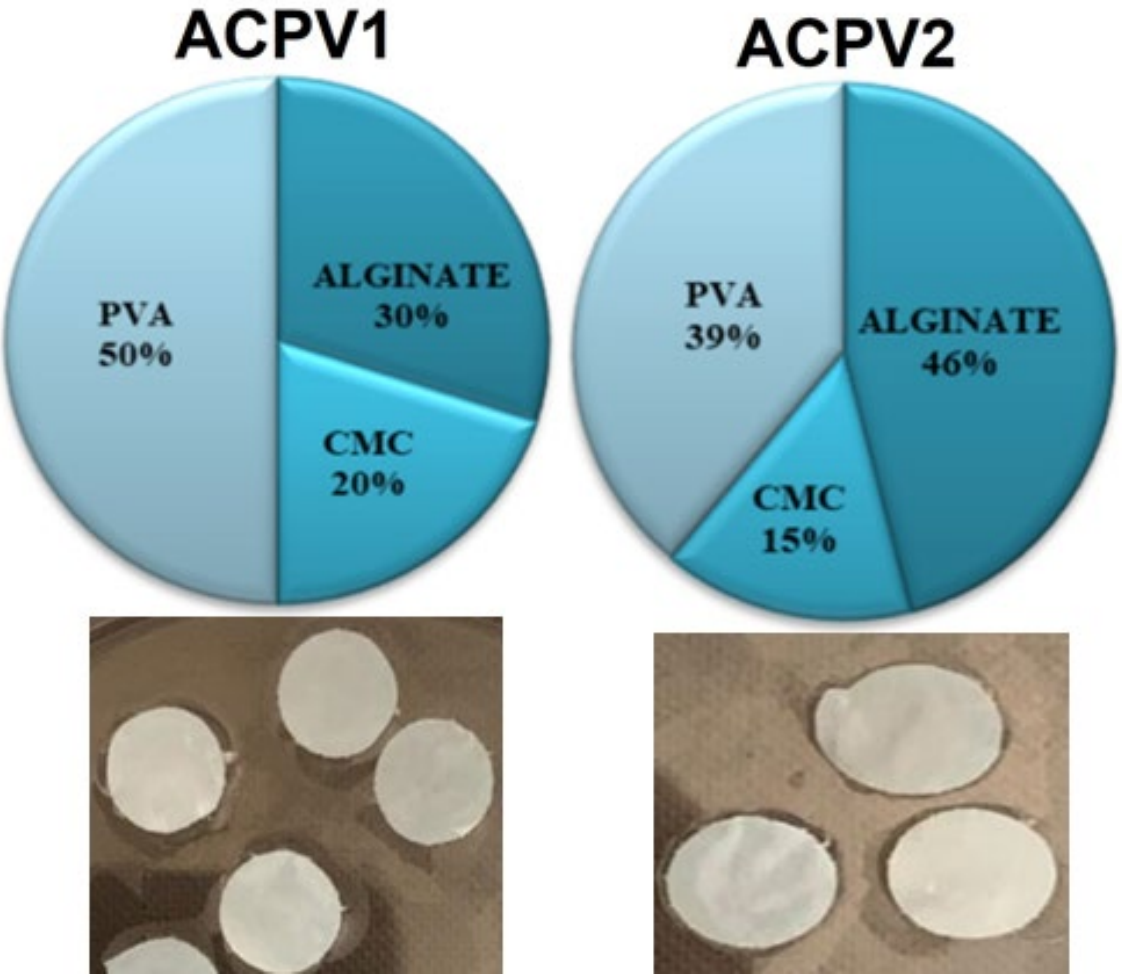

Figure 8: *Percentage composition of constituent polymers in ACPV1 and ACPV2 hybrid hydrogel subsets .*

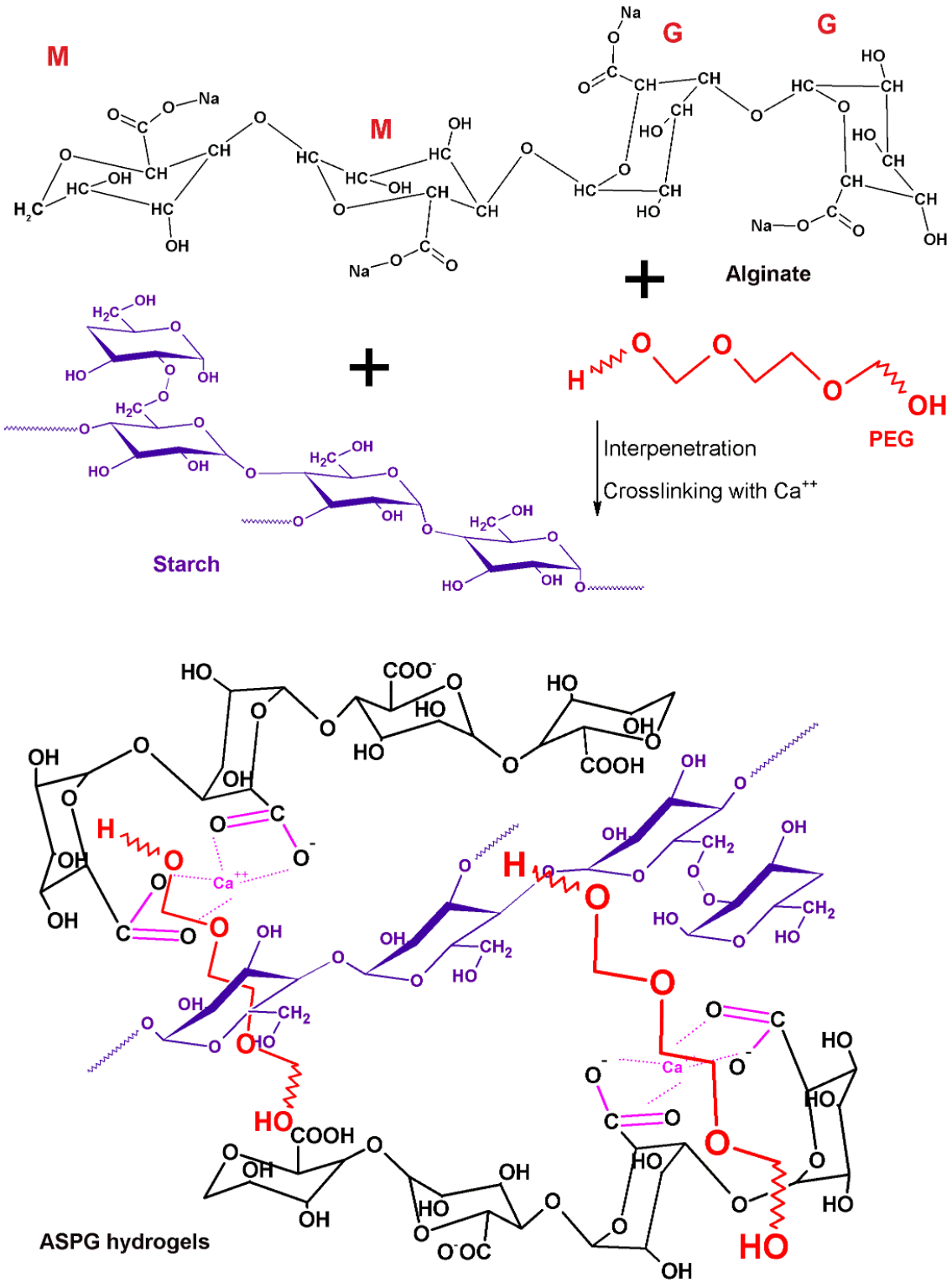

Figure 9: *Proposed structure of ASPG hydrogels.*

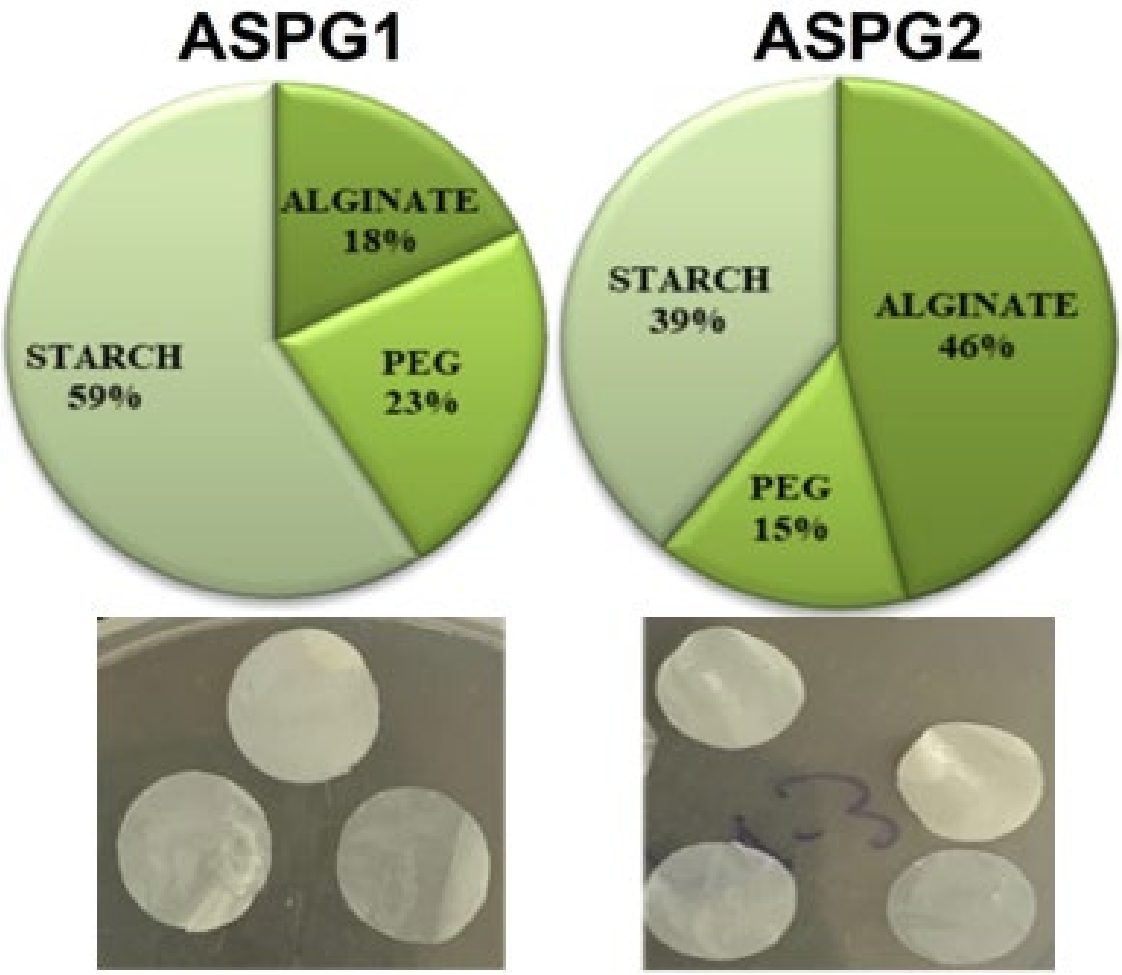

Figure 10: *Percentage composition of constituent polymers in ASPG1 and ASPG2 hybrid hydrogel subsets.*

Physiochemical Characterizations

Surface functional groups

ATR spectra demonstrated peaks in all the four hydrogels suggesting the existence of similar functional groups on their surface (**Figures 11A-11D**). The broad peak around 3500 cm^{-1} in all the four hydrogels represented -OH stretching vibrations contained in alginate, starch, CMC, PVA and PEG. The sharp peak 1700 cm^{-1} attributed to the stretching vibrations of carbonyl groups presented by the alginate fragments. The sharp peak around 1750 cm^{-1} representing stretching vibrations of -COOH suggesting the presence of alginate and CMC. The sharp peak around 1000 cm^{-1} was due to the C-O-C stretching vibrations of the glycosidic bonds in the polysaccharides and PVA. Hence, the IR analysis suggests the presence of alginate, starch, CMC, PVA and PEG fractions in the surface of all the four hydrogels.

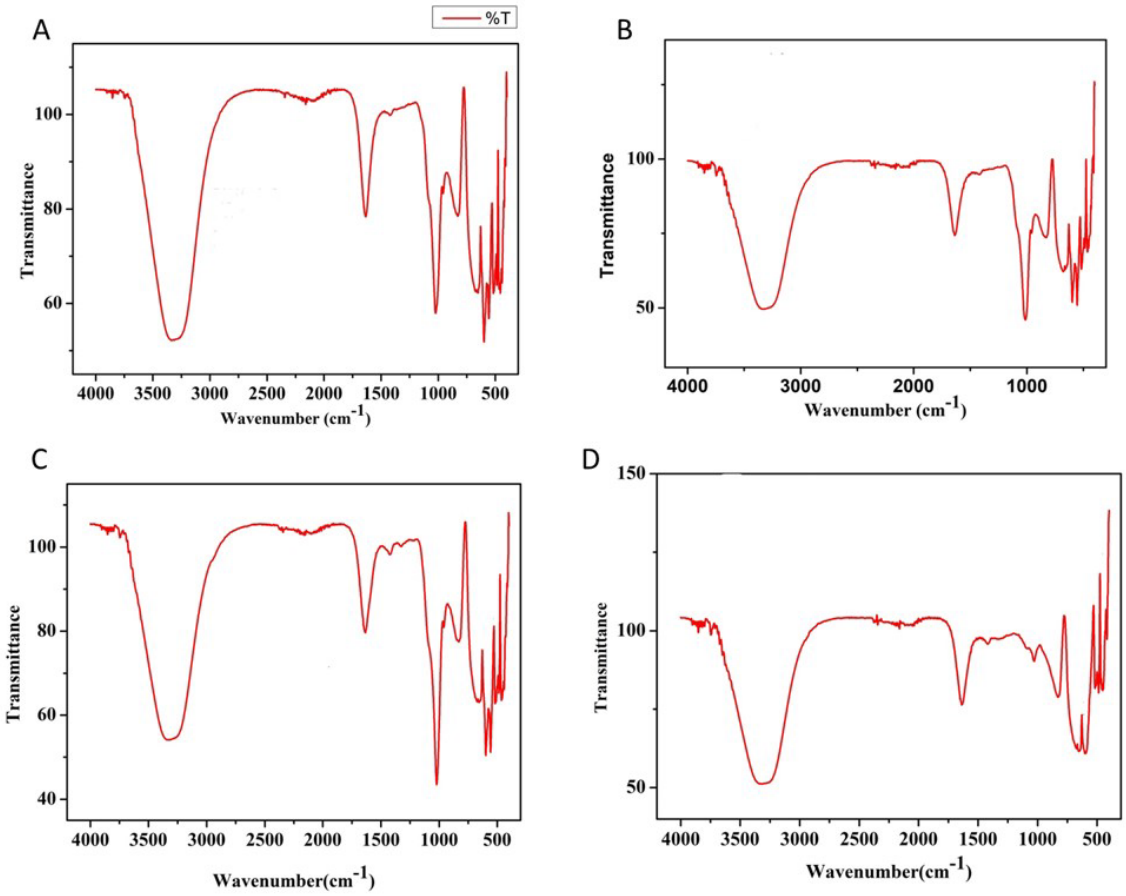

Figure 11: *ATR spectra of hybrid hydrogels: (A) ACPV1, (B) ACPV2, (C) ASPG1 and (D) ASPG2.*

Water Profile

The hybrid hydrogels displayed EWC >79% and swelling ratio >5; however, were statistically not significant among the groups except for the EWC between ASPG2 and ACPV2 (P=0.0207) (**Table 1**). Interestingly, ACPV2 exhibited increased level of EWC (88.40±2.51) suggesting the superabsorbent nature. Overall, the four hydrogels exhibited similar water profile (**Table 1**). Also, the diffusional exponent (n) was 0.1574, 0.1124, 0.2478 and 0.4089 respectively for ACPV1, ACPV2, ASPG1 and ASPG2 whereas the swelling constant (k) was 0.4336, 0.7165, 0.3169 and 0.1562 respectively for ACPV1, ACPV2, ASPG1 and ASPG2 (**Table 1**) (**Figures 12A-12D**). Additionally,

total water absorption sites (TWAS) were $6.8x10^{24} \pm 1.93\ x10^{23}$, $4.24x10^{24} \pm 5.11\ x10^{23}$, $2.22x10^{24} \pm 1.99\ x10^{23}$ and$1.67x10^{24} \pm 3.34\ x10^{23}$ respectively for ACPV1, ACPV2, ASPG1 and ASPG2. The ACPV hydrogels displayed significantly increased TWAS than the ASPG hydrogels; however, the alterations with ASPG hydrogels were statistically not significant (P=0.2559) compared to all others (**Table 1**) (**Figures 13**).

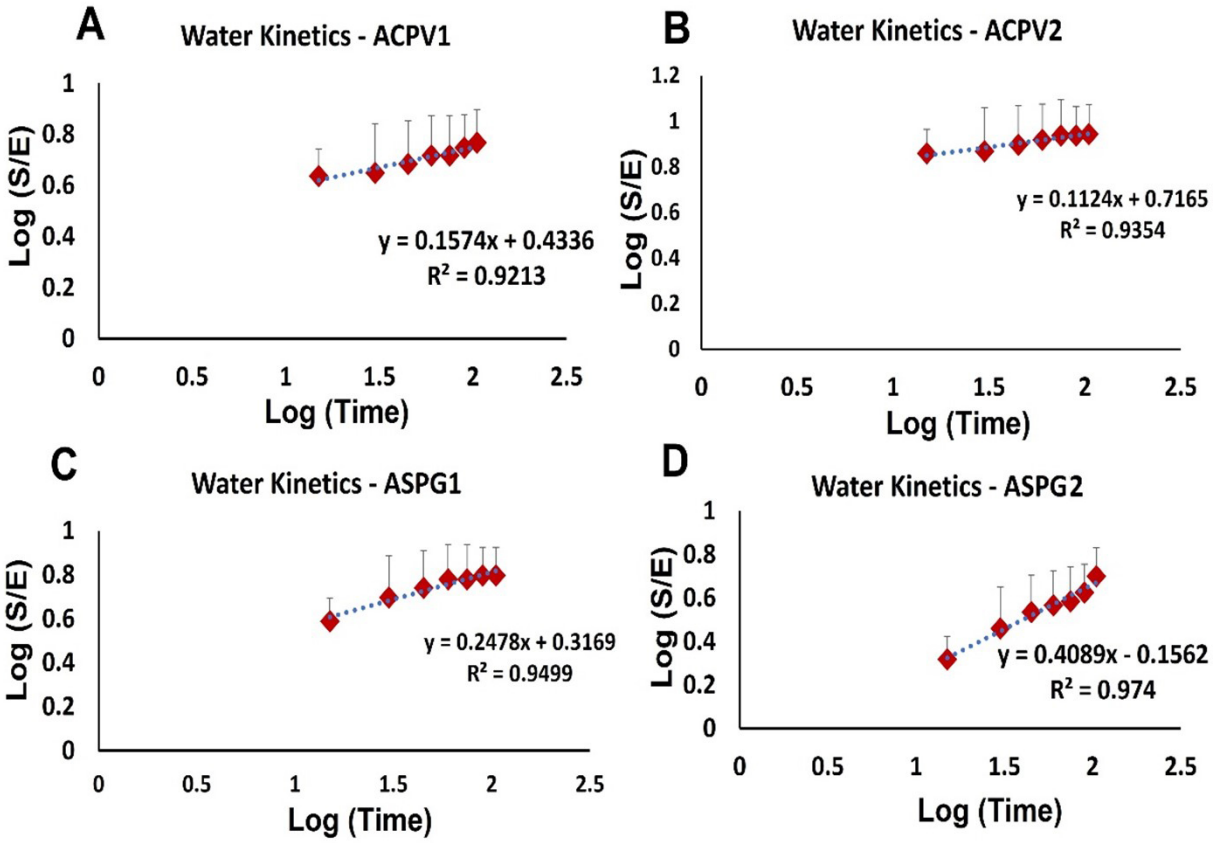

Figure 12: *Determination of diffusional exponent (n) and the swelling constant (k) from the plot of log(S/E) along the Y-axis and log(time) along the X-axis of the hybrid hydrogel scaffolds: (A) ACPV1, (B) ACPV2, (C) ASPG1 and (D) ASPG2.*

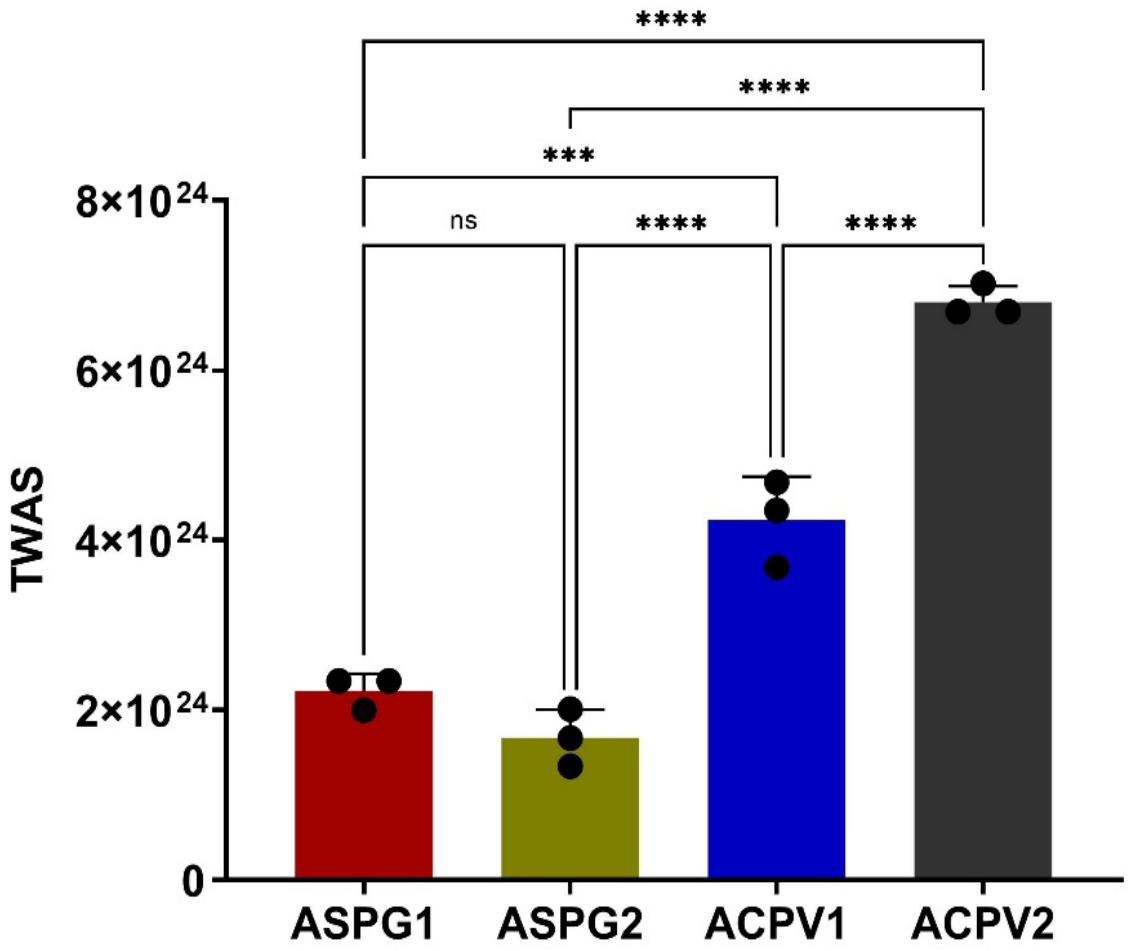

Figure 13: *TWAS of ACPV and ASPG hybrid hydrogels (***P<0.001, ****P<0.0001, ns= not significant).*

Table 1: Characterization of ACPV and ASPG hydrogels.

Parameters	ACPV 1	ACPV2	ASPG1	ASPG2
Equilibrium water content	82.44±4.58	88.40±2.51	83.5±5.09	78.57±10.37
Swelling	6±1.76	8.94±2.21	6.43±1.77	5.33±2.08
Diffusional exponent (n)	0.1574	0.1124	0.2478	0.4089
Swelling constant (k)	0.4336	0.7165	0.3169	0.1562
TWAS	$6.8x10^{24} \pm 1.93\ x10^{23}$	$4.24x10^{24} \pm 5.11\ x10^{23}$	$2.22x10^{24} \pm 1.99\ x10^{23}$	$1.67x10^{24} \pm 3.34\ x10^{23}$
Pore length	6.67±3.31	10.35±3.6	11.76±4.2	4.03±2.41
Pore breadth	5.2±2.9	7.63±2.7	7.96±2.5	2.84±1.72
Pore aspect ratio	1.34±0.31	1.36±0.20	1.48±0.35	1.41±0.29
Receding contact angle	44.44±5.21	52.46±4.40	45.14±3.58	46.09±7.94
Advancing contact angle	43.33±4.51	48.88±4.40	45.146 ± 4.8	47.2±7.98
Tensile Strength	0.387±0.06	0.474±0.125	0.147±0.07	0.911±0.003
Young's Modulus	0.98±0.15	1.51±0.36	1.66±0.37	4.5±0.02
Protein adsorption (%)	41.05±31.24	41.40±19.60	75.42±14.88	46.73±26.83

Surface morphology

SEM imaging demonstrated the surface morphology and pore distribution of the hydrogels unveiling the porous morphology, pore density and pore interconnectivity (**Figures 14A-14D**). ACPV2 and ASPG1 exhibited increased pore diameter when compared to ACPV1 and ASPG2 (**Table 1**). However, the difference in pore length and breadth between ACPV1 ($P=0.0753$) and ACPV2 ($P=0.1089$), ACPV1 ($P=0.3158$) and ASPG2 ($P=0.1348$) and ACPV2 ($P=0.7082$) and ASPG1 ($P=0.9839$) were statistically not significant. Interestingly, the pore length and breadth in ACPV1 ($P=0.0017$) and ASPG1 ($P=0.0229$), ACPV2 ($P=0.0007$) and ASPG2 ($P=0.0002$) and ASPG1 ($P<0.0001$) and ASPG2 ($P<0.0001$) were statistically significant. Additionally, the pore aspect ratio of the hydrogels exhibited similar values and were statistically not significant suggesting the similar pore morphology (**Table 1**).

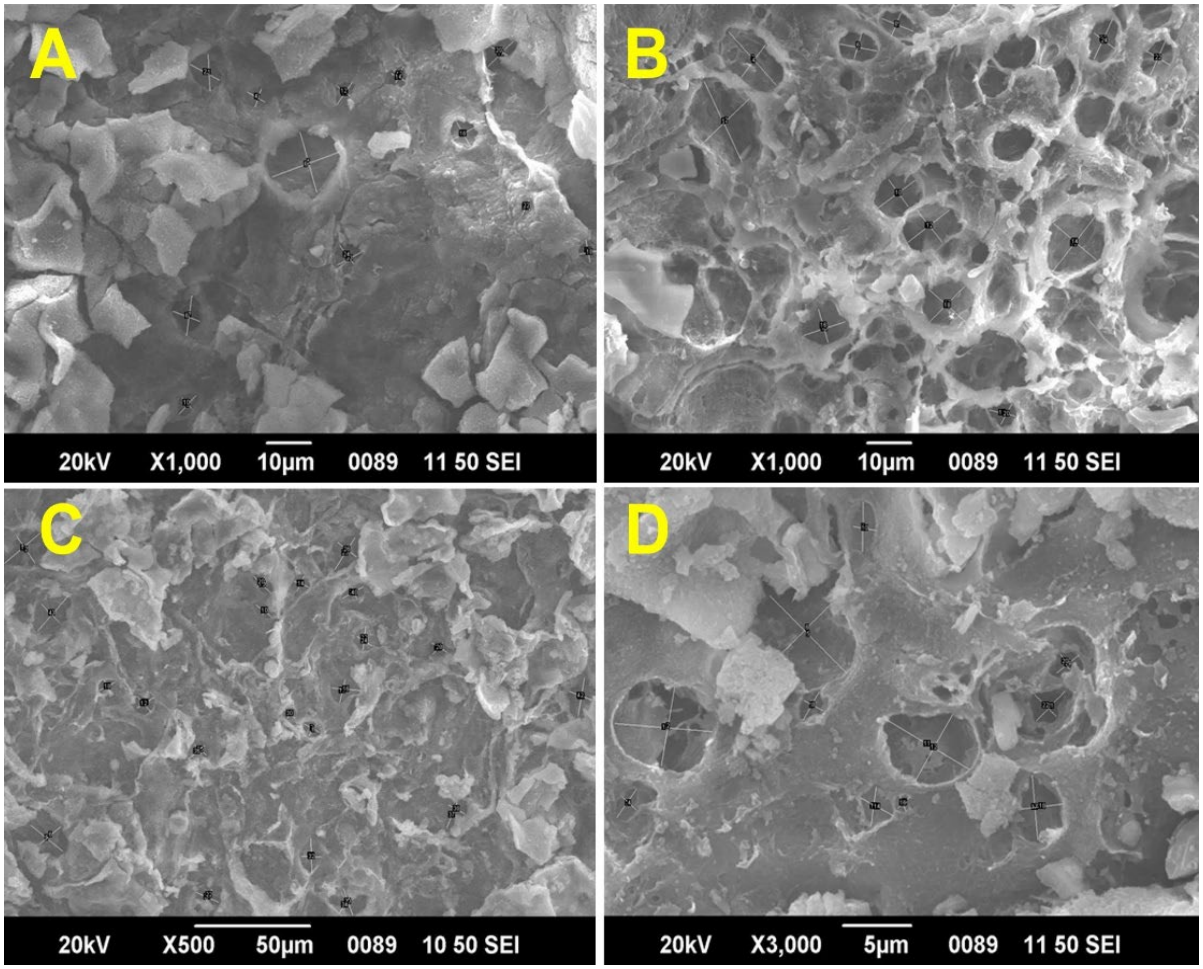

Figure 14: *SEM images showing the pore distribution and size of hybrid hydrogel scaffolds: (A) ACPV1, (B) ACPV2, (C) ASPG1 and (D) ASPG2.*

Surface Hydrophilicity

The advancing contact angles (ACA) of the hydrogels ranged between 43° to 48° whereas the receding contact angles (RCA) were between 44° and 52° suggesting the amphiphilic nature of the hydrogels; however, difference between ACA or RCA among the ACPV and ASPG hydrogels were statistically not significant (**Table 1**).

Tensile Strength

ASPG2 exhibited significantly greater tensile properties when compared with other three hydrogels. The tensile strength of ACPV1 (P=0.7138) was higher than ASPG1 and lower than ACPV2 (P=0.1213 respectively); however, the difference was statistically not significant. ASPG2 exhibited increased Young's modulus compared to

the other three hydrogels; however, the increase was statistically not significant (**Table 1**).

Biodegradation and Stability

Weight loss in ASPG1 hydrogel was minimal till day 10 when compared to the initial dry weight ($P>0.05$) followed by significant increase in weight loss as observed in days 20 and 30. A significant weight loss was shown by ASPG2 hydrogels in days 10 and 20; however, the weight loss after 20 days was statistically not significant ($P>0.05$). Minimal weight loss was observed in both ACPV1 and ACPV2 hydrogels till day 10 and was significantly increased in day 30 ($P<0.05$) (**Figure 15**). TDS showed gradual increase throughout the experiment which was significantly higher in day 30 when compared with day 1 ($P<0.05$) for both ACPV and ASPG hydrogels (**Table 2**). The pH was slightly acidic during the initial phase and turned to neutral or slightly alkaline on day 30 for both ACPV and ASPG hydrogels. The initial and final pH of the medium was statistically not significant ($p>0.05$). However, the variations were significant on day 10 and 20 when compared with day 1 for both ACPV and ASPG hydrogels ($p<0.05$) (**Table 2**). Biostability studies of the hydrogels in culture medium showed that all the hydrogels were stable in cell culture medium without exhibiting any disintegration.

Table 2: Biodegradation of ACPV and ASPG hydrogels showing the alterations in TDS and pH.

Hydrogel	TDS (ppm)	pH
DAY 1 (n=3)		
ACPV1	3582±0	7.1±0
ACPV2	3582±0	7.1±0
ASPG1	3582±0	7.1±0
ASPG2	3582±0	7.1±0
DAY 10 (n=3)		
ACPV1	4609±257.56	6.9±0.03
ACPV2	4453.3±198.84	6.9±0.10
ASPG1	4343.6±40.41	6.8±0.05
ASPG2	4137.3±1723.08	6.75±0.07
DAY 20 (n=3)		
ACPV1	5010.3±428.00	6.8±0.015
ACPV2	5213.3±328.51	6.85±0.02
ASPG1	5429.6±46.19	6.75±0.05
ASPG2	5399±519.07	6.80±0.005
DAY 30 (n=3)		
ACPV1	5864.3±596.98	7.08±0.06
ACPV2	5691.6±361.42	7.13±0.02
ASPG1	6041.3±462.83	7.03±0.15
ASPG2	6006±540.93	7.1±0

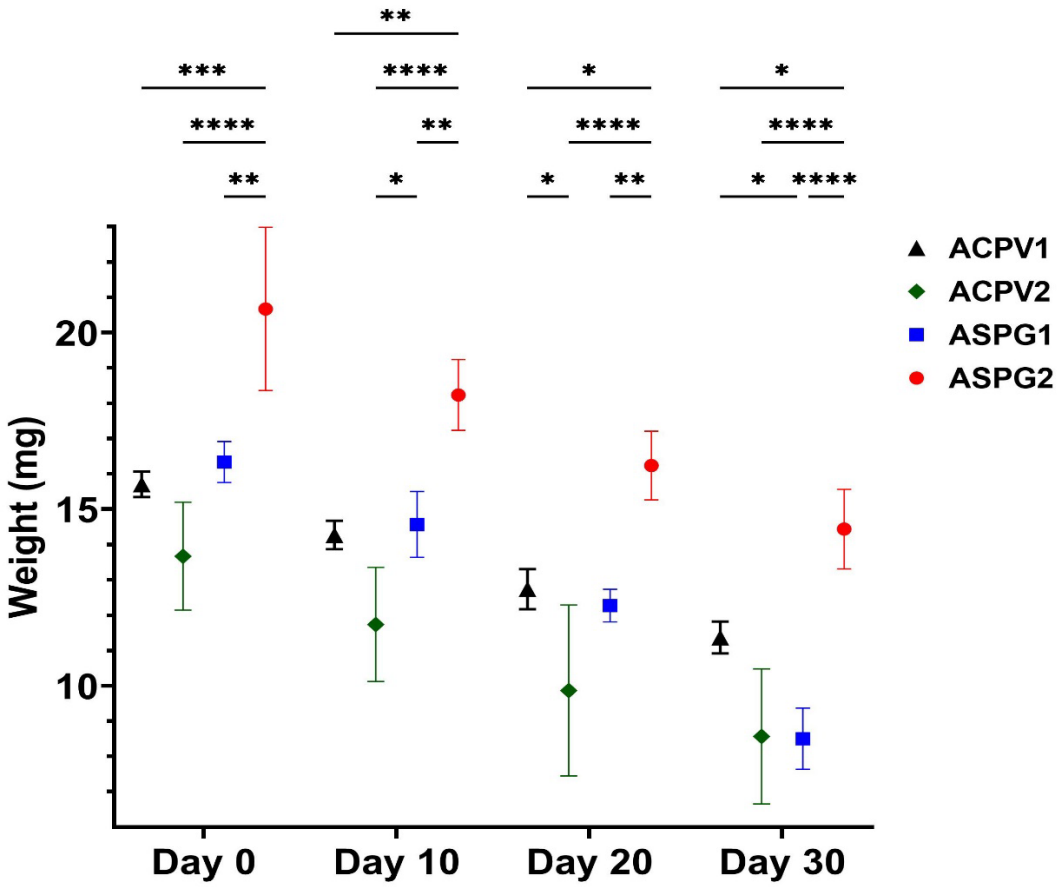

Figure 15: Biodegradation of ACPV and ASPG hydrogels showing the progressive loss in dry weight (*P<0.05, **P<0.01, ***P<0.001, ****P<0.0001, ns= not significant).

Examinations on Cell-material Interaction and Compatibility of the Hybrid Hydrogels

Protein Adsorption

The total proteins adsorbed on hydrogel surfaces were 41.05%, 49.4%, 75.4% and 46.7% for ACPV1, ACPV2, ASPG1 and ASPG2 respectively (**Table 1**). The level of protein adsorption was significantly higher (P=0.0466) ASPG1 hydrogel; however, was statistically not significant in ACPV1, ACPV2 and ASPG2 (P=0.2283, P=0.1036 and P=0.0752 respectively). SDS PAGE analysis revealed predominant albumin adsorption onto the surface of all hydrogels. The relative albumin adsorption was 60.33%, 53.75%, 50.17% and 56.25% respectively for ACPV1, ACPV2, ASPG1 and ASPG2 where plasma control presented 80.47% (**Figure 16**).

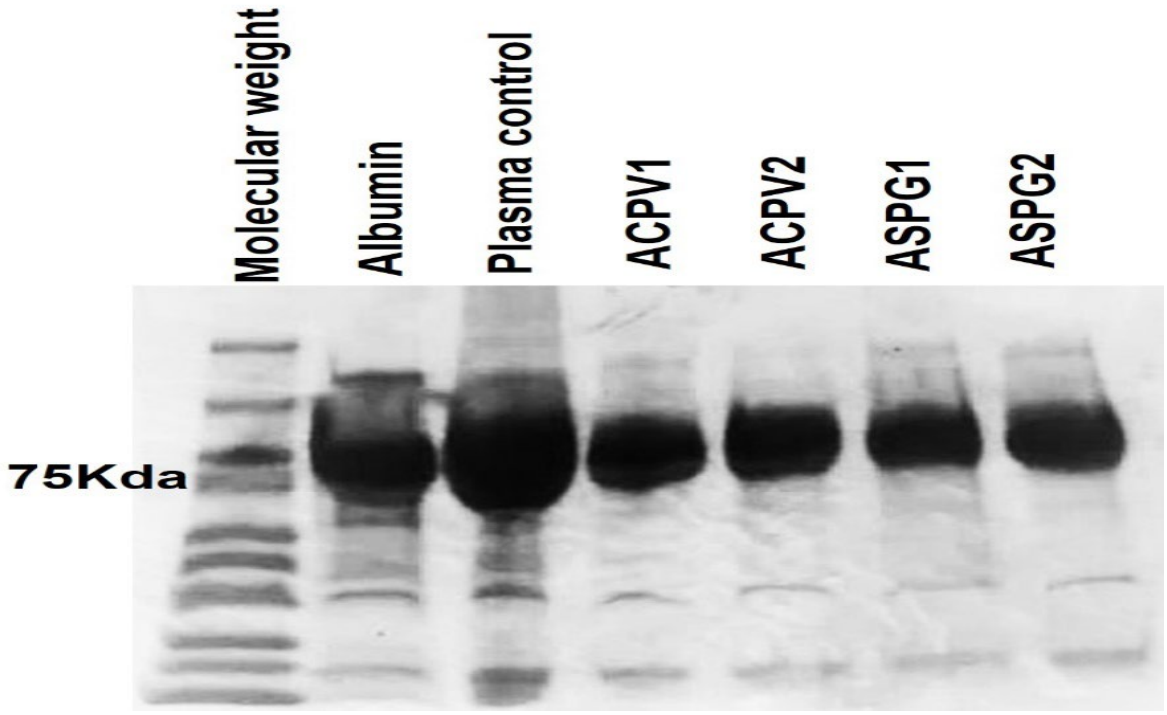

Figure 16: *SDS-PAGE analysis of hybrid hydrogels after treatment with plasma demonstrating the conspicuous band corresponding to adsorption of albumin in comparison with control plasma and bovine serum albumin.*

Cytocompatibility

The H9c2 cells on contact with ACPV and ASPG hydrogels retained their normal spindle morphology and deviation from the normal morphology was completely absent suggesting the non-toxic nature of the hydrogels revealing their biocompatibility (**Figures 17A-17E**). MTT assay using H9c2 cells cultured with hydrogel extract revealed the viability 82%, 105.37%, 89.12% and 104.75% for ACPV1, ACPV2, ASPG1 and ASPG2 respectively when compared with the control cells grown on 2D cell culture wells (**Figure 17F**). The difference in viability was statistically not significant among the groups ($p>0.05$).

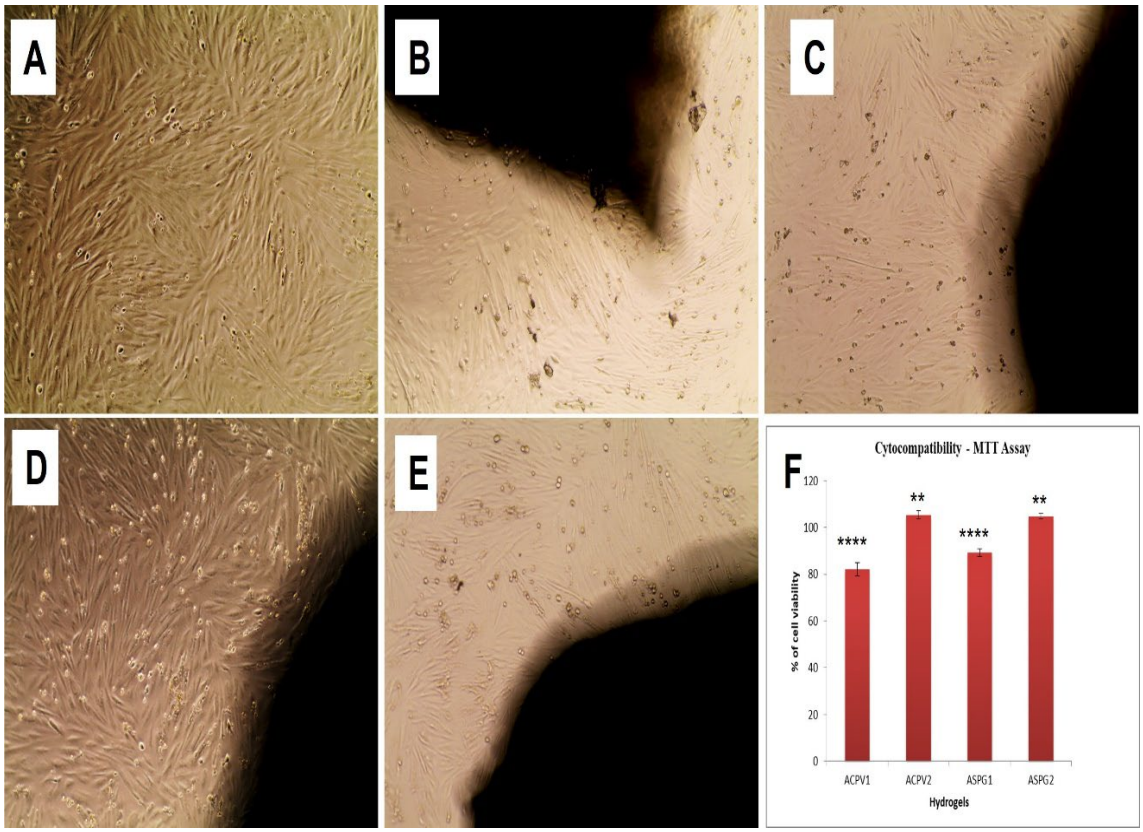

Figure 17: *Direct contact assay of hydrogels using H9c2 cells showing the biocompatibility: (A) Control, (B) ACPV1, (C) ACPV2, (D) ASPG1 and (E) ASPG2. (F) MTT assay using hydrogel extract treated H9c2 cells showing increased cell viability (*P<0.05, **P<0.01, ***P<0.001, ****P<0.0001).*

Cell-hydrogel Interaction

Cell adhesion

Both ACPV and ASPG hydrogels displayed adhesion and viability as evident from the FDA signals. Among the four systems, ASPG1 was superior in cell attachment and proliferation. The ACPV1, ACPV2 and ASPG2 displayed a moderate level of cell attachment. (**Figures 18A-18E**).

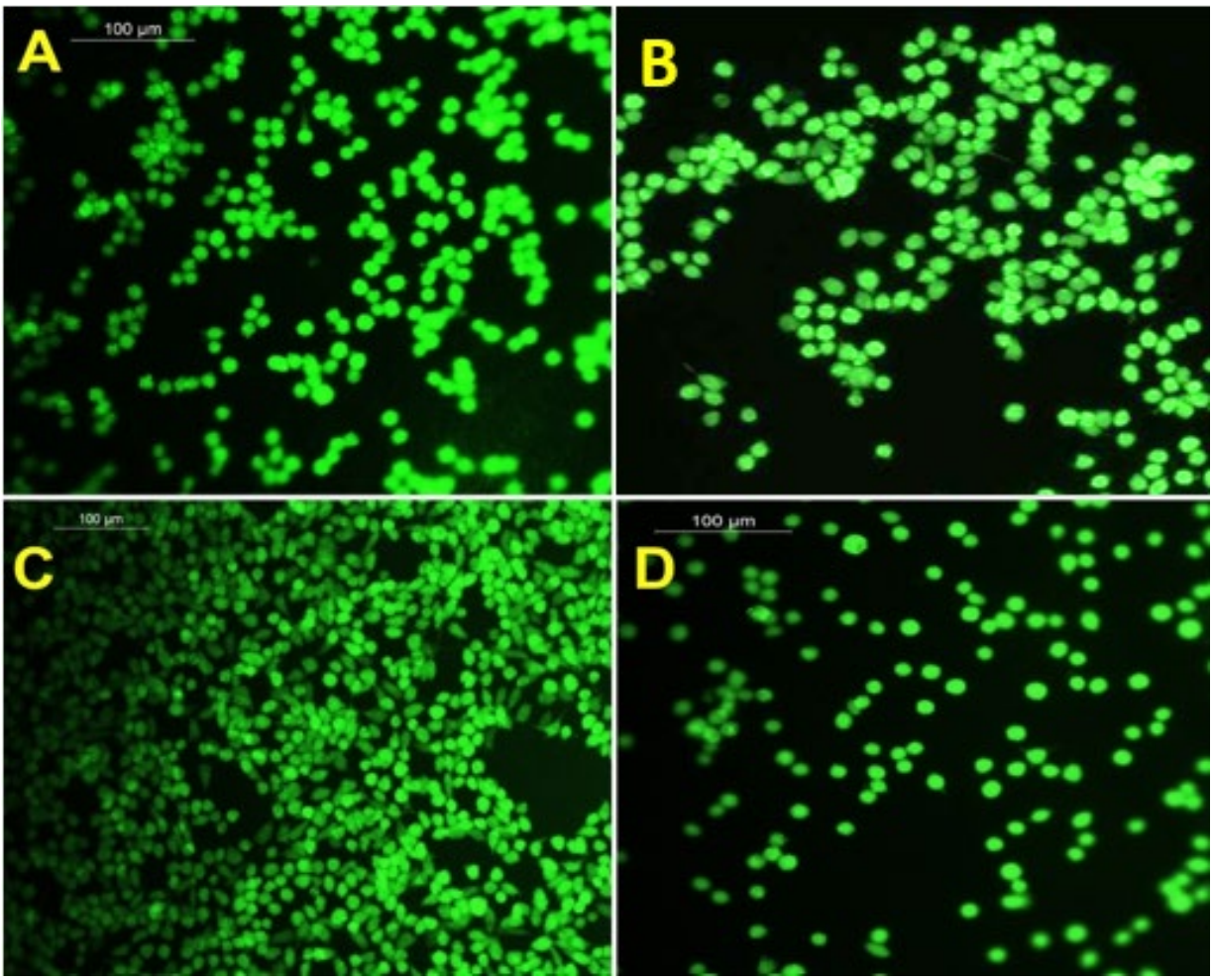

Figure 18: *Cell adhesin assay of hydrogels using H9c2 cells showing their healthy being: (A) ACPV1, (B) ACPV2, (C) ASPG1 and (D) ASPG2.*

Cell penetration

The penetration of H9c2 cells onto the ACPV and ASPG hydrogels were examined by Z-stack analysis the cells with DAPI which revealed the penetration depth

of 23.88 µm, 79.04 µm, 108.91 µm, 107.65 µm and 152.56 µm for control, ACPV1, ACPV2, ASPG1 and AGPG2 hydrogels, respectively. The cell penetration was superior in both the ACPV and ASPG hydrogels compared to the control where ASPG hydrogels displayed increased penetration depth than ACPV1 (**Figures 19A-19J**).

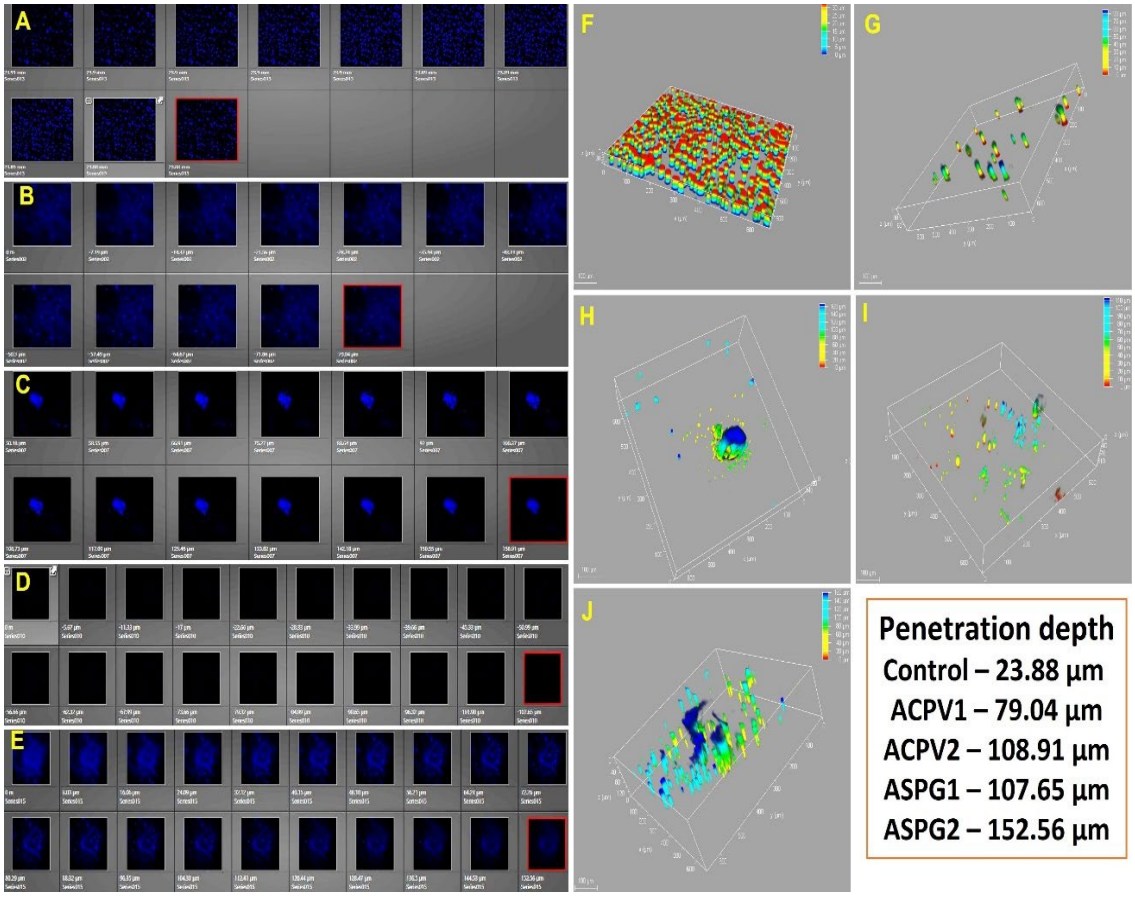

Figure 19: *The gallery images of Z-stacks representing the infiltration of H9c2 cells stained with DAPI toward the interior of (A) Control, (B) ACPV1, (C) ACPV2, (D) ASPG1 and (E) AGPG2 hydrogels respectively. 3D renders of (F) Control, (G) ACPV1, (H) ACPV2, (I) AGPG1 and (J) ASPG2 hydrogels were obtained from the Z-stack visualization of the penetration depth of H9c2 cells.*

Biological Responses of Biosynthetic Hydrogels for CTE

Antimicrobial Efficiency

ACPV and ASPG hydrogel subsets loaded with varying doses of amikacin and vancomycin displayed significantly increased zone of inhibition against Gram positive and Gram-negative bacteria when compared with the control (**Table 3**) (**Figure 20A-20P**). Statistically significant increase in the zone of inhibition was observed between ACPV1(5_{Ami}) and ASPG1(5_{Ami}). However, the variations in zone of inhibition were statistically not significant for the other hydrogels incorporated with 5, 10 and 20µl of amikacin ($p>0.05$). In addition, ACPV1(5_{Vanc}) showed significant difference ($p<0.05$) between ACPV2(5_{Vanc}) and ASPG1(5_{Vanc}); however, was statistically not significant compared to ACPV1(5_{Vanc}) and ASPG2(5_{Vanc}) ($p>0.05$). Similarly, ACPV2(5_{Vanc}) displayed significantly increased zone of inhibition compared to ASPG1(5_{Vanc}) and ASPG2(5_{Vanc}) ($p<0.05$); however, ASPG1(5_{Vanc}) and ASPG2(5_{Vanc}) displayed similar trend. ACPV1(10_{Vanc}) and ACPV2(10_{Vanc}) exhibited significant increase in zone of inhibition when compared with ASPG1(10_{Vanc}) and ASPG2(10_{Vanc}) ($p<0.05$); however, the zone of inhibition among ACPV1(10_{Vanc}) and ACPV2(10_{Vanc}) and ASPG1(10_{Vanc}) and ASPG2(10_{Vanc}) were statistically not significant ($p>0.05$). Also, non-significant variation was observed for all the hydrogels incorporated with 20µl of vancomycin ($p>0.05$).

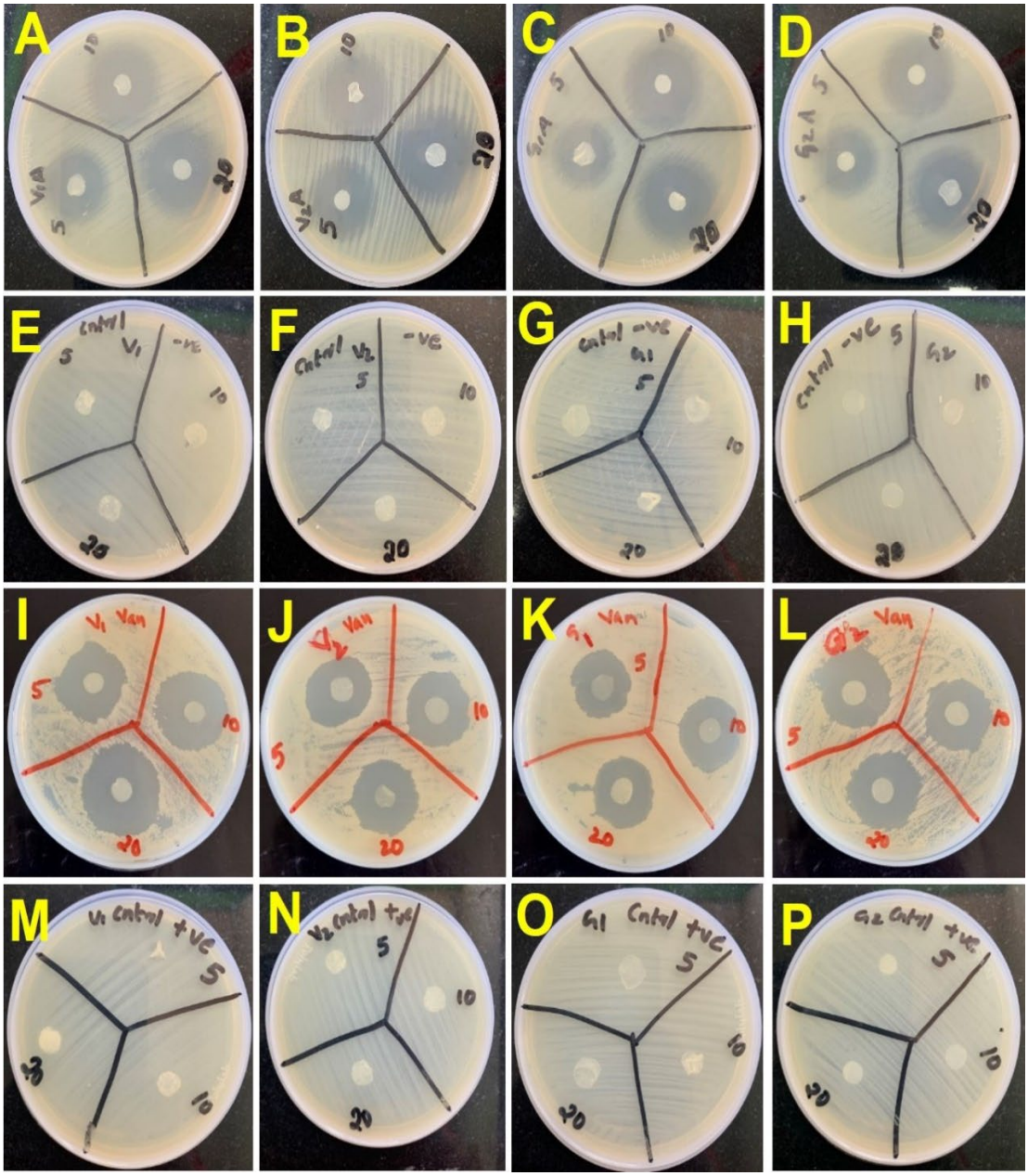

Figure 20: *Antibiotic releasing efficiency of ACPV and ASPG hybrid hydrogel scaffolds (A) ACPV1 incorporated with different concentrations of amikacin (B) ACPV2 incorporated with different concentrations of amikacin (C) ASPG1 incorporated with different concentrations of amikacin, (D) ASPG2 incorporated with different concentrations of amikacin, (E) ACPV1 control for amikacin (F) ACPV2 control for amikacin (G) ASPG1 control for amikacin (H) ASPG2 control for amikacin (I) ACPV1 incorporated with different concentrations of vancomycin (J) ACPV2 incorporated with different concentrations of vancomycin (K) ASPG1 incorporated with different concentrations of vancomycin (L) ASPG2 incorporated with different concentrations of vancomycin (M) ACPV1 control for vancomycin (N) ACPV2 control for vancomycin (O) ASPG1 control for vancomycin (P) ASPG2 control for vancomycin.*

Table 3: Antimicrobial efficiency of Amikacin and Vancomycin loaded hydrogels revealing the zone of inhibition (cm).

Hydrogel	Amikacin			Vancomycin		
	5µG/ML	**10 µG/ML**	**20µG/ML**	**5µG/ML**	**10µG/ML**	**20µG/ML**
ACPV1	2.37±0.05	2.47±0.05	2.73±0.11	2.53±0.11	3.03±0.05	3.16±0.05
ACPV2	2.3±0.10	2.53±0.11	2.87±0.05	2.87±0.05	3.2±0.20	3.06±0.05
ASPG1	2.06±0.05	2.53±0.05	2.66±0.05	2.2±0.10	2.63±0.05	2.96±0.15
ASPG2	2.23±0.11	2.47±0.11	2.76±0.05	2.3±0.20	2.63±0.11	3.06±0.05

Studies on Antioxidant Response

In cell free system

DPPH scavenging was significantly decreased in the ACPV1 ($P<0.0001$), ACPV2 ($P<0.0001$), ASPG1 ($P<0.0001$) and ASPG2 ($P<0.0001$); however, was comparable with untreated control. Similar level of scavenging was observed for ACPV1, ACPV2, ASPG1 and ASPG2 and were statistically not significant (**Figure 21A**). Additionally, NO scavenging was significantly decreased in the ACPV1 ($P<0.0001$), ACPV2 ($P<0.0001$), ASPG1 ($P<0.0001$) and ASPG2 ($P<0.0001$) compared with the ascorbic acid control. ACPV1 displayed increased scavenging and ACPV2 exhibited decreased scavenging among the four hydrogels whereas ASPG1 and ASPG2 displayed similar levels of NO scavenging (**Figure 21B**).

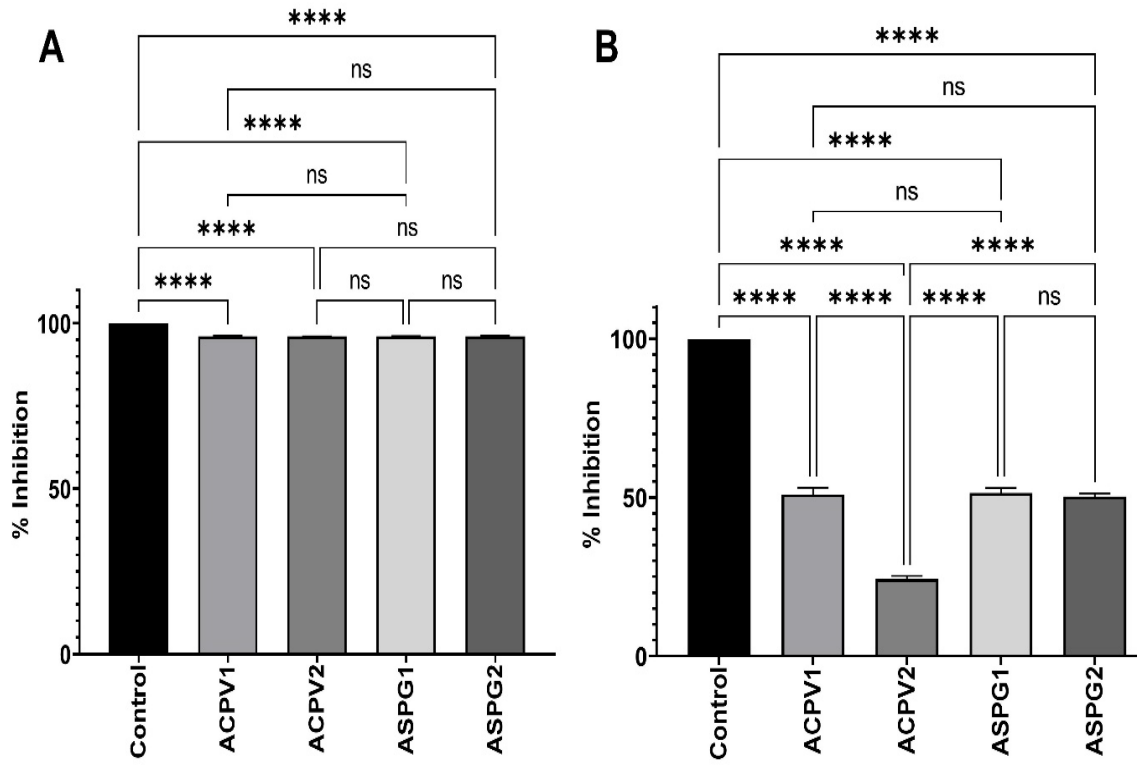

Figure 21: *Bar diagram showing the (A) DPPH and (B) NO scavenging activities of ACPV1, ACPV2, ASPG1 and ASPG2 compared to the respective controls. (**** P<0.0001, ns – non-significant).*

In cellular system

Direct contact oxidative stress

The level of oxidative stress was significantly increased in the H_2O_2 treatment group compared to the control (P<0.0001). The antioxidant potential of hydrogels was exhibited by the significantly decreased level of oxidative stress in ACPV1 (P<0.0001), ACPV2 (P<0.0001), ASPG1 (P<0.0001) and ASPG2 (P<0.0001) treated RAW 267.4 cells compared to H_2O_2 treatment group where the maximum effect was displayed by ACPV2 (**Figure 22A-22B**).

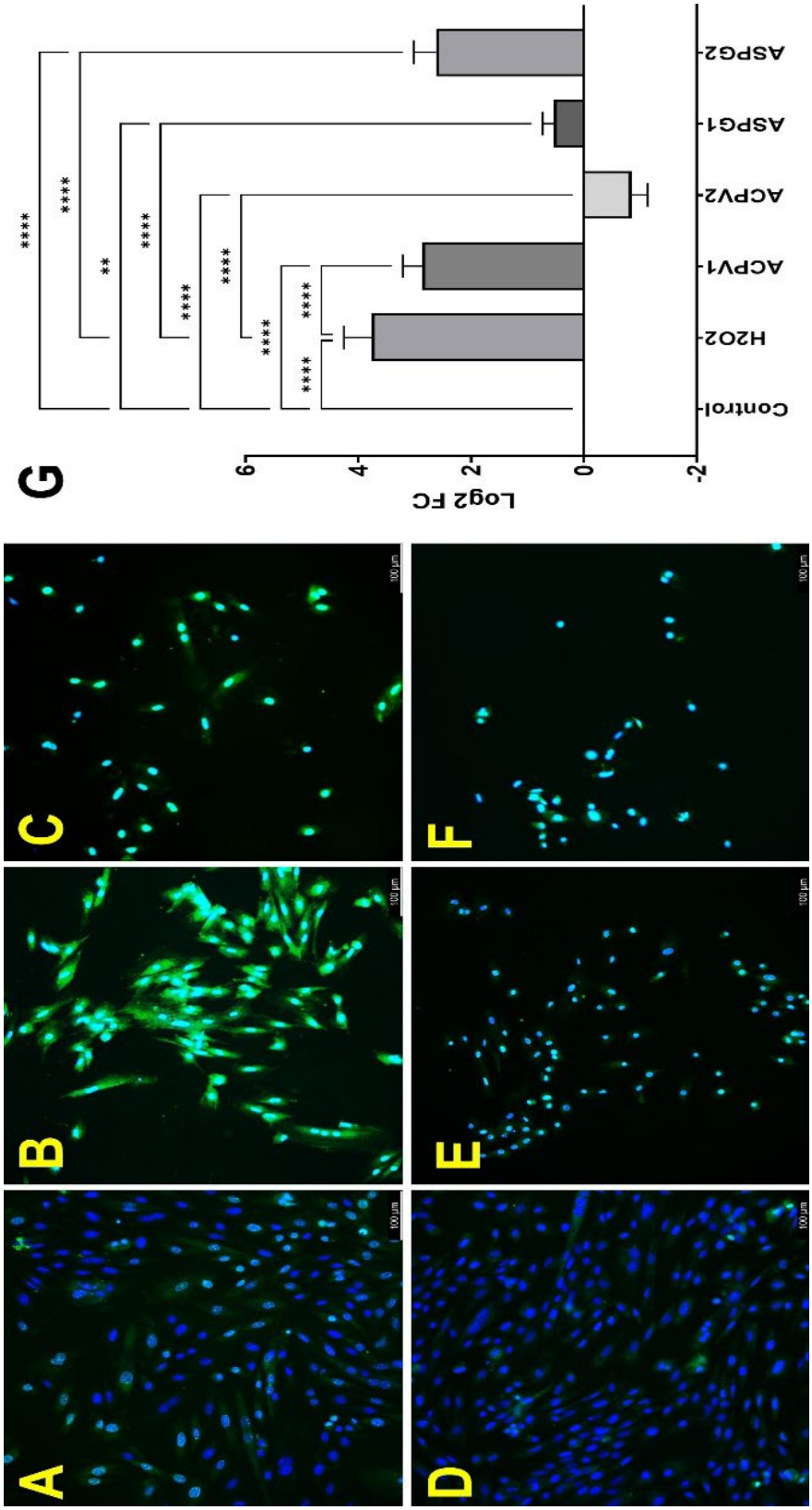

Figure 22: *Cell-ROX assay of hydrogels using RAW267.4 cells showing the antioxidant nature: (A) Control, (B) H2O2, (C) ACPV1, (D) ACPV2, (E) ASPG1 and (F) ASPG2. (G) Bar diagram showing the comparison of antioxidant effects of ACPV and ASPG hybrid hydrogel scaffolds. (*P<0.05, **P<0.01, ***P<0.001, ****P<0.0001)*

Studies on Immunocompatibility and Gene Interactions

Direct contact assay

The toxicity and the macrophage activation of the ACPV and ASPG hydrogels under the direct influence of cell contact was determined by direct contact assay. The RAW267.4 cells on contact with ACPV and ASPG hydrogels retained their normal morphology and deviation from the normal morphology was completely absent suggesting the absence of macrophage activation revealing their immunocompatibility (**Figures 23A-23E**).

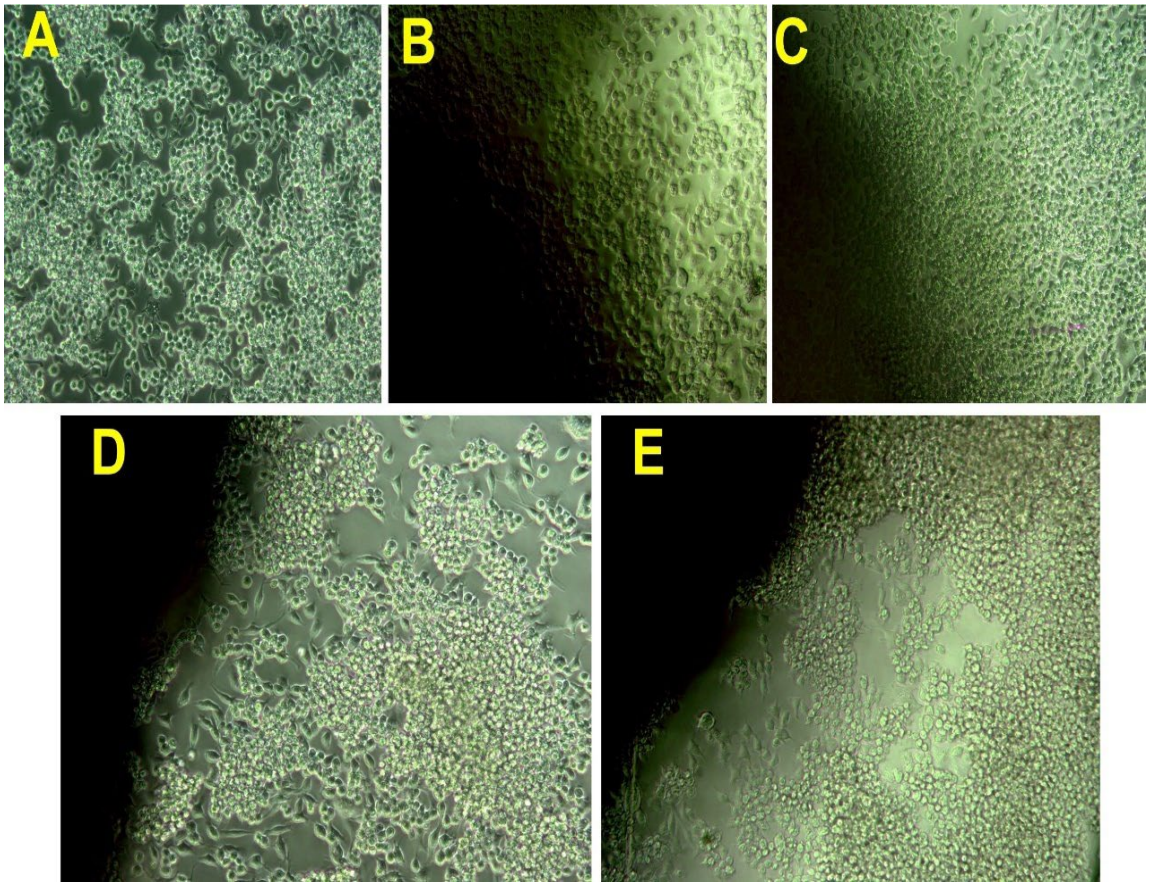

Figure 23: *Direct contact assay of hydrogels using RAW264.7 cells showing the immunocompatibility: (A) Control, (B) ACPV1, (C) ACPV2, (D) ASPG1 and (E) ASPG2.*

Immunofluorescence

The level of IL6 was significantly increased in the LPS group compared to the normal control (P=0.0007). Interestingly, ACPV1 and ACPV2 displayed a significantly decreased expression of IL6 compared to the LPS control; however, ASPG1 and ASPG2 displayed significantly increased expression (**Figures 24A and 24B**). The expression level of TNFα was significantly increased in the LPS control compared to the normal control (P<0.0001). ASPG1displayed significantly decreased (P<0.0001) expression of TNFα; however, the alteration in ASPG2 (P=0.6825) was statistically not significant compared to the LPS group. Interestingly, ACPV1 (P<0.0001) and ACPV2 (P<0.0001) displayed a significantly decreased expression of TNFα (P<0.0001) compared to the LPS control where the level of TNFα in ACPV2 (P<0.0001) was significantly lower than the control (**Figures 25A and 25B**). The expression level of NFκB was significantly increased in the LPS control compared to the normal control (P<0.0001). The level of NFκB was significantly lower in ASPG1 (P<0.0001), ACPV1 (P<0.0001) and ACPV2 (P<0.0001) than LPS and control groups whereas ASPG2 (P=0.0005) displayed significantly increased expression of NFκB than LPS; however, was increased compared to the control (P=0.0053) (**Figures 26A and 26B**). The expression level of IKB was significantly increased in the LPS control compared to the normal control (P<0.0001). The level of IKB was significantly decreased in ASPG2 (P<0.0001) and ACPV2 (P<0.0001) than LPS group; however, the decrease was statistically not significant in ASPG1 (P=0.1475) and ACPV1 (P=0.0968). All the hydrogels displayed significantly increased level of IKB compared to the control (**Figures 27A and 27B**). The expression level of IL10 was significantly increased in the LPS control compared to the normal control (P<0.0001). The level of IL10 was significantly decreased in ASPG1 (P=0.0018), ASPG2 (P=0.0004), ACPV1 (P<0.0001) and ACPV2 (P<0.0001) than LPS group. All

the hydrogels except ACPV2 displayed significantly increased level of IL10 compared to the control (**Figures 28A and 28B**). The expression level of TGFβ was significantly increased in the LPS control compared to the normal control ($P<0.0001$). The level of TGFβ was decreased in ASPG1 ($P=0.0003$) and ACPV1 ($P<0.0001$) than LPS group; however, was statistically not significant in ASPG2 ($P=0.9604$) and ACPV2 ($P=0.8500$). All the hydrogels displayed significantly increased level of TGFβ compared to the control (**Figures 29A and 29B**).

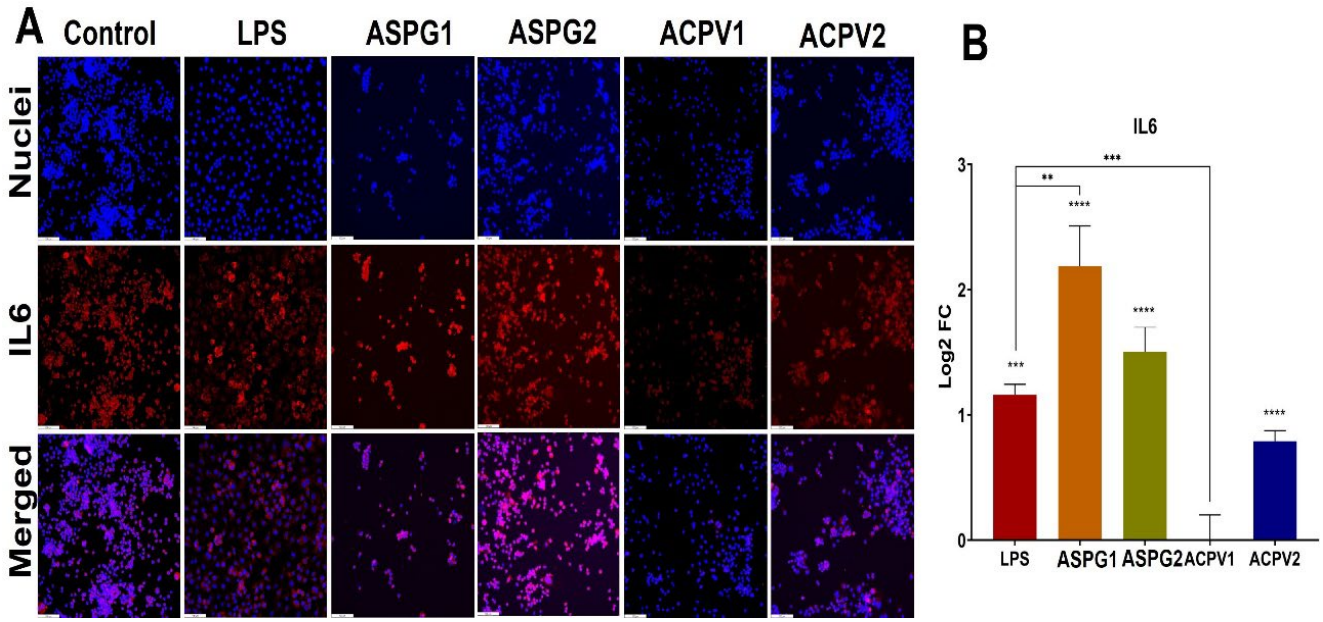

Figure 24: *(A) Representative images for the immunofluorescence analysis for the expression of IL6 in the RAW264.7 cells (N=3) following the treatment ACPV and ASPG hydrogels and (B) the quantification of protein expression of IL6 in the RAW264.7 cells calculated from MFI. Immunofluorescence images in the left column show nuclear staining with DAPI; the images in the middle column show expression of IL6 and the images in the right column show overlay of IL6 staining with DAPI. Images were acquired at 20x magnification. (**** P<0.0001, *** P<0.001, ** P<0.01).*

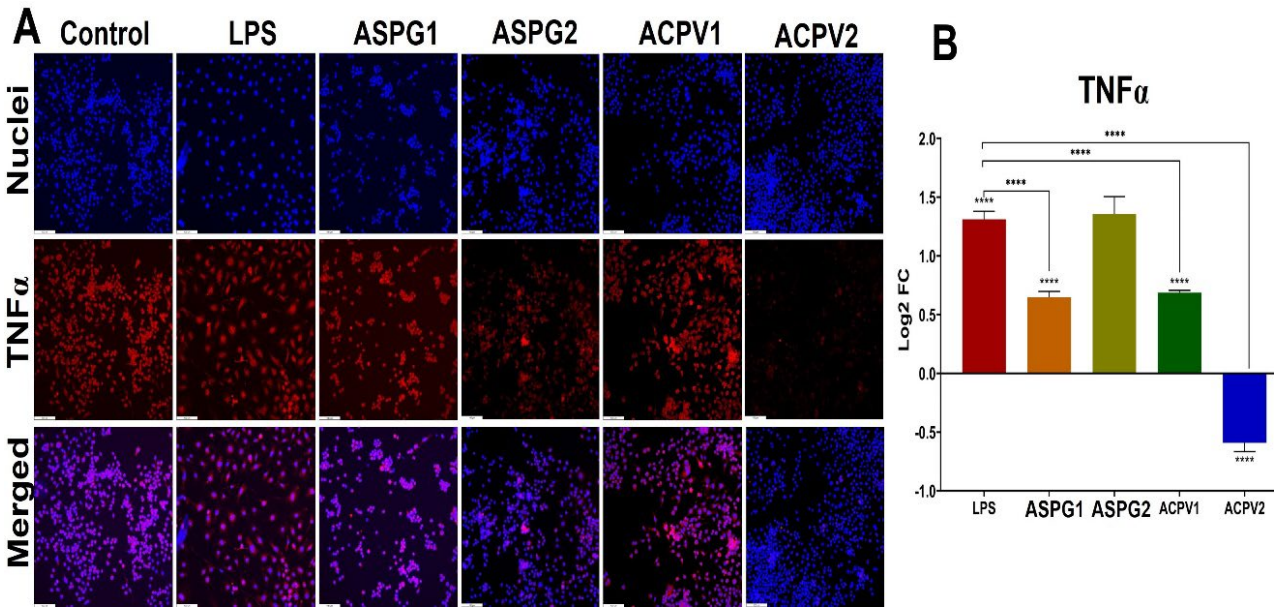

Figure 25: *(A) Representative images for the immunofluorescence analysis for the expression of TNFα in the RAW264.7 cells (N=3) following the treatment ACPV and ASPG hydrogels and (B) the quantification of protein expression of TNFα in RAW264.7 calculated from MFI. Immunofluorescence images in the left column show nuclear staining with DAPI; the images in the middle column show expression of TNFα and the images in the right column show overlay of TNFα staining with DAPI. Images were acquired at 20x magnification. (**** P<0.0001 and unlabelled groups represent NS).*

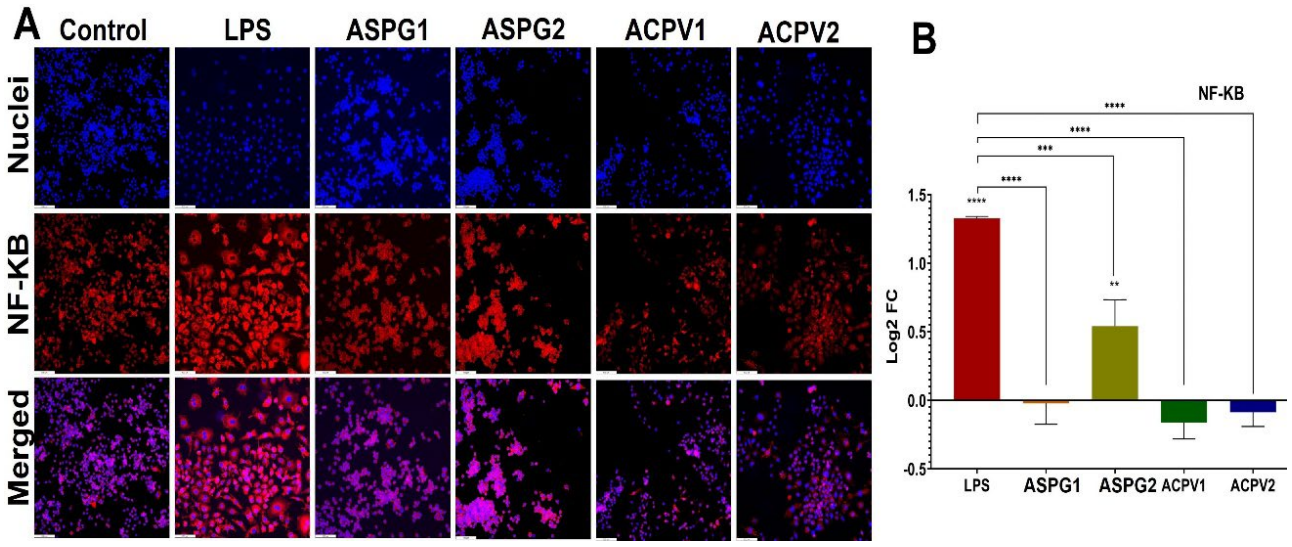

Figure 26: *(A) Representative images for the immunofluorescence analysis for the expression of NFkβ in the RAW264.7 cells (N=3) following the treatment ACPV and ASPG hydrogels and (B) the quantification of protein expression of NFkβ in RAW264.7 calculated from MFI. Immunofluorescence images in the left column show nuclear staining with DAPI; the images in the middle column show expression of NFkβ and the images in the right column show overlay of NFkβ staining with DAPI. Images were acquired at 20x magnification. (**** P<0.0001 and unlabelled groups represent NS).*

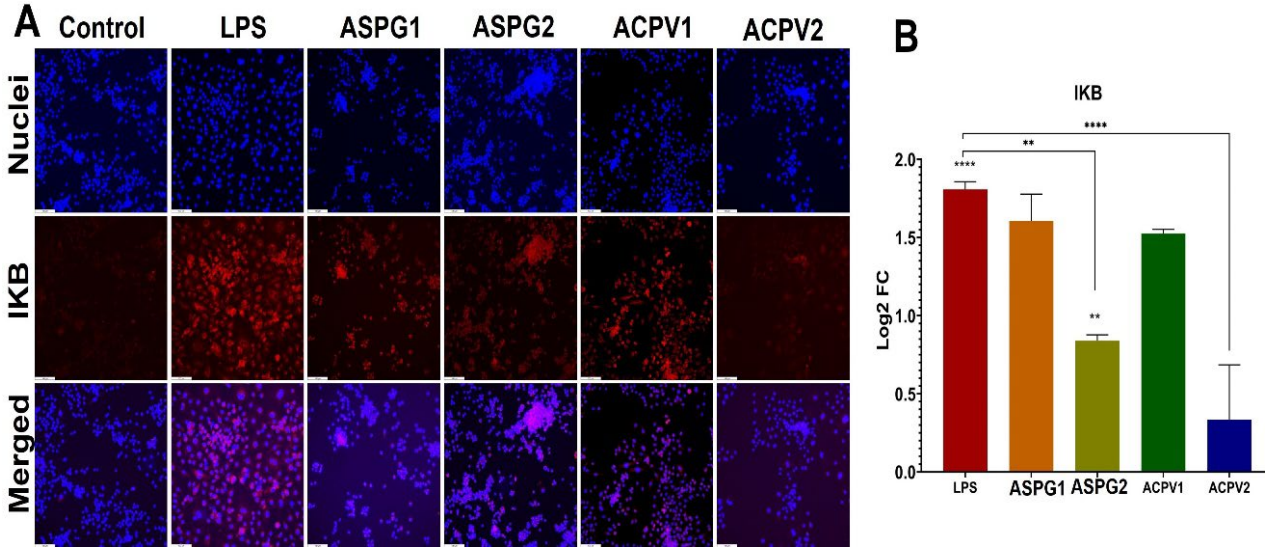

Figure 27: *(A) Representative images for the immunofluorescence analysis for the expression of IKB in the RAW264.7 cells (N=3) following the treatment ACPV and ASPG hydrogels and (B) the quantification of protein expression of IKB in RAW264.7 calculated from MFI. Immunofluorescence images in the left column show nuclear staining with DAPI; the images in the middle column show expression of IKB and the images in the right column show overlay of IKB staining with DAPI. Images were acquired at 20x magnification. (**** P<0.0001, ** P<0.01 and unlabeled groups represent NS).*

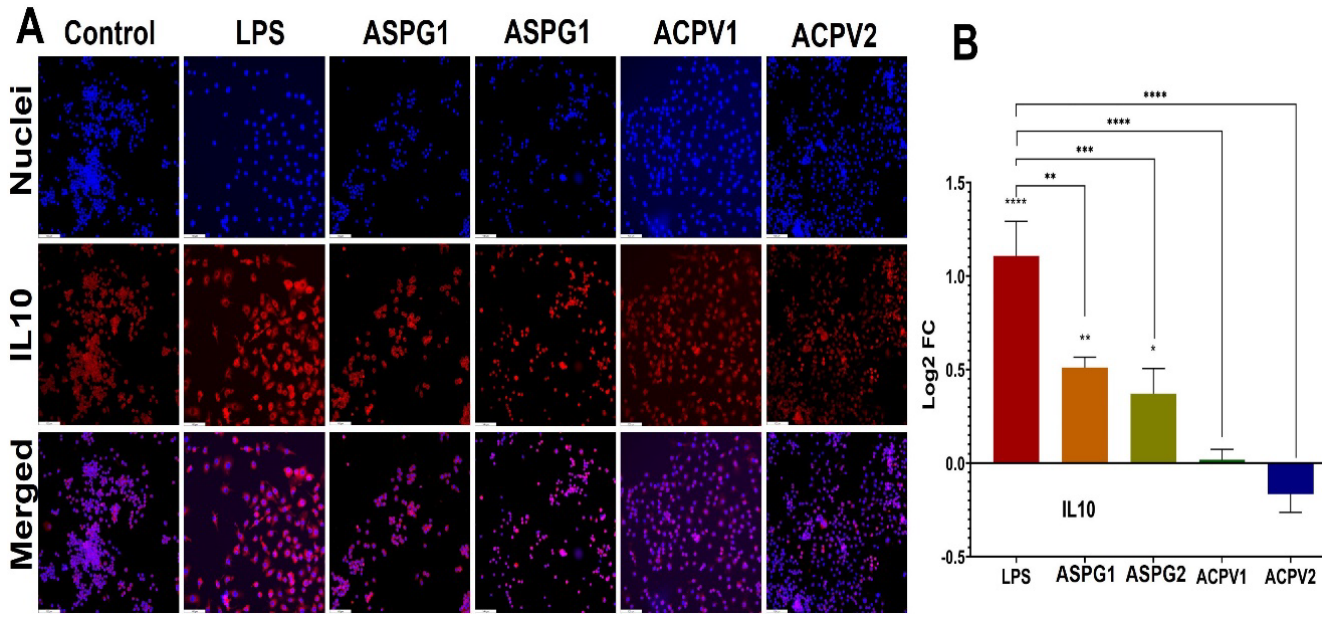

Figure 28: *(A) Representative images for the immunofluorescence analysis for the expression of IL10 in the RAW264.7 cells (N=3) following the treatment ACPV and ASPG hydrogels and (B) the quantification of protein expression of IL10 in RAW264.7 calculated from MFI. Immunofluorescence images in the left column show nuclear staining with DAPI; the images in the middle column show expression of IL10 and the images in the right column show overlay of IL10 staining with DAPI. Images were acquired at 20x magnification. (**** P<0.0001, ** P<0.01 and unlabelled groups represent NS).*

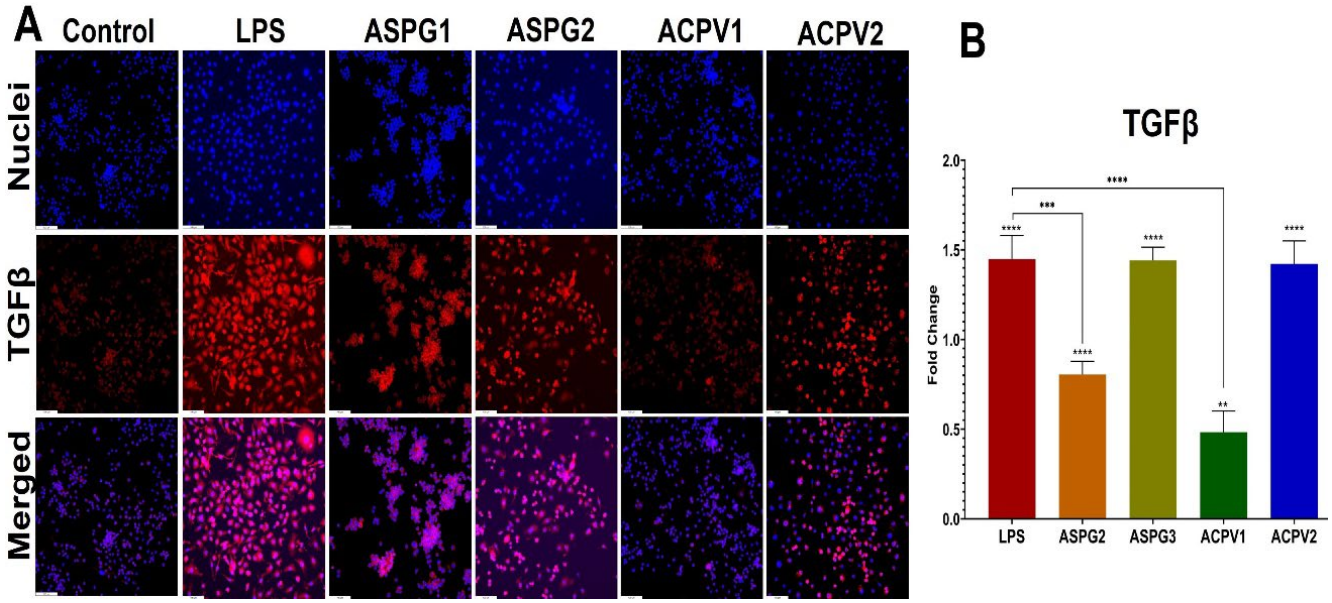

Figure 29*: (A) Representative images for the immunofluorescence analysis for the expression of TGFβ in the RAW264.7 cells (N=3) following the treatment ACPV and ASPG hydrogels and (B) the quantification of protein expression of TGFβ in RAW264.7 calculated from MFI. Immunofluorescence images in the left column show nuclear staining with DAPI; the images in the middle column show expression of TGFβ and the images in the right column show overlay of TGFβ staining with DAPI. Images were acquired at 20x magnification (**** P<0.0001, *** P<0.001, ** P<0.01 and unlabelled groups represent NS).*

Gene interactions and network analysis

The genes interconnected with six proteins (IL6, NF-Kβ, IL-10, TGF-β, TNF-α and IKβ) were constituted the subnetworks composed of 370 genes (**Figure 30A**) (**Table 4**). These 370 genes are associated with 120 pathways involving various biological processes; especially the pathways associated with, regulation of metabolic process, pro-survival events and signal transduction (**Figure 30B**) (**Table 5**). The volcano plot revealed that intra cellular protein kinase cascade, positive regulation of metabolic processes and regulation of apoptosis to be the most prevalent pathways involved by the interconnected genes (**Figure 30C**).

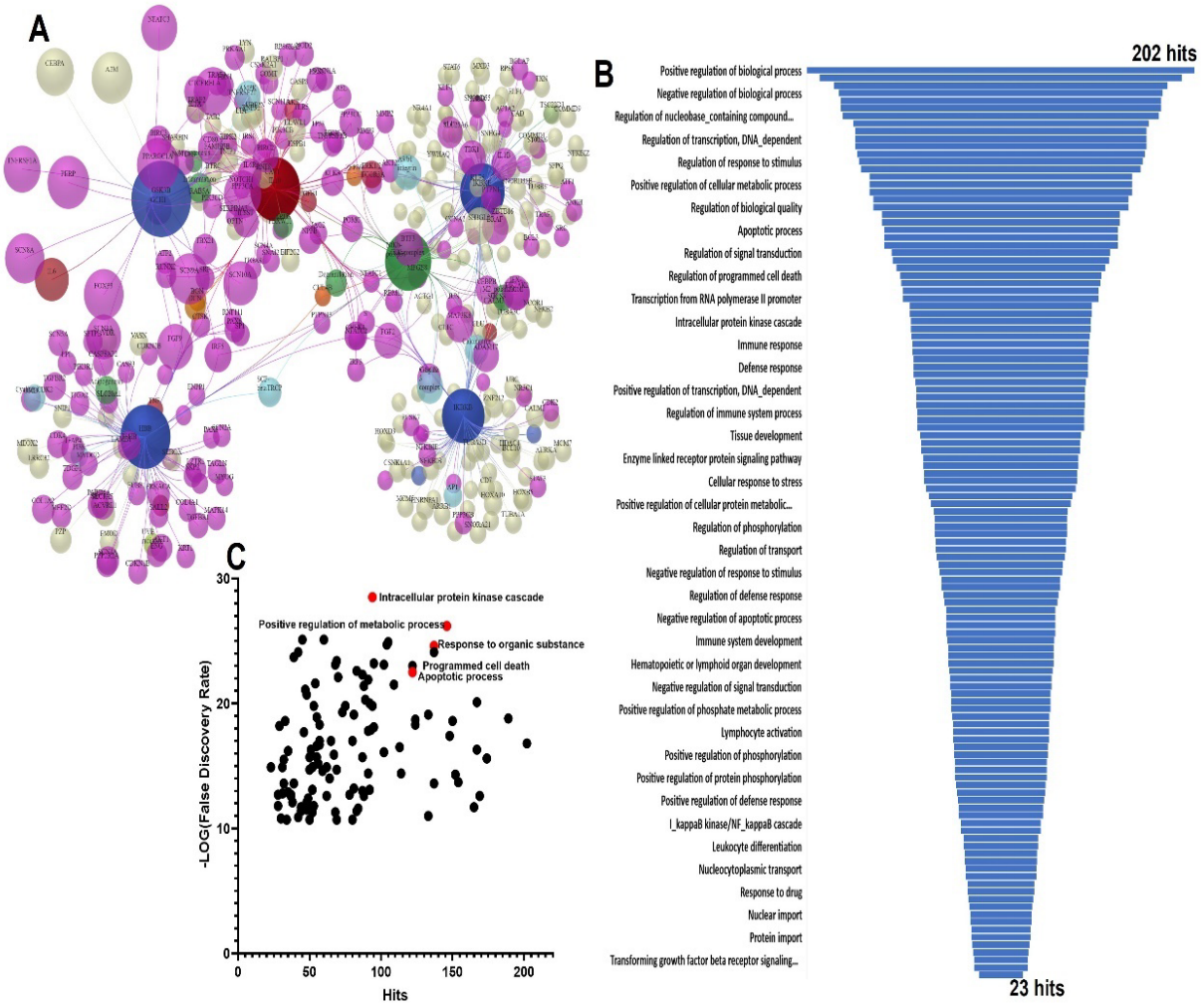

Figure 30: *(A) Network visualization showing the interconnecting network of the genes IL6, NF-Kβ, IL-10, TGF-β, TNF-α and IKβ. (B) Funnel diagram displaying the total interactions for each biological process connected to the input genes based on GO:BP database (P<0.05 for all hits). (C) Volcano plot showing the key biological processes based on the -Log (FDR).*

Table 4: The genes interconnected with IL6, NF-Kβ, IL-10, TGF-β, TNF-α and IKβ. (*Deg - Degree)

Gene Id	Label	*Deg
4790	IKBKE	119
7124	IL10	96
4792	IKBKB	87
7040	HBB	77
3569	IKK-complex	29
3586	GSK3B	26
SIGNOR-C13	CHEK1	5
6774	IRF5	3
29110	MFGE8	3
1147	NFATC1	3
5966	NfKb-p65/p50	3
6885	RBM10	3
5970	M2_polarization	3
8450	CUL4B	2
6667	PTPN13	2
7538	ZFP36	2
330	MMP2	2
329	MMP9	2
4851	AKT2	2
208	FCGR3A	2
1432	NFATC2	2
23291	S	2
7132	IRF3	2
6722	PTPN1	2
1634	DCN	2
633	BGN	2
3043	SRF	2
3039	SP1	2
SIGNOR-PH97	ATF2	2
4023	PAX6	2
SIGNOR-C156	RNF111	2
5294	RUNX2	2
SIGNOR-PH46	CTSK	2
7157	SCF-betaTRCP	2
3663	TBX21	2
6336	AMPK	2
11280	GCH1	2
6323	IL6R	2
6326	IL6ST	2
6328	Inflammation	2
6329	BIRC2	2
6331	BIRC3	2
6334	CD80	2
6335	CTCF	2
9611	NCOR1	2
7278	TUBA3C	2
9021	SOCS3	2
808	CALM3	2
3551	JUN	2
801	CALM1	2
1191	CLU	2
6188	RPS3	2
4791	NFKB2	2
71	ACTG1	2
1213	CLTC	2
2908	NFKB1	2
8841	HDAC3	2
P59594	Degranulation	2
CHEBI:3638	POMC	2
SIGNOR-PH92	PPP3CC	2
SIGNOR-C166	ERK1/2	2
2643	KLK3	2
SIGNOR-PH12	NPPB	2
3570	IL1B	1
3587	IL6	1
1050	CEBPA	1
7295	TXN	1
1326	ITGB8	1
1997	ELF1	1
1831	TSC22D3	1
4221	MEN1	1
1244	ABCC2	1
4794	KLF4	1
7175	TPR	1
10987	COPS5	1
23054	NCOA6	1
9532	BAG2	1
5716	PSMD10	1
602	LCK	1
1832	DSP	1
3164	NR4A1	1
2752	GLUL	1
92609	TIMM50	1

7536	SF1	1
7431	VIM	1
5468	PPARG	1
54951	COMMD8	1
10636	RGS14	1
10891	LTBP1	1
84557	MAP1LC3A	1
3313	HSPA9	1
3146	HMGB1	1
8648	NCOA1	1
51397	COMMD10	1
54971	BANP	1
5092	PCBD1	1
7846	TUBA1A	1
3065	HDAC1	1
26259	FBXW8	1
9883	POM121	1
9759	HDAC4	1
823	CAPN1	1
3305	HSPA1L	1
7988	ZNF212	1
5971	RELB	1
8915	BCL10	1
3206	HOXA10	1
6790	AURKA	1
7052	TGM2	1
3215	HOXB5	1
805	CALM2	1
3178	HNRNPA1	1
6195	RPS6KA1	1
79191	IRX3	1
619505	SNORA21	1
25	ABL1	1
3232	HOXD3	1
580	BARD1	1
409	ARRB2	1
10382	TUBB4A	1
924	CD7	1
1	A1BG	1
51341	ZBTB7A	1
9349	RPL23	1
301	ANXA1	1
468	ATF4	1
219541	MED19	1
8518	IKBKAP	1
1316	KLF6	1

11167	FSTL1	1
50855	PARD6A	1
7046	MAP3K7	1
79753	SNIP1	1
2331	FMOD	1
2022	MC1R	1
2615	LRRC32	1
3912	LAMB1	1
7421	VDR	1
5858	PZP	1
1994	ELAVL1	1
7186	TRAF2	1
27161	EIF2C2	1
841	CASP8	1
81858	SHARPIN	1
10133	OPTN	1
90268	FAM105B	1
4049	LTA	1
55072	RNF31	1
10928	RALBP1	1
10318	TNIP1	1
9025	RNF8	1
2	A2M	1
94	ACVRL1	1
291	SLC25A4	1
293	SLC25A6	1
307	ANXA4	1
408	ARRB1	1
688	KLF5	1
708	C1QBP	1
790	CAD	1
857	CAV1	1
998	CDC42	1
1452	CSNK1A1	1
1499	CTNNB1	1
1869	E2F1	1
1917	EEF1A2	1
2033	EP300	1
2280	FKBP1A	1
3064	HTT	1
3066	HDAC2	1
3185	HNRNPF	1
3192	HNRNPU	1
3212	HOXB2	1
3315	HSPB1	1
3840	KPNA4	1

4052	NFKBIA	1
4067	LYN	1
4174	MCM5	1
4176	MCM7	1
4223	MEOX2	1
4627	MYH9	1
4670	HNRNPM	1
4793	NFKBIB	1
4841	NONO	1
5371	PML	1
5442	POLRMT	1
5531	PPP4C	1
5783	NFKBIE	1
5868	RAB5A	1
6202	RPS8	1
6421	SFPQ	1
6456	SH3GL2	1
6778	STAT6	1
7133	RPS6KA2	1
7316	UBC	1
7334	UBE2N	1
7528	YY1	1
7704	ZBTB16	1
8110	DPF3	1
8193	DPF1	1
8451	CUL4A	1
8454	CUL1	1
8655	DYNLL1	1
8717	TRADD	1
8772	FADD	1
8945	BTRC	1
9043	SPAG9	1
9093	DNAJA3	1
9612	NCOR2	1
9782	MATR3	1
9908	SIRT6	1
10454	TAB1	1
10477	UBE2E3	1
10627	MYL12A	1
10892	MALT1	1
10971	YWHAQ	1
11345	GABARAPL2	1
22984	PDCD11	1
23118	TAB2	1
26811	SNORD55	1
27043	PELP1	1

29099	COMMD9	1
51295	ECSIT	1
51400	PPME1	1
51678	MPP6	1
57805	KIAA1967	1
64332	NFKBIZ	1
83463	MXD3	1
84617	TUBB6	1
94163	SNORD38B	1
113457	TUBA3D	1
114990	VASN	1
150684	COMMD1	1
347733	TUBB2B	1
645832	SEBOX	1
724102	SNHG4	1
2932	SRC	1
9641	STAG2	1
SIGNOR-C14	STAT3	1
3553	TBK1	1
3696	TNF	1
3725	TDGF1	1
9314	TGFB1	1
3932	TLR8	1
SIGNOR-PH55	TNFRSF1A	1
4157	TP53	1
4240	TRAF3	1
4313	UVB radiation	1
4318	CASP3	1
4772	Caspase 3 complex	1
4773	CEBPB	1
5770	chloroquine	1
8241	CHUK	1
6196	CREB1	1
SIGNOR-C5	CRP	1
51548	CSNK2A1	1
6714	doramapimod	1
10735	FBN1	1
30009	FOXP3	1
6997	HBA1	1
51311	IL1A	1
7187	NFATC3	1
SIGNOR-ST17	NOTCH1	1
836	NR3C1	1
SIGNOR-C221	PCSK7	1
1051	PERP	1

1111	Phagocytosis	1
1385	PPARGC1A	1
1401	PPP3CA	1
1457	PPP3CB	1
CHEBI:40953	PRKAA1	1
2200	PRKACA	1
50943	RELA	1
3552	TLR5	1
3661	A9/b1 integrin	1
4775	ADAM17	1
9159	AP1	1
64065	ATF1	1
5443	BCL3	1
5530	BRAF	1
5532	BTF3	1
5533	Calcineurin	1
5562	CASP8AP2	1
5566	RBX1	1
7100	EIF2AK2	1
6868	FBXW11	1
SIGNOR-C154	FGF2	1
466	FGF9	1
1386	FLI1	1
673	FUBP1	1
689	G3BP2	1
SIGNOR-C155	GGCX	1
9994	IL10RA	1
9978	IL10RB	1
5610	IL1RN	1
SIGNOR-PF1	SCN10A	1
2214	SCN11A	1
2247	SCN1A	1
2254	SCN2A	1
2313	SCN3A	1
8880	SCN4A	1
2677	SCN5A	1
3588	SCN8A	1
3557	SCN9A	1
SIGNOR-C15	IEX-1L	1
3572	MAP3K8	1
941	THBD	1
10664	TRAF1	1
O75353	S100A6	1
354	ACTA2	1
4879	ANKH	1
7056	BGLAP	1

7185	CCNA2	1
6277	CDK2	1
59	CDK4	1
56172	CDKN1B	1
632	CDKN2B	1
890	COL1A2	1
1017	COL4A1	1
1019	CyclinE/CDK2	1
1027	ENG	1
1030	ENPP1	1
1278	ITGA2	1
1282	KRT1	1
SIGNOR-C16	LPL	1
5167	MEF2D	1
3673	MYOG	1
3848	OMD	1
4209	PAX8	1
4656	PI3K	1
4958	PIK3CG	1
5080	PIK3R1	1
7849	PPP2R2A	1
5295	SALL2	1
5520	SFTPB	1
54778	SHC1	1
860	SKP2	1
6297	SLC20A1	1
6439	SLC5A5	1
6464	TAGLN	1
6502	TFAP4	1
6574	TGFBR1	1
6528	TGFBR2	1
6876	TSHB	1
7023	LZTR1	1
7048	Adipogenesis	1
7252	AKT1	1
8216	AKT	1
SIGNOR-PH26	Angiogenesis	1
207	ARDS	1
SIGNOR-PF24	COMT	1
SIGNOR-PH128	HES1	1
1312	IRS1	1
1513	JAG2	1
3280	NOD2	1
3667	NOTCH4	1
3714	PIK3CA	1

64127	PIK3CB	1
4855	PIK3CD	1
5290	REL	1
5291	RIPK2	1
5293	SNAI2	1
8767	SCNN1A	1
6591	SERPINA3	1

6337	TNFRSF1B	1
12	TNFRSF21	1
27242	ITGA3	1
3675	LPP	1
4026	MYOCD	1
93649	MAPK14	1

Table 5: The biological pathways associated with the genes interconnected with IL6, NF-Kβ, IL-10, TGF-β, TNF-α and IKβ.

Pathways	**Hits**	**P Value**
Intracellular protein kinase cascade	94	2.95E-29
Positive regulation of metabolic process	146	6.02E-27
Positive regulation of defence response	45	7.54E-26
Regulation of defence response	60	8.84E-26
Regulation of programmed cell death	105	1.30E-25
Regulation of apoptotic process	104	2.05E-25
Response to organic substance	137	2.41E-25
Positive regulation of cellular metabolic process	137	7.35E-25
I-kappaB kinase/NF-kappaB cascade	42	8.69E-25
Regulation of I-kappaB kinase/NF-kappaB cascade	39	1.80E-24
Positive regulation of immune system process	69	3.94E-24
Response to endogenous stimulus	95	7.04E-24
Regulation of immune response	68	8.10E-24
Positive regulation of response to stimulus	102	8.22E-24
Apoptotic process	122	9.87E-24
Apoptotic process	122	9.87E-24
Positive regulation of protein metabolic process	83	2.31E-23
Programmed cell death	122	3.04E-23
Regulation of immune system process	87	4.52E-23
Positive regulation of transcription from RNA polymerase II promoter	70	7.75E-23
Response to wounding	91	1.22E-22
Positive regulation of immune response	54	2.45E-22
Regulation of protein metabolic process	109	2.91E-22
Positive regulation of transcription, DNA dependent	88	4.10E-22
Positive regulation of transcription, DNA dependent	88	4.10E-22
Regulation of sequence specific DNA binding transcription factor activity	47	7.11E-22
Activation of immune response	48	2.09E-21
Positive regulation of RNA metabolic process	89	5.31E-21
Response to chemical stimulus	167	8.55E-21
Immune response	92	1.04E-20
Positive regulation of nucleobase containing compound metabolic process	94	1.56E-20
Positive regulation of signal transduction	75	1.65E-20
Regulation of cytokine production	53	1.65E-20
Positive regulation of cellular protein metabolic process	73	4.94E-20
Enzyme linked receptor protein signalling pathway	81	7.34E-20
Immune system process	133	7.98E-20
Cytokine production	55	1.15E-19
Positive regulation of cellular process	189	1.61E-19
Intracellular signal transduction	124	1.82E-19
Positive regulation of sequence specific DNA binding transcription factor activity	33	2.56E-19
Cell surface receptor signaling pathway	150	2.72E-19
Regulation of multicellular organismal process	124	5.29E-19

Innate immune response	57	5.36E-19
Positive regulation of I-kappa-B kinase/NF-kappaB cascade	29	6.09E-19
Regulation of transcription from RNA polymerase II promoter	95	8.68E-19
Regulation of cellular protein metabolic process	93	1.17E-18
Défense response	91	1.61E-18
T cell activation	46	2.20E-18
Regulation of response to stimulus	148	4.06E-18
Negative regulation of apoptotic process	57	9.77E-18
Negative regulation of apoptotic process	57	9.77E-18
Regulation of protein modification process	80	1.04E-17
Positive regulation of protein modification process	65	1.12E-17
Positive regulation of biological process	202	1.55E-17
Negative regulation of programmed cell death	57	2.19E-17
Positive regulation of multicellular organismal process	55	2.62E-17
Regulation of molecular function	113	3.26E-17
Positive regulation of cell differentiation	51	4.97E-17
Response to stress	167	5.00E-17
Positive regulation of cytokine production	35	6.04E-17
Transcription from RNA polymerase II promoter	102	7.52E-17
Cell activation	67	1.28E-16
Hematopoietic or lymphoid organ development	55	1.93E-16
Response to external stimulus	87	2.00E-16
Inflammatory response	50	2.04E-16
Regulation of gene expression	174	2.32E-16
Nuclear import	32	2.82E-16
Immune system development	56	6.73E-16
Response to abiotic stimulus	62	1.14E-15
Hemopoiesis	52	1.27E-15
Protein import into nucleus	31	1.27E-15
Positive regulation of NFkappaB transcription factor activity	23	1.33E-15
Lymphocyte activation	50	1.87E-15
Regulation of phosphorylation	69	2.05E-15
Positive regulation of developmental process	59	2.58E-15
Multi organism process	91	4.17E-15
Regulation of signal transduction	114	4.44E-15
Regulation of transcription, DNA dependent	152	4.79E-15
Regulation of transcription, DNA dependent	152	4.79E-15
Regulation of transcription, DNA dependent	152	4.79E-15
Negative regulation of response to stimulus	64	8.94E-15
Regulation of RNA metabolic process	154	1.89E-14
Intracellular receptor mediated signaling pathway	32	2.30E-14
Organ development	137	2.55E-14
Leukocyte differentiation	39	2.74E-14
Protein phosphorylation	81	6.47E-14
Leukocyte activation	52	7.23E-14
Negative regulation of metabolic process	92	7.67E-14

Phosphorylation	87	1.05E-13
Response to drug	35	1.35E-13
Protein import	31	1.74E-13
Nucleocytoplasmic transport	37	1.93E-13
Transforming growth factor beta receptor signaling pathway	28	1.95E-13
Regulation of cell proliferation	78	2.02E-13
Negative regulation of biological process	169	2.25E-13
Regulation of catalytic activity	88	2.32E-13
Nuclear transport	37	2.65E-13
Regulation of protein phosphorylation	62	2.68E-13
MAPK cascade	49	3.92E-13
Angiogenesis	38	7.22E-13
Interaction with host	38	7.22E-13
Vasculature development	48	7.25E-13
Negative regulation of signal transduction	53	1.55E-12
Adaptive immune response	28	1.70E-12
Regulation of nucleobase containing compound metabolic process	165	1.85E-12
Immune effector process	44	2.11E-12
Positive regulation of phosphorylation	49	2.23E-12
Tissue development	84	2.77E-12
Positive regulation of protein phosphorylation	48	3.52E-12
Negative regulation of cell proliferation	44	3.58E-12
Negative regulation of cellular metabolic process	83	3.80E-12
Regulation of transport	68	4.90E-12
Positive regulation of phosphate metabolic process	52	5.13E-12
Regulation of biological quality	133	9.79E-12
Regulation of MAPK cascade	42	1.21E-11
Gland development	30	1.65E-11
Regulation of cell differentiation	69	1.81E-11
Cellular response to stress	80	2.07E-11
Transmembrane receptor protein serine/threonine kinase signalling pathway	34	2.09E-11
Regulation of transferase activity	50	2.18E-11

CHAPTER 5
DISCUSSION

Synthesis and Characterization of Novel Biodegradable Hybrid Hydrogel Scaffolds Using the Copolymers Sodium Alginate, CMC, Starch, PEG and PVA

The performance of CTE hydrogel significantly relies on the adequate mechanical strength, controlled degradation, nontoxic degradation products, interconnected pores for nutrient trafficking, support cell adhesion, proliferation, viability and differentiation, favouring cell integration and contractile function under ischemic conditions of the injured heart. Conventional hydrogels possessing all these hallmarks are limited. The challenges have been analysed by hybridizing the natural polymers alginate, cellulose and starch with the synthetic polymers PVA and PEG to synthesize a panel of four hydrogels ACPV1 and ACPV2 and ASPG1 and ASPG2. These hybrid hydrogels displayed superior properties supporting CTE applications.

Interestingly, the four hydrogel scaffolds synthesized in this study were decorated with ample functional moieties contributing to the biological performance for cardiac applications. Evidently, IR analysis revealed the presence of abundant hydrophilic functional groups such as hydroxyl, carboxyl and carbonyl on scaffold surface. The sharp peak near 1000 cm^{-1} which indicated C-O-C stretching in all hydrogels confirms the presence of polysaccharides as this vibration is characteristic for the glycosidic bonds in polysaccharides. Also, the weakening of C-O stretching vibration in ASPG2 reflects increased hydrogen bond formation between glycosidic oxygen and -OH groups indicative of a hydrophilic surface stabilized by hydrogen bonding. Evidentially, the presence of hydrophilic moieties on scaffold surface greatly enhances the water absorption capacity of the hydrogels by promoting hydrogen bonding with water molecules [165]. Moreover, the abundance of surface functional moieties provide opportunities for chemical immobilization of biomolecules and other growth factors for

improving cell adhesion and maturation [166]. Overall, all the hydrogels displayed abundant surface functional groups which are crucial for guiding the cellular and biological performance for CTE applications.

Water content of the hydrogels is a function of osmotic driving forces and the cohesive force exerted by the polymer network [167]. Both ACPV and ASPG hydrogel subsets demonstrated an EWC greater than 80% suggesting their super-absorbent nature and swelling ratio between 5-7 attributing to ample hydrophilic functional groups and porosity as evidenced by IR analysis and SEM respectively. The superior water content is beneficial for the trafficking of metabolite and mass transfer. In addition, the increased water level relaxes the polymer chains to increase the surface area and pore size facilitating the cell survival and performance [168]. Furthermore, the increased water content prevents dehydration thereby accelerating the wound healing responses [169]. Imperatively, the superior water content in the hydrogels, favour for the successful CTE. Remarkably, the superabsorbent hydrogels are characterized by superior water content and holding capability, controlled by diffusion [170]. Generally, the diffusion of water in the hydrogels is controlled by the diffusional exponent (n), which drives the movement of water via Fickian diffusion (regulated by swelling), or super case II transport (SCIIT) (regulated by network relaxation). If $n \leq 0.5$m, the swelling favours Fickian diffusion and favours SCIIT if $n \geq 1.0$ [127]. All the ACPV1, ACPV2, ASPG1 and ASPG2 hydrogels displayed $n \leq 0.5$m, reflecting their Fickian diffusion. Moreover, Fickian diffusion depends on diffusive flux which is the amount of substance per unit area per unit time, which in turn is related to the TWAS. Interestingly, the increased level of TWAS on both ACPV and ASPG hydrogels favours significant uptake of water within a short period of time as revealed in the swelling data.

The growth and survival of cells seeded onto CTE hydrogels are greatly influenced by its porosity pore density and pore size as the cell adhesion, migration, proliferation,

differentiation and cell-cell interaction are dependent on pore architecture [171]. Furthermore, the efficiency of nutrient trafficking and removal of metabolic exhaust is greatly influenced by pore morphology and density. The surface morphometry reveals that the four scaffolds displayed pore architecture with pore length ranging between 4 μm to 12 μm and pore breadth ranging between 3 μm to 8 μm corresponding to the micro porous architecture of an ideal tissue engineering scaffold [172]. Multiple reports conclude that microporous scaffold architecture improves cell migration, attachment and anchorage dependent cell to cell communication [173]. Moreover, neovascularization, cell infiltration and survival are optimum in scaffolds with pore size range of 5 μm to 15 μm [174]. Notably, human embryonic stem cells (hESCs) demonstrated appreciable attachment on the scaffolds with pore size ranging between 3 to 8 μm [175]. Additionally, poly(ethylene glycol) scaffolds with pore size of 12μm promoted better migration of mesenchymal stem cells (MSCs) [176]. These observations suggest that the porosity in both the ASPG and ACPV hydrogels pose immense potential to support the growth of multiple cell types onto the interstices suggesting the potential for CTE.

Mechanical properties of the CTE scaffolds influence the cell adhesion, cell signaling pathways, angiogenesis and neo-tissue formation. The superior tensile properties of ACPV2 and ASPG2 hydrogels reflect the increased crosslinking density owing to the higher alginate content. Mechanical strength and swelling are the functions of crosslinking density within the co-polymers which determine the thermodynamic stability of the hydrogels [177]. Moreover, Young's modulus of a healthy human cardiac tissue is ~50 kPa which increases up to 100 kPa during scarring and fibrosis [178]. Moreover, the Youngs modulus of the hydrogels ranged between 1 to 4 MPa which has been reported to be ideal for soft tissue engineering. For instance, the electrospun polyester ether(urethane urea) scaffold, with an elastic modulus ranging between 1-2 MPa, was loaded with adeno associated viral genes and implanted into left ventricle of rat resulted in improved LV function owing to the mechanical properties of the

scaffold [179]. Hence, the healing responses and beating function in CTE hydrogels warrant mechanical properties superior to native heart tissue. Interestingly, the ACPV and ASPG hydrogels are mechanocompatible for CTE allowing for tuneable mechanical properties by manipulating the cross-linking density by divalent cations.

Biomolecules including the adhesin proteins and ECM components involved in the regenerative responses in the native cardiac tissues composed of amphiphilic due to hydrophilic and hydrophobic domains. The contact angle data for all the hydrogels were in the range of amphiphilicity which is crucial in enhancing cell adhesion and proliferation [180]. Hence, the hydrophilicity of ACPV and ASPG hybrid hydrogel subsets are mainly due to -COOH and -OH on hydrogel surfaces as indicated by IR analysis. However, extreme hydrophilic or hydrophobic surfaces impair cell adhesion and proliferation whereas moderately wettable surfaces are optimal [181–183]. Hence, the amphiphilic nature of ACPV and ASPG hydrogels supports protein adsorption and the binding, proliferation and migration of cells facilitating the integration of CTE at the tissue interface.

Biodegradation of ACPVI and ACPV2 hydrogels was studied using PBS buffer for 30 days where all the hydrogels maintained their structure for the initial three weeks period followed by slower withering. ACPVI and ACPV2 hydrogels lost 72% and 63.5% of their dry weight respectively after 30 days study. Similarly, ASPG1 and ASPG 2 hydrogels lost 52% and 81.6% of their dry weight respectively. TDS were increased in a time dependent fashion owing to the erosion of ions and other solid particles from the hydrogel surfaces confirming the degradation. Cross-linking of the polymer chain with calcium is affected by the formation of covalent bond between calcium ions and guluronic acid residues in the G block of alginate chains forming the characteristic egg box structure [151]. Interactions of the cross-linked alginate with monovalent ions such as sodium and potassium result in the replacement of calcium ions with monovalent ions resulting in the collapse of egg box leading to gel-sol

transition and subsequent weakening of the hydrogel [184]. Additionally, the slight drop in pH suggests the release of mild acidic degradation products which elicits minimal physiological responses following the implantation owing to the efficient buffering capacity of circulating fluids [151].

Examinations on cell-material Interaction and Compatibility of the Hybrid Hydrogels

The in vivo biocompatibility of a scaffold is greatly driven by the type and amount of protein adsorbed on the surface [185]. Post-implantation, cellular attachment on any scaffold surface is largely affected and regulated by the adsorbed protein layer as scaffold-protein interaction occurs prior to cell infiltration/adhesion. Protein adsorption on a hydrophobic scaffold surface is largely governed by hydrophobic interactions whereas a hydrophilic surface favour electrostatic force. Interestingly, the hydrophilic surfaces retain confirmation of adsorbed proteins whereas hydrophobic results in structural deformities [186]. The adherence of albumin in the surface of scaffold results in smoothness and a rough surface is detrimental as the RBC membrane rupture occurs upon encountering circulation resulting in haemolysis and activation and aggregation of platelets leading to thrombosis [187]. Importantly, adsorption of plasma albumin prevents unfavourable cell-scaffold interactions contributing to hemocompatibility and created favourable environment for the infiltrating cells [188]. Additionally, albumin binding on scaffold surface prevents the adsorption of fibrinogen preventing thrombosis and inflammation [189]. Also, there are reports on using albumin itself as biomaterial for fabricating tissue engineering scaffolds due to its exceptional biocompatibility [190]. In the present study, ACPV1, ACPV2 and ASPG2 exhibited superior adsorption of albumin from the serum whereas ASPG1 demonstrated a significantly higher adsorption (75%) which is attributed to the microporous and amphiphilic nature of scaffolds [191].

Direct contact assay and test on extract were used to assess the cytotoxicity of the hydrogels assessing the characteristic cell morphology and cell viability respectively. Both the ACPV and ASPG hydrogels were cytocompatible as evident from H9c2 cell adhesion, proliferation and survival which significantly depends on the hydrogel properties such as extent

of porosity, protein adsorption and surface hydrophilicity [192]. Significantly, the hydrogels are biocompatible and the degradation products are non-toxic to the cells. Direct contact revealed the absence of morphological changes in H9c2 cells demonstrating the cytocompatibility of ACPV and ASPG hydrogels. Moreover, the cell spreading and health status determined by FDA staining unveiled the healthy being of H9c2 cells in the interstices of both ACPV and ASPG hydrogels. Hence, the ACPV and ASPG hydrogel systems represent biocompatible templates for CTE applications.

Furthermore, the infiltration of cells exhibited increased migration onto the inner network of ACPV and ASPG hydrogels which is crucial for the mobility of seeded and the host cells from the surviving cardiac tissue post implantation. Moreover, the cells infiltrated >100 μm within the ACPV2, ASPG1 and ASPG2 hydrogels through the interconnecting pores unveiled the capability of the healthy cells to occupy the inner rooms of the hydrogel [193]. Also, the increased density of H9c2 cell homes the hydrogel network. Logically, the rate of biodegradation of ACPV and ASPG before the expansion rate of seeded cells is crucial for triggering the cell migration towards the interstices of the hydrogels. However, the uncontrolled biodegradation destabilizes the hydrogels thereby preventing the cell attachment and proliferation which lead to apoptosis [170]. Moreover, the biodegradation of the hydrogels provides additional space for the proliferating cell population suggesting the potential applications of the hydrogels in cardiac regeneration.

Biological Responses of Biosynthetic Hydrogels for CTE

Antimicrobial Efficiency

The translational challenges in tissue engineering strategy including infection following the invasive procedures are alarming [194]. Such infections result in unpredictable aftermaths including sustained inflammatory responses leading to treatment/implant failure. Oral/intravenous administration of antibiotics help to prevent infections; however, limited bioavailability and bioretention of antibiotics at the surgery site and antibiotic resistance are challenging. In addition, the higher doses of antibiotics cause off-target side effects including liver damage and kidney disorders. A possible alternative to treat implant-driven infection is to incorporate antibiotics into scaffolds aiding in a sustained and localized delivery of antibiotics and eliminates the chances of systemic toxicity. In the present study, all the hydrogels incorporated with varying concentrations of amikacin and vancomycin demonstrated excellent inhibition of bacterial proliferation. The exceptional amphiphilicity and water profile of the ACPV and ASPG enabled the loading/release of antibiotics by simple diffusion.

Studies on Antioxidant Response

Several ROS including superoxide anions, hydroxyl radical and hydrogen peroxide are upregulated in the infarct zone aggravating the MI pathology by inducing oxidative stress. Increased oxidative stress significantly damage the proteins, nucleic acids, lipids and membranes associated with the surviving cardiac tissue as well as the cells seeded onto the scaffolds [195]. Hence, addressing the oxidative stress using hydrogels warrants careful consideration while designing CTE-based strategies. Unfortunately, such hydrogels with ROS scavenging effects are rare in the literature. Translationally, the present study adopted a simple approach of incorporating the natural antioxidant ascorbic acid onto the ACPV and ASPG

hydrogels for improved antioxidant effects. The rationale for choosing ascorbic acid owes to its vast biological functions including potent antioxidant and radical scavenger effects protecting the cells/tissues against oxidative stress, redox homeostasis of antioxidant mediators including glutathione and α–tocopherol (vitamin E), cofactor for biosynthetic enzymes including monooxygenase and dioxygenase enzymes and synthesis and homeostasis of collagen subtypes [196]. Importantly, ascorbic acid administration has significantly reduced the risk of CVDs and improved the cardiac healing following MI [197] [198]. Hence, the incorporation of ascorbic acid offers dual benefits of providing antioxidant property to the hydrogels and acts as a cardioprotective mediator accelerating the healing responses at the infarct zone.

Pathologically, localized implantation sites are at the highest risk of ROS and subsequent oxidative stress potentially impairing the bystander cells by inducing cytotoxic effects such as DNA/protein modification and the triggering of apoptosis [199]. Such detrimental effects often result in the failure of the implants demanding ROS-responsive scaffold system. Strategically, we adopted the simple and clinically feasible approach of incorporating a natural, nontoxic, water soluble and cardioprotective antioxidant, ascorbic acid, in our hydrogel system which showed propounding antioxidant effects in cellular and cell free system as consistent with reported literature [200]. Importantly, ASPG and ACPV hydrogel systems significantly shielded the oxidative stress induced by H_2O_2 in vitro and protected the RAW 267.4 cells from apoptosis. These observations promote the potential translational applications of ASPG and ACPV hydrogel systems in regenerative cardiology for the management of heart failure. However, further in vivo and pre-clinical validations are warranted to extrapolate this approach in clinical arena.

Studies on Immunocompatibility and Gene Interactions

Inflammation is the initial phase of wound healing which progresses through the activation of mononuclear immune cells including macrophages. Essentially, the balance between pro-inflammatory M1 (classically activated) phenotype and pro-healing M2 (alternatively activated) phenotype of macrophage is crucial for the resolution of inflammation [201]. Besides, the macrophages are highly plastic cells that alters their morphology and functions based on the nature and chemistry of the micro-environment determining the M1 and M2 phenotypes [202]. Moreover, the M0 (unstimulated) phenotype constitutes normal macrophages reflecting the normal physiological milieu [201]. Also, the existence of M0 macrophages is evident by the absence of alterations in the characteristic morphology upon contact with any foreign materials [201] [203]. Interestingly, the contact of ACPV and ASPG hydrogels failed to activate the RAW264.7 macrophages in the culture as evident from the absence of changes in their classical morphology, suggesting their normal phenotype. Hence, the possible immune system activation upon implantation of ACPV and ASPG is bare minimal, suggesting their potential application in CTE.

IL6 is a pleotropic cytokine playing a crucial role in inflammatory responses which has been intimately associated with MI and has been an ideal target for CVDs [204]. Also, elevated circulatory IL6 has been reported in clinical specimen and animal models of MI [204] [205]. Moreover, increased IL6 level 4 months following STEMI correlates with the increased infarct size, reduced LVEF and adverse clinical outcomes suggesting the potential role in cardiac inflammation following MI [206]. Translationally, the downregulation of IL6 has been encouraging to prevent the inflammatory episodes and to alleviate the pathological symptoms involved in MI [207]. Hence, the CTE scaffolds/hydrogels exhibiting minimal trigger in IL6 upregulation offer successful cardiac regeneration. Interestingly, the ACPV hydrogels, as observed in our findings, displayed a significant downregulation of IL6 upon encountering the

macrophage cells suggesting the minimal immune activation and immense translational potential. However, such IL6 lowering effects of CTE hydrogels are rare in the scientific literature and the underlying mechanism possibly owes to the biocompatible functionalities in the parent co-polymers.

The pro-inflammatory cytokine, TNFα, has been extensively investigated as a biomarker associated with MI. Both the membrane bound and secretory forms of TNFα elicit complex molecular interactions resulting in the aggravated pathology in MI which has been demonstrated in vitro and in vivo models and in clinical subjects [208]. Additionally, TNFα sustains the reversible contractile dysfunction and the irreversible MI injury in response to ischemic insults as evident from the TNFα knockout experimental models in CVDs [209]. The cardiac rescue strategies and reperfusion have been accompanied by the upregulation of TNFα as evident by myocardial ailments in clinical examinations. Moreover, the increased oxidative stress associated with myocardial ischemia fuel TNFα induction promoting the apoptosis/necrosis of cardiomyocytes along with impairing the calcium homeostasis resulting in aggravated pathology and delayed healing [210]. Hence, the careful consideration of TNFα biology is crucial for successful CTE. Interestingly, ACPV hydrogel system displayed a significant downregulation of TNFα in the RAW267.4 macrophages upon direct contact benefitting their promise in CTE applications.

NFκB is a super family of transcription factors consisting of the genes encoding the members RelA (p65), RelB, c-Rel, p50 and p52 and included in two sub-families. The sub-family comprising p50 and p52 is mainly involved in mediating inflammatory responses where NFκB exist as a heterodimer [211]. In the absence of an activation signal, NFκB remain as inactive form, bound to IKB (inhibitors of κB) in the cytosol. The phosphorylation-dependent degradation of IKB activates NFκB promoting its translocation to nucleus accelerating the expression of a battery of pro-inflammatory genes including IL6 [211]. Hence, the binding and

expression of IKB determine the NFκB activity. The active upregulation of NFκB has been well established in the ischemic and reperfused myocardium suggesting the pro-inflammatory milieu aggravating the complications [212]. Additionally, NFκB has been intimately associated with pro-inflammatory cytokine burst, hypertrophy and apoptosis along with oxidative stress in CM [213]. Interestingly, a seminal study demonstrated that the selective inhibition of NFκB significantly improved the myocardial function and alleviated the pathology following MI. Hence, in the context of CTE the downregulation of NFκB signalling with a concomitant upregulation of IKB is essential for the successful cardiac regenerative outcomes.

Interestingly, the contact of ASPG and ACPV hydrogels failed to upregulate NFκB in the RAW267.4 macrophages suggesting the minimal possibilities associated with the activation of proinflammatory genes. Contrastingly, the increased level of IKB expression reflects the increased possibility of NFκB activation. However, the information regarding the phosphorylation status of IKB is required to confirm the activation status of NFκB [214]. Considering the decreased level of NFκB and other proinflammatory mediators, it is reasonable to speculate that the increased IKB is insufficient to mobilize and activate NFκB upon contact with ACPV and AGPG hydrogels. However, further mechanistic studies are warranted to validate these conclusions.

IL10 is an anti-inflammatory cytokine functioning in the restoration of myocardial homeostasis following ischemic injury [215]. Importantly, IL10 regulates the activation of monocytes with the concomitant suppression of a school of proinflammatory mediators thereby accelerating the healing responses [215]. Clinically, the upregulation of circulatory IL10 has been correlated with the progressive healing of myocardial ischemia and reperfusion, limiting the burst of proinflammatory mediators. Interestingly, the endogenous IL10 inhibits TNF-α and NO, thereby protecting the ischemic myocardium via suppressing the recruitment and activation of neutrophils [216]. Additionally, IL10 reduced the infarct zone expansion and

improved the cardiac function by improving the capillary density, preventing the apoptosis and minimizing inflammation as demonstrated in MI mice models [217]. Hence, the basal expression or upregulation of IL10 is an indication of resolution of ischemic damage in the myocardium. Taken together, the decreased level of IL10 by RAW267.4 macrophages upon contact with ASPG and ACPV hydrogels is suggestive of the absence of macrophage activation and proinflammatory signalling.

TGFβ superfamily plays a crucial role in ECM homeostasis, cell survival, proliferation and differentiation along with the modulation of inflammation following MI [218] [219]. TGFβ is constitutively expressed in the adult mammalian heart supporting homeostatic cardiac function by sustaining the spontaneous beating [218] [219]. In addition, TGFβ promotes the transdifferentiation and proliferation of myofibroblasts to accelerate the healing responses especially by secreting the ECM components [220]. Importantly, TGFβ accelerates the phenotype switch of proinflammatory M1 macrophages to pro-healing M2 phenotypes by suppressing the expression of inflammatory cytokines and chemokines [218] [219]. Furthermore, TGFβ is a well-known activator for angiogenesis which in turn is the key to cardiac healing and neo-tissue formation [221]. Interestingly, TGFβ loaded hydrogels have been considered to be a successful approach in promoting healing responses as demonstrated in seminal reports dealing with multiple tissue engineering approaches [222] [223]. Considering the potential healing benefits, the upregulation of TGFβ in RAW267.4 macrophages upon contact with ACPV and AGPG hydrogels suggest their promise in CTE applications.

Interestingly, the mediators (IL6, NF-Kβ, IL-10, TGF-β, TNF-α and IKβ) chosen for immunocompatibility assessment were involved in multiple pathways of inflammation and/or immunomodulation. Hence, the assessment of their gene interactions unveiled the possible pathways of inflammation or repair correlating with the cellular/tissue level expression of these

mediators. Interestingly, IL6, NF-Kβ, IL-10, TGF-β, TNF-α and IKβ are intimately connected with 370 genes and 120 pathways unveiling their potential network. As highlighted in the NetworkAnalysis data, signal transductions involving protein kinases play a critical role in resolving cellular stress including inflammatory, metabolic and oxidative stress in macrophages [224]. Similarly, the metabolic regulation plays a critical role in the inflammatory responses elicited by macrophages [225]. For instance, the M1 macrophages rely mostly on glycolytic pathways leading to succinate accumulation and subsequent HIF1α activation for upregulating the glycolytic genes [225]. On the other hand, the M2 macrophages rely on oxidative phosphorylation for replenishing the substrates for the electron transport chain [225] [226]. These observations suggest that pro- and anti-inflammatory phenotypes of macrophages are featured with specific metabolic signature pathways and these pathways could be targeted for designing therapeutic approaches in minimizing the adverse effects involved in biomaterial implantation. Additionally, the regulation of apoptotic process in the macrophages are crucial in determining the success of implants regarding their plasticity [227].

On considering CTE, a thorough understanding and screening regarding the interconnecting pathways and networks and its assessment regarding functional properties and immunobiology of the biomaterial implants are highly recommended for successful outcomes. Interestingly, our data provides novel insights into the cytokine profiling and possible gene interactions in determining the success of ACPV and ASPG hydrogels. However, further mechanistic studies are warranting to apply such preliminary findings to translational regenerative cardiology.

CHAPTER 6
SUMMARY & CONCLUSION

According to World Health Organization (WHO), CVDs accounts ~17.9 million global deaths globally which is supported by the estimate by AHA pointing a 21.1% increase in global CVD deaths [228] [229]. MI incidence is alarming [230] and the ischemic episodes following the MI significantly affects cardiac performance. Current treatment strategies depend on pharmacotherapy and surgical interventions to restore the blood flow and functional output; however, heart transplantation remains the ultimate management option. Unfortunately, the lack of organ donors, higher risk of infection and adverse immunological responses pose challenges in transplantation approach. At this juncture, CTE has emerged as a promising strategy in regenerative cardiology [231]. CTE exploits the inherent regenerative potential of cardiac tissue utilizing a supporting scaffold grown with specific cell phenotypes and growth factors providing a 3D micro- architecture mimicking the native cardiac tissue.

Pathologically, the infarcted myocardium displays a hostile microenvironment as evident from oxidative stress, inflammatory explosion, metabolic dysfunction, hypoxic maladaptation and reperfusion injury [232]. In addition, the cardiac sufferers are highly susceptible to infections limiting the recovery rate and functional outcome [233] [171]. Hence, the approaches for the early detection of these risk factors and effective CTE strategies to address such challenges are critical for cardiac regeneration. As hydrogel scaffolds simulate native cardiac ECM along with the benefits including biological cues for adherence, proliferation and differentiation of cells and excellent immunocompatibility, the hydrogel-based biomaterials have gained prior appreciation in CTE [103]. Hence, the current trend of CTE has been inclined to injectable and implantable hydrogels and multiple synthetic approaches have been evolved to engineer ideal scaffolds for successful CTE.

Interestingly, the hydrogel scaffolds possessing multiple talents for simultaneously addressing the biological issues associated with cardiac pathology and healing are highly demanding for CTE. For example, the increased chance of infection warrants the hydrogels

with antimicrobial properties and hydrogels with antioxidant properties are required to tame the pathological infarct zone tissue. CTE demands an ideal hydrogel template and the performance of engineered myocardial construct is driven by the parameters including physiochemical properties, mechanical strength, non-toxic degradation products, cell-material interaction, interconnected porosity and favourable microniche for cellular viability and differentiation along with tunablility for addressing pathological insults including infection and oxidative stress. Unfortunately, the hydrogel materials addressing these stringent and complementary requirements are rare in the literature. At this juncture, the major focus of this research was to engineer and evaluate biologically favourable and cardiac compatible hydrogel scaffolds using biosynthetic the copolymers polysaccharide alginate, starch and the polysaccharide derivative CMC reinforced with synthetic polymers PVA and PEG for CTE.

Two hydrogel families ACPV and ASPG were successfully synthesized. ACPV hybrid hydrogel system was prepared by interpenetrating alginate and cellulose with the synthetic polymer PVA and the subsets ACPV1 and ACPV2 were prepared by varying the composition of the co-polymers. Similarly, PEG was used in ASPG system instead of PVA and the two subsets ASPG1 and ASPG2 were prepared by altering the constituent ratio of co-polymers. Divalent cation, Ca^{2+} was used as the crosslinking agent in both the preparations. ATR spectral analysis demonstrated the surface functional groups unveiling ample -OH, -C=O, -COOH and C-O-C groups on the surface suggesting the presence of alginate, starch, CMC, PVA and PEG fractions in the surface of respective hydrogels. SEM analysis displayed the surface morphology and pore organization of both ACPV and ASPG hydrogels, where ACPV2 and ASPG1 exhibited superior pore features compared to ACPV1 and ASPG2. The similar level of pore aspect ratio suggests similar pore morphology in both the systems. These observations suggest that the porosity in both the ASPG and ACPV hydrogels pose immense potential to support the growth of multiple cell types onto the interstices suggesting the potential for CTE.

Both the hydrogels, ACPV and ASPG, were superabsorbent in nature as evident from the EWC >79% and swelling ratio >5. Similar level of water profile was displayed by all the four hydrogels in terms of diffusional exponent, swelling constant and TWAS whereas ACPV hydrogels displayed significantly increased TWAS than the ASPG hydrogels. Overall, all the ACPV1, ACPV2, ASPG1 and ASPG2 hydrogels displayed Fickian diffusion suggesting the diffusion-controlled performance which is crucial for successful CTE. Additionally, both the hydrogels are amphiphilic.

Interestingly, ASPG2 exhibited superior mechanocompatibility compared with other three hydrogels as evident from the increased tensile strength and modulus. In addition, the tunable mechanical properties could be manipulated by the crosslinking density using divalent cations which support protein adsorption and the binding, proliferation and migration of cells facilitating the integration of CTE at the tissue interface. Additionally, the contact angle studies revealed the amphiphilic nature of both the ACPV and ASPG hydrogel system. The amphiphilic nature of ACPV and ASPG hydrogels are crucial to support protein adsorption and the binding, proliferation and migration of cells facilitating the integration of CTE at the tissue interface.

Both ACPV and ASPG hydrogel system were biodegradable and the degradation products are nontoxic and failed to elicit alterations in pH of the surrounding media. The progressive increase in TDS reflects the biodegradation and accumulation of degradation products. Biodegradation is facilitated by the cross-linking chemistry of alginate with monovalent ions such as sodium and potassium which results in the replacement of calcium ions with monovalent ions resulting in the collapse of egg box leading to gel-sol transition and subsequent weakening the hydrogel [184].

Both ACPV and ASPG hydrogel system promoted plasma protein adsorption on their interstices where the major fraction of adsorbed protein was contributed by albumin. The in

vivo biocompatibility of a scaffold is greatly driven by the type and amount of protein adsorbed on the surface [185] and the albumin passivation supports the adhesion and proliferation of cardiac cells which depends on the amphiphilicity. Among the four subsets of hydrogels, ASPG1 demonstrated a significantly higher adsorption (75%) which is attributed to the microporous and amphiphilic nature of scaffolds [191].

Direct contact assay using H9c2 cardiomyoblast cells on contact with ACPV and ASPG hydrogels resulted in the retention of their normal spindle morphology and deviation from the normal morphology was completely absent suggesting the non-toxic nature of the hydrogels revealing their biocompatibility. Additionally, the MTT assay using H9c2 cells cultured with hydrogel extract revealed viability of >80% in all subsets when compared with the control cells. These data confirmed the cytocompatibility of ACPV and ASPG hydrogels.

Both ACPV and ASPG hydrogels displayed adhesion and spreading of H9c2 cells as evident from the FDA staining. Among the four systems, ASPG1 was superior in cell attachment and proliferation. Also, the penetration of H9c2 cells onto the ACPV and ASPG hydrogels were examined by Z-stack analysis revealing the superior cell penetration in both the ACPV and ASPG hydrogels compared to the control where ASPG hydrogels displayed increased penetration depth than ACPV1. The penetration of cells exhibited increased migration onto the inner network of ACPV and ASPG hydrogels and the cells infiltrated >100 μm within the ACPV2, ASPG1 and ASPG2 hydrogels through the interconnecting pores unveiled the capability of the healthy cells to occupy the inner rooms of the hydrogel [193].

ACPV and ASPG hydrogel subsets loaded with varying doses of amikacin and vancomycin displayed significantly increased zone of inhibition than the control. The exceptional amphiphilicity and water profile of the ACPV and ASPG enabled the loading/release of antibiotics by simple diffusion. Hence, the hydrogels are tuneable for addressing the possible infections associated with implantation in the surviving cardiac tissue.

ACPV and ASPG hydrogels loaded with ascorbic acid displayed appreciable antioxidant response in vitro cell free system. DPPH scavenging was decreased in the ACPV1, ACPV2, ASPG1 and ASPG2 comparable with untreated control. ACPV1 displayed increased scavenging and ACPV2 exhibited decreased scavenging among the four hydrogels whereas ASPG1 and ASPG2 displayed similar levels of NO scavenging. The incorporation of ascorbic acid offers dual benefits of providing antioxidant property to the hydrogels and act as a cardioprotective mediator accelerating the healing responses at the infarct zone.

ACPV and ASPG hydrogels exhibited protection against H_2O_2 induced oxidative stress in RAW267.4 macrophage cells. The antioxidant potential of hydrogels was exhibited by the significantly decreased level of oxidative stress in RAW267.4 cells upon direct contact with ACPV and ASPG hydrogels compared to H_2O_2 treatment group. Hence, ASPG and ACPV hydrogel systems significantly shielded the oxidative stress induced by H_2O_2 in vitro and protected the RAW267.4 cells from apoptosis unveiling the potential translational applications in regenerative cardiology. Also, the RAW267.4 cells on contact with ACPV and ASPG hydrogels retained their normal morphology and deviation from the normal morphology was completely absent suggesting the absence of macrophage activation revealing their immunocompatibility.

IL6 was decreased in ACPV1 and ACPV2 upon contact with RAW267.4 cells compared to the LPS control; however, ASPG1 and ASPG2 displayed significantly increased expression. TNFα was decreased in ASPG1, ACPV1 and ACPV2 treated RAW267.4 cells compared to the LPS control where the level of TNFα in ACPV2 was lower than the control. The level of NFκB was lower in ASPG1, ACPV1 and ACPV2 than LPS and control groups whereas ASPG2 displayed increased expression of NFκB than LPS and was increased compared to the control. All the four hydrogel subsets displayed increased levels of IKB and TGFβ compared to the control upon contact with RAW267.4 cells. All the hydrogel subsets

except ACPV2 displayed increased level of IL10 compared to the control upon contact with RAW267.4 cells. The mediators (IL6, NFκB, IL-10, TGF-β, TNF-α and IKB) chosen for immunocompatibility assessment were involved in multiple pathways of inflammation and/or immunomodulation as assessed by Network Analyst program. Hence, the assessment of their gene interactions unveiled the possible pathways of inflammation or repair correlating with the cellular/tissue level expression of these mediators. Importantly, the current data provide novel insights into the cytokine profiling and possible gene interactions in determining the success of ACPV and ASPG hydrogels. However, further mechanistic studies are warranted to apply such preliminary findings to translational regenerative cardiology.

To conclude, two sets of hybrid hydrogels, ACPVs and ASPGs, were prepared and examined for physical, biocompatibility and biological performance for cardiac tissue engineering. The hydrogels were biodegradable with appreciable mechanical strength, optimum surface features and water profile with immense biocompatibility. The hydrogels exhibited cell survival, antimicrobial potential and ROS scavenging responses, suggesting their ability to promote healing under hostile conditions of infarct zone. Despite the promising findings generated from ACPV and ASPG hydrogels, our study is not exempted from limitations. In vivo validations of these hydrogels are the beyond the focus of this study. The strategies to assess the invitro 3D performance of the hydrogels are currently unavailable. Electrical conductivity assessment of the hydrogels requires additional engineering strategies. Controlling calcium homeostasis and mitochondrial dynamics for improving functional outcomes warrants further validations. Future research is required for addressing these limitations to extend the applications of ACPV and ASPG hydrogels in therapeutic arena.

CHAPTER 7
RECOMMENDATIONS

The culmination of the current study, in addition to generating information, has also identified certain gaps in this area. The recommendations listed below, aim to provide insights into these unmet needs and to direct future research in this field. Such endeavours will help in revolutionizing and advancing knowledge in the field. A few suggestions are listed below:

Management of Ca^{2+} ions at the infarct site using hydrogel systems:

The dysregulation of calcium cycling during myocardial infarction causes shift in its cytosolic baseline concentration. This in turn can cause an increased uptake of Ca^{2+} ions into mitochondria leading to mitochondrial calcium overload and oxidative stress, further exacerbating the condition. Thus, the management of Ca^{2+} ions at the infarcted zone is essential to counter the advancement of the disease. Hydrogels that can sequester and balance Ca^{2+} ion concentration at the site of infarction will represent a significant advancement in CTE. Decorating the hydrogel surfaces with molecules that can sequester Ca^{2+} ions will effectively remove excess calcium ions from infarction zone thereby diminishing its deleterious effects. Further research is also needed to fine-tune the properties of the hydrogels in terms of its crosslinking density, biodegradability, mechanical properties etc. to optimize it for effective management of Ca^{2+} ions.

Molecular biology and mechanism of ROS and RNS scavenging using hydrogels:

Numerous studies have shown that excess ROS released primarily from mitochondria and other cellular components causes the progression of MI. ROS activates multiple signalling cascades leading to inflammation. Scavenging of ROS species from site of injury can prevent such catastrophic events thus curtailing the advancement of MI. Developing CTE hydrogels with inherent ROS scavenging property or tailoring ROS scavenging molecules on hydrogel surfaces will aid in managing ROS levels in infarct site. Present study has revealed inherent ROS scavenging effects in ACPV and ASPG hydrogels. But further study is required to elucidate the exact mechanism of this inherent ROS scavenging property. Moreover, ACPV

and ASPG hydrogels functionalized with the antioxidant ascorbic acid also demonstrated superior ROS scavenging effects. But different aspects such as the chemistry of ascorbic acid - hydrogel surface interaction, release kinetics of ascorbic acid and ROS scavenging kinetics need to be elucidated. Such information is essential for developing more efficient CTE scaffolds with improved ROS scavenging potential. Such systems will unquestionably protect myocardial tissue from the damages posed by ROS.

Incorporation of growth factors, MMP inhibitors and other mediators:

Decorating the CTE hydrogels with the regenerative cues including growth factors, matrix metalloproteinase (MMP) inhibitors and other mediators offers a promising strategy to tame the hostile micro-environment at the infarct zone promoting myocardial repair. Ongoing and future investigations warrant to explore novel hydrogel engineering strategies and sustained delivery systems to achieve optimal therapeutic outcomes while minimizing potential off-target effects. Furthermore, elucidating the synergistic interactions between multiple therapeutic agents using smart/intelligent hydrogel systems further enhance their efficacy in accelerating the myocardial regeneration post-MI.

Co-culture with primary endothelial cells, cardiac fibroblasts and cardiomyocytes:

Biological modification of hydrogels by co-culture with primary endothelial cells, cardiac fibroblasts and cardiomyocytes holds significant promise for ensuring angiogenesis and promoting better integration within the infarcted myocardium. Future research is warranted on optimizing co-culture conditions, including cell ratios, ECM homeostasis, culture medium composition and scaffold characteristics, to trigger cellular interactions. Additionally, the strategies to track the fate of co-cultured cell populations that mimic native cardiac tissue architecture needs to be developed. This approach fuels in designing advanced hydrogel constructs triggering functional myocardial regeneration through enhanced vascularization, ECM deposition and cellular integration.

Development of in vitro and in vivo 3D models to study MI:

Cardiomimetic in vitro and in vivo 3D models to study myocardial infarction (MI) is essential for advancing the translational potential of hydrogel-based CTE. These models simulate and recapitulate the pathophysiology of infarct zone, including histomorphometry, tissue architecture, cellular interactions and biochemical gradients. Moreover, integrating advanced imaging techniques including fluoroscopy and functional assays enable comprehensive characterization of hydrogel performance in terms of cardiac function restoration, tissue remodelling and long-term therapeutic efficacy. Multidisciplinary research collaboration is warranted in establishing standardized cardiac models that mimic the complex milieu of infarct zone, thereby fuelling the translation of hydrogel-based therapies to clinical arena.

In conclusion, incorporating these suggestions into future research will aid in developing innovative and promising hydrogels with better therapeutic performance for MI. In this way, scientists can contribute meaningfully for significant developments in the field of cardiac tissue engineering and regenerative medicine.

REFERENCES

[1] S.S. Virani, A. Alonso, E.J. Benjamin, M.S. Bittencourt, C.W. Callaway, A.P. Carson, A.M. Chamberlain, A.R. Chang, S. Cheng, F.N. Delling, L. Djousse, M.S.V. Elkind, J.F. Ferguson, M. Fornage, S.S. Khan, B.M. Kissela, K.L. Knutson, T.W. Kwan, D.T. Lackland, T.T. Lewis, J.H. Lichtman, C.T. Longenecker, M.S. Loop, P.L. Lutsey, S.S. Martin, K. Matsushita, A.E. Moran, M.E. Mussolino, A.M. Perak, W.D. Rosamond, G.A. Roth, U.K.A. Sampson, G.M. Satou, E.B. Schroeder, S.H. Shah, C.M. Shay, N.L. Spartano, A. Stokes, D.L. Tirschwell, L.B. VanWagner, C.W. Tsao, On behalf of the American Heart Association Council on Epidemiology and Prevention Statistics Committee and Stroke Statistics Subcommittee, Heart Disease and Stroke Statistics—2020 Update: A Report From the American Heart Association, Circulation. 141 (2020). https://doi.org/10.1161/CIR.0000000000000757.

[2] S.K. Al-Kaabi, A. Atherton, Impact of noncommunicable diseases in the State of Qatar, Clin. Outcomes Res. (2015) 377. https://doi.org/10.2147/CEOR.S74682.

[3] G. Lippi, B.M. Henry, F. Sanchis-Gomar, Physical inactivity and cardiovascular disease at the time of coronavirus disease 2019 (COVID-19), Eur. J. Prev. Cardiol. 27 (2020) 906–908. https://doi.org/10.1177/2047487320916823.

[4] A.E. Berezin, A.A. Berezin, Adverse Cardiac Remodelling after Acute Myocardial Infarction: Old and New Biomarkers, Dis. Markers. 2020 (2020) 1215802. https://doi.org/10.1155/2020/1215802.

[5] M.F. Kilkenny, L. Dunstan, D. Busingye, T. Purvis, M. Reyneke, M. Orgill, D.A. Cadilhac, Knowledge of risk factors for diabetes or cardiovascular disease (CVD) is poor among individuals with risk factors for CVD, PloS One. 12 (2017) e0172941. https://doi.org/10.1371/journal.pone.0172941.

[6] M. Ezzati, Z. Obermeyer, I. Tzoulaki, B.M. Mayosi, P. Elliott, D.A. Leon, Contributions of risk factors and medical care to cardiovascular mortality trends, Nat. Rev. Cardiol. 12 (2015) 508–530. https://doi.org/10.1038/nrcardio.2015.82.

[7] F.G. Thankam, D.K. Agrawal, Infarct Zone: a Novel Platform for Exosome Trade in Cardiac Tissue Regeneration, J Cardiovasc. Transl. Res. 13 (2020) 686–701. https://doi.org/10.1007/s12265-019-09952-8.

[8] G.T. Finosh, M. Jayabalan, Regenerative therapy and tissue engineering for the treatment of end-stage cardiac failure, Biomatter. 2 (2012) 1–14. https://doi.org/10.4161/biom.19429.

[9] F.G. Thankam, J.G. Ayoub, M.M.R. Ahmed, A. Siddique, T.C. Sanchez, R.A. Peralta, T.J. Pennington, D.K. Agrawal, Association of hypoxia and mitochondrial damage associated molecular patterns in the pathogenesis of vein graft failure: a pilot study, Transl. Res. (2020). https://doi.org/10.1016/j.trsl.2020.08.010.

[10] C. Kane, C.M.N. Terracciano, Concise Review: Criteria for Chamber-Specific Categorization of Human Cardiac Myocytes Derived from Pluripotent Stem Cells, Stem Cells Dayt. Ohio. 35 (2017) 1881–1897. https://doi.org/10.1002/stem.2649.

[11] K.T. MacLeod, S.B. Marston, P.A. Poole-Wilson, N.J. Severs, P.H. Sugden, Cardiac myocytes and the cardiac action potential, in: D.A. Warrell, T.M. Cox, J.D. Firth (Eds.), Oxf. Textb. Med., Oxford University Press, 2010: pp. 2604–2618. https://doi.org/10.1093/med/9780199204854.003.160102.

[12] R.J. Stenger, D. Spiro, Structure of the cardiac muscle cell, Am. J. Med. 30 (1961) 653–665. https://doi.org/10.1016/0002-9343(61)90205-4.

[13] C.A. Walker, F.G. Spinale, The structure and function of the cardiac myocyte: A review of fundamental concepts, J. Thorac. Cardiovasc. Surg. 118 (1999) 375–382. https://doi.org/10.1016/S0022-5223(99)70233-3.

[14] R. Laird, Cardiovascular Structure and Function, in: Cardiopulm. Phys. Ther., Elsevier, 1999: pp. 3–38. https://doi.org/10.1016/B978-032301840-1.50005-0.

[15] J.W. Calvert, D.J. Lefer, Overview of Cardiac Muscle Physiology, in: Muscle, Elsevier, 2012: pp. 57–66. https://doi.org/10.1016/B978-0-12-381510-1.00006-5.

[16] R. Bassel-Duby, E.N. Olson, Biochemistry of Development: Striated Muscle, in: Encycl. Biol. Chem., Elsevier, 2013: pp. 179–186. https://doi.org/10.1016/B978-0-12-378630-2.00091-8.

[17] F. Z. Asumda, Troponin and Tropomyosin in the Cardiomyocyte Nucleus:What for?, Int. J. Cardiovasc. Res. 02 (2013). https://doi.org/10.4172/2324-8602.1000137.

[18] N. Bildyug, Extracellular Matrix in Regulation of Contractile System in Cardiomyocytes, Int. J. Mol. Sci. 20 (2019). https://doi.org/10.3390/ijms20205054.

[19] J.G. Lichter, E. Carruth, C. Mitchell, A.S. Barth, T. Aiba, D.A. Kass, G.F. Tomaselli, J.H. Bridge, F.B. Sachse, Remodeling of the sarcomeric cytoskeleton in cardiac ventricular myocytes during heart failure and after cardiac resynchronization therapy, J. Mol. Cell. Cardiol. 72 (2014) 186–195. https://doi.org/10.1016/j.yjmcc.2014.03.012.

[20] M. Chu, C.C. Gregorio, C.T. Pappas, Nebulin, a multi-functional giant, J. Exp. Biol. 219 (2016) 146–152. https://doi.org/10.1242/jeb.126383.

[21] M. Pruna, E. Ehler, The intercalated disc: a mechanosensing signalling node in cardiomyopathy, Biophys. Rev. 12 (2020) 931–946. https://doi.org/10.1007/s12551-020-00737-x.

[22] C.B. Estigoy, F. Pontén, J. Odeberg, B. Herbert, M. Guilhaus, M. Charleston, J.W.K. Ho, D. Cameron, C.G. Dos Remedios, Intercalated discs: multiple proteins perform multiple functions in non-failing and failing human hearts, Biophys. Rev. 1 (2009) 43. https://doi.org/10.1007/s12551-008-0007-y.

[23] N.G. Frangogiannis, The Extracellular Matrix in Ischemic and Nonischemic Heart Failure, Circ. Res. 125 (2019) 117–146. https://doi.org/10.1161/CIRCRESAHA.119.311148.

[24] I. Valiente-Alandi, A.E. Schafer, B.C. Blaxall, Extracellular matrix-mediated cellular communication in the heart, J. Mol. Cell. Cardiol. 91 (2016) 228–237. https://doi.org/10.1016/j.yjmcc.2016.01.011.

[25] H. Ju, I.M.C. Dixon, Cardiac Extracellular Matrix and its Role in the Development of Heart Failure, in: P.K. Singal, I.M.C. Dixon, R.E. Beamish, N.S. Dhalla (Eds.), Mech. Heart Fail., Springer US, Boston, MA, 1995: pp. 75–90. https://doi.org/10.1007/978-1-4615-2003-0_7.

[26] M. Zwitter, J.S. Tobias, A survey of the ethical considerations in randomised trials for lung cancer, Lung Cancer Amst. Neth. 19 (1998) 197–210. https://doi.org/10.1016/s0169-5002(97)00099-8.

[27] G.C. Yeo, F.W. Keeley, A.S. Weiss, Coacervation of tropoelastin, Adv. Colloid Interface Sci. 167 (2011) 94–103. https://doi.org/10.1016/j.cis.2010.10.003.

[28] L. Timmers, G. Pasterkamp, V.C. de Hoog, F. Arslan, Y. Appelman, D.P.V. de Kleijn, The innate immune response in reperfused myocardium, Cardiovasc. Res. 94 (2012) 276–283. https://doi.org/10.1093/cvr/cvs018.

[29] F.G. Thankam, Z.K. Roesch, M.F. Dilisio, M.M. Radwan, A. Kovilam, R.M. Gross, D.K. Agrawal, Association of Inflammatory Responses and ECM Disorganization with HMGB1 Upregulation and NLRP3 Inflammasome Activation in the Injured Rotator Cuff Tendon, Sci. Rep. 8 (2018) 8918. https://doi.org/10.1038/s41598-018-27250-2.

[30] J.M. Wells, A. Gaggar, J.E. Blalock, MMP generated matrikines, Matrix Biol. 44–46 (2015) 122–129. https://doi.org/10.1016/j.matbio.2015.01.016.

[31] N.G. Frangogiannis, The extracellular matrix in myocardial injury, repair and remodeling, J. Clin. Invest. 127 (2017) 1600–1612. https://doi.org/10.1172/JCI87491.

[32] M. Domenech, L. Polo-Corrales, J.E. Ramirez-Vick, D.O. Freytes, Tissue Engineering Strategies for Myocardial Regeneration: Acellular Versus Cellular Scaffolds?, Tissue Eng. Part B Rev. 22 (2016) 438–458. https://doi.org/10.1089/ten.teb.2015.0523.

[33] M. Qasim, P. Arunkumar, H.M. Powell, M. Khan, Current research trends and challenges in tissue engineering for mending broken hearts, Life Sci. 229 (2019) 233–250. https://doi.org/10.1016/j.lfs.2019.05.012.

[34] A. Hasan, A. Khattab, M.A. Islam, K.A. Hweij, J. Zeitouny, R. Waters, M. Sayegh, M.M. Hossain, A. Paul, Injectable Hydrogels for Cardiac Tissue Repair after Myocardial Infarction, Adv. Sci. Weinh. Baden-Wurtt. Ger. 2 (2015) 1500122. https://doi.org/10.1002/advs.201500122.

[35] H.M. Nugent, E.R. Edelman, Tissue Engineering Therapy for Cardiovascular Disease, Circ. Res. 92 (2003) 1068–1078. https://doi.org/10.1161/01.RES.0000073844.41372.38.

[36] M. Boffito, S. Sartori, G. Ciardelli, Polymeric scaffolds for cardiac tissue engineering: requirements and fabrication technologies: Polymeric scaffolds for cardiac tissue engineering, Polym. Int. 63 (2014) 2–11. https://doi.org/10.1002/pi.4608.

[37] M. Arnal-Pastor, J. C., M. Monlen, A. Valls- Lluch, Biomaterials for Cardiac Tissue Engineering, in: J.A. Andrades (Ed.), Regen. Med. Tissue Eng., InTech, 2013. https://doi.org/10.5772/56076.

[38] G. Camci-Unal, H. Aubin, A.F. Ahari, H. Bae, J.W. Nichol, A. Khademhosseini, Surface-modified hyaluronic acid hydrogels to capture endothelial progenitor cells, Soft Matter. 6 (2010) 5120–5126. https://doi.org/10.1039/c0sm00508h.

[39] Z. Li, J. Guan, Hydrogels for Cardiac Tissue Engineering, Polymers. 3 (2011) 740–761. https://doi.org/10.3390/polym3020740.

[40] F.G. Thankam, J. Muthu, Biosynthetic hydrogels-Studies on chemical and physical characteristics on long-term cellular response for tissue engineering: Biosynthetic Hydrogels, J. Biomed. Mater. Res. A. 102 (2014) 2238–2247. https://doi.org/10.1002/jbm.a.34895.

[41] G.N. Grover, N. Rao, K.L. Christman, Myocardial matrix–polyethylene glycol hybrid hydrogels for tissue engineering, Nanotechnology. 25 (2014) 014011. https://doi.org/10.1088/0957-4484/25/1/014011.

[42] C.L. McGann, E.A. Levenson, K.L. Kiick, Resilin-Based Hybrid Hydrogels for Cardiovascular Tissue Engineering, Macromol. Chem. Phys. 214 (2013) 203–213. https://doi.org/10.1002/macp.201200412.

[43] B. Peña, M. Laughter, S. Jett, T.J. Rowland, M.R.G. Taylor, L. Mestroni, D. Park, Injectable Hydrogels for Cardiac Tissue Engineering, Macromol. Biosci. 18 (2018) e1800079. https://doi.org/10.1002/mabi.201800079.

[44] S.D. Anker, A.J.S. Coats, G. Cristian, D. Dragomir, E. Pusineri, M. Piredda, L. Bettari, R. Dowling, M. Volterrani, B.-A. Kirwan, G. Filippatos, J.-L. Mas, N. Danchin, S.D. Solomon, R.J. Lee, F. Ahmann, A. Hinson, H.N. Sabbah, D.L. Mann, A prospective comparison of alginate-hydrogel with standard medical therapy to determine impact on functional capacity and clinical outcomes in patients with advanced heart failure (AUGMENT-HF trial), Eur. Heart J. 36 (2015) 2297–2309. https://doi.org/10.1093/eurheartj/ehv259.

[45] Y. Song, C. Zhang, J. Zhang, N. Sun, K. Huang, H. Li, Z. Wang, K. Huang, L. Wang, An injectable silk sericin hydrogel promotes cardiac functional recovery after ischemic myocardial infarction, Acta Biomater. 41 (2016) 210–223. https://doi.org/10.1016/j.actbio.2016.05.039.

[46] J.L. Drury, D.J. Mooney, Hydrogels for tissue engineering: scaffold design variables and applications, Biomaterials. 24 (2003) 4337–4351. https://doi.org/10.1016/S0142-9612(03)00340-5.

[47] A.M. Kloxin, M.W. Tibbitt, K.S. Anseth, Synthesis of photodegradable hydrogels as dynamically tunable cell culture platforms, Nat. Protoc. 5 (2010) 1867–1887. https://doi.org/10.1038/nprot.2010.139.

[48] S. Mantha, S. Pillai, P. Khayambashi, A. Upadhyay, Y. Zhang, O. Tao, H.M. Pham, S.D. Tran, Smart Hydrogels in Tissue Engineering and Regenerative Medicine, Mater. Basel Switz. 12 (2019). https://doi.org/10.3390/ma12203323.

[49] I.C.P. Rodrigues, A. Kaasi, R. Maciel Filho, A.L. Jardini, L.P. Gabriel, Cardiac tissue engineering: current state-of-the-art materials, cells and tissue formation, Einstein Sao Paulo Braz. 16 (2018) eRB4538. https://doi.org/10.1590/S1679-45082018RB4538.

[50] A. Eltom, G. Zhong, A. Muhammad, Scaffold Techniques and Designs in Tissue Engineering Functions and Purposes: A Review, Adv. Mater. Sci. Eng. 2019 (2019) 1–13. https://doi.org/10.1155/2019/3429527.

[51] G. Turnbull, J. Clarke, F. Picard, P. Riches, L. Jia, F. Han, B. Li, W. Shu, 3D bioactive composite scaffolds for bone tissue engineering, Bioact. Mater. 3 (2018) 278–314. https://doi.org/10.1016/j.bioactmat.2017.10.001.

[52] C.J. Bettinger, J.T. Borenstein, R. Langer, Micro- and Nanofabricated Scaffolds, in: Princ. Tissue Eng., Elsevier, 2007: pp. 341–358. https://doi.org/10.1016/B978-012370615-7/50028-7.

[53] E.M. Prieto, S.A. Guelcher, Tailoring properties of polymeric biomedical foams, in: Biomed. Foams Tissue Eng. Appl., Elsevier, 2014: pp. 129–162. https://doi.org/10.1533/9780857097033.1.129.

[54] F. Wahid, T. Khan, Z. Hussain, H. Ullah, Nanocomposite scaffolds for tissue engineering; properties, preparation and applications, in: Appl. Nanocomposite Mater. Drug Deliv., Elsevier, 2018: pp. 701–735. https://doi.org/10.1016/B978-0-12-813741-3.00031-5.

[55] H. Liu, X. Ding, G. Zhou, P. Li, X. Wei, Y. Fan, Electrospinning of Nanofibers for Tissue Engineering Applications, J. Nanomater. 2013 (2013) 1–11. https://doi.org/10.1155/2013/495708.

[56] I. Jun, H.-S. Han, J.R. Edwards, H. Jeon, Electrospun Fibrous Scaffolds for Tissue Engineering: Viewpoints on Architecture and Fabrication, Int. J. Mol. Sci. 19 (2018). https://doi.org/10.3390/ijms19030745.

[57] F. Xing, Z. Xiang, P.M. Rommens, U. Ritz, 3D Bioprinting for Vascularized Tissue-Engineered Bone Fabrication, Mater. Basel Switz. 13 (2020). https://doi.org/10.3390/ma13102278.

[58] J. Gopinathan, I. Noh, Recent trends in bioinks for 3D printing, Biomater. Res. 22 (2018) 11. https://doi.org/10.1186/s40824-018-0122-1.

[59] M.J. Hodgson, C.C. Knutson, N. Momtahan, A.D. Cook, Extracellular Matrix from Whole Porcine Heart Decellularization for Cardiac Tissue Engineering, Methods Mol. Biol. Clifton NJ. 1577 (2018) 95–102. https://doi.org/10.1007/7651_2017_31.

[60] A. Porzionato, E. Stocco, S. Barbon, F. Grandi, V. Macchi, R. De Caro, Tissue-Engineered Grafts from Human Decellularized Extracellular Matrices: A Systematic Review and Future Perspectives, Int. J. Mol. Sci. 19 (2018). https://doi.org/10.3390/ijms19124117.

[61] P. Kc, Y. Hong, G. Zhang, Cardiac tissue-derived extracellular matrix scaffolds for myocardial repair: advantages and challenges, Regen. Biomater. 6 (2019) 185–199. https://doi.org/10.1093/rb/rbz017.

[62] Lewis MR., Muscular contraction in tissue cultures., Contrib Embryol Carnegie Inst. 9 (1920) 191–212.

[63] A.A. MOSCONA, Tissues from dissociated cells, Sci. Am. 200 (1959) 132-134 passim.

[64] T.F. McDonald, H.G. Sachs, R.L. DeHaan, Development of Sensitivity to Tetrodotoxin in Beating Chick Embryo Hearts, Single Cells and Aggregates, Science. 176 (1972) 1248–1250. https://doi.org/10.1126/science.176.4040.1248.

[65] D.G. Simpson, L. Terracio, M. Terracio, R.L. Price, D.C. Turner, T.K. Borg, Modulation of cardiac myocyte phenotype in vitro by the composition and orientation of the extracellular matrix, J. Cell. Physiol. 161 (1994) 89–105. https://doi.org/10.1002/jcp.1041610112.

[66] H.H. Vandenburgh, P. Karlisch, L. Farr, Maintenance of highly contractile tissue-cultured avian skeletal myotubes in collagen gel, Vitro Cell. Dev. Biol. J. Tissue Cult. Assoc. 24 (1988) 166–174.

[67] L. Terracio, B. Miller, T.K. Borg, Effects of cyclic mechanical stimulation of the cellular components of the heart: in vitro, Vitro Cell. Dev. Biol. J. Tissue Cult. Assoc. 24 (1988) 53–58.

[68] M.S. Kolodney, E.L. Elson, Correlation of myosin light chain phosphorylation with isometric contraction of fibroblasts, J. Biol. Chem. 268 (1993) 23850–23855.

[69] R.L. Carrier, M. Papadaki, M. Rupnick, F.J. Schoen, N. Bursac, R. Langer, L.E. Freed, G. Vunjak-Novakovic, Cardiac tissue engineering: cell seeding, cultivation parameters and tissue construct characterization, Biotechnol. Bioeng. 64 (1999) 580–589.

[70] R.K. Li, Z.Q. Jia, R.D. Weisel, D.A. Mickle, A. Choi, T.M. Yau, Survival and function of bioengineered cardiac grafts, Circulation. 100 (1999) II63-69.

[71] J. Leor, S. Aboulafia-Etzion, A. Dar, L. Shapiro, I.M. Barbash, A. Battler, Y. Granot, S. Cohen, Bioengineered cardiac grafts: A new approach to repair the infarcted myocardium?, Circulation. 102 (2000) III56-61.

[72] M. Radisic, H. Park, H. Shing, T. Consi, F.J. Schoen, R. Langer, L.E. Freed, G. Vunjak-Novakovic, Functional assembly of engineered myocardium by electrical stimulation of cardiac myocytes cultured on scaffolds, Proc. Natl. Acad. Sci. U. S. A. 101 (2004) 18129–18134. https://doi.org/10.1073/pnas.0407817101.

[73] T. Shimizu, M. Yamato, Y. Isoi, T. Akutsu, T. Setomaru, K. Abe, A. Kikuchi, M. Umezu, T. Okano, Fabrication of pulsatile cardiac tissue grafts using a novel 3-dimensional cell sheet manipulation technique and temperature-responsive cell culture surfaces, Circ. Res. 90 (2002) e40.

[74] V. Mironov, T. Boland, T. Trusk, G. Forgacs, R.R. Markwald, Organ printing: computer-aided jet-based 3D tissue engineering, Trends Biotechnol. 21 (2003) 157–161. https://doi.org/10.1016/S0167-7799(03)00033-7.

[75] C. Doescher, A. Thai, E. Cha, P.V. Cheng, D.K. Agrawal, F.G. Thankam, Intelligent Hydrogels in Myocardial Regeneration and Engineering, Gels Basel Switz. 8 (2022) 576. https://doi.org/10.3390/gels8090576.

[76] B.C. Kallukalam, M. Jayabalan, V. Sankar, Studies on chemically crosslinkable carboxy terminated-poly(propylene fumarate-co-ethylene glycol)-acrylamide hydrogel as an injectable biomaterial, Biomed. Mater. Bristol Engl. 4 (2009) 015002. https://doi.org/10.1088/1748-6041/25/1/015002.

[77] H. Naito, Y. Takewa, T. Mizuno, S. Ohya, Y. Nakayama, E. Tatsumi, S. Kitamura, H. Takano, S. Taniguchi, Y. Taenaka, Three-dimensional cardiac tissue engineering using a thermoresponsive artificial extracellular matrix, ASAIO J. Am. Soc. Artif. Intern. Organs 1992. 50 (2004) 344–348.

[78] T. Sakai, R.K. Li, R.D. Weisel, D.A. Mickle, E.T. Kim, Z.Q. Jia, T.M. Yau, The fate of a tissue-engineered cardiac graft in the right ventricular outflow tract of the rat, J. Thorac. Cardiovasc. Surg. 121 (2001) 932–942. https://doi.org/10.1067/mtc.2001.113600.

[79] T.C. McDevitt, S.P. Palecek, Innovation in the culture and derivation of pluripotent human stem cells, Curr. Opin. Biotechnol. 19 (2008) 527–533. https://doi.org/10.1016/j.copbio.2008.08.005.

[80] T. Shinoka, C.K. Breuer, R.E. Tanel, G. Zund, T. Miura, P.X. Ma, R. Langer, J.P. Vacanti, J.E. Mayer, Tissue engineering heart valves: valve leaflet replacement study in a lamb model, Ann. Thorac. Surg. 60 (1995) S513-516. https://doi.org/10.1016/0003-4975(95)00733-4.

[81] T. Shinoka, P.X. Ma, D. Shum-Tim, C.K. Breuer, R.A. Cusick, G. Zund, R. Langer, J.P. Vacanti, J.E. Mayer, Tissue-engineered heart valves. Autologous valve leaflet replacement study in a lamb model, Circulation. 94 (1996) II164-168.

[82] O. Ishii, M. Shin, T. Sueda, J.P. Vacanti, In vitro tissue engineering of a cardiac graft using a degradable scaffold with an extracellular matrix-like topography, J. Thorac. Cardiovasc. Surg. 130 (2005) 1358–1363. https://doi.org/10.1016/j.jtcvs.2005.05.048.

[83] N. Baheiraei, R. Gharibi, H. Yeganeh, M. Miragoli, N. Salvarani, E. Di Pasquale, G. Condorelli, Electroactive polyurethane/siloxane derived from castor oil as a versatile cardiac patch, part I: Synthesis, characterization,and myoblast proliferation and differentiation, J. Biomed. Mater. Res. A. 104 (2016) 1570–1570. https://doi.org/10.1002/jbm.a.35712.

[84] S. Trombino, F. Curcio, R. Cassano, M. Curcio, G. Cirillo, F. Iemma, Polymeric Biomaterials for the Treatment of Cardiac Post-Infarction Injuries, Pharmaceutics. 13 (2021) 1038. https://doi.org/10.3390/pharmaceutics13071038.

[85] S. Vigneswari, J.M. Chai, K.H. Kamarudin, A.-A.A. Amirul, M.L. Focarete, S. Ramakrishna, Elucidating the Surface Functionality of Biomimetic RGD Peptides Immobilized on Nano-P(3HB-co-4HB) for H9c2 Myoblast Cell Proliferation, Front. Bioeng. Biotechnol. 8 (2020) 567693. https://doi.org/10.3389/fbioe.2020.567693.

[86] A. Liberski, N. Latif, C. Raynaud, C. Bollensdorff, M. Yacoub, Alginate for cardiac regeneration: From seaweed to clinical trials, Glob. Cardiol. Sci. Pract. 2016 (n.d.) e201604. https://doi.org/10.21542/gcsp.2016.4.

[87] N. Landa, L. Miller, M.S. Feinberg, R. Holbova, M. Shachar, I. Freeman, S. Cohen, J. Leor, Effect of injectable alginate implant on cardiac remodeling and function after recent and old infarcts in rat, Circulation. 117 (2008) 1388–1396. https://doi.org/10.1161/CIRCULATIONAHA.107.727420.

[88] J. Leor, S. Tuvia, V. Guetta, F. Manczur, D. Castel, U. Willenz, O. Petneházy, N. Landa, M.S. Feinberg, E. Konen, O. Goitein, O. Tsur-Gang, M. Shaul, L. Klapper, S. Cohen, Intracoronary injection of in situ forming alginate hydrogel reverses left ventricular remodeling after myocardial infarction in Swine, J. Am. Coll. Cardiol. 54 (2009) 1014–1023. https://doi.org/10.1016/j.jacc.2009.06.010.

[89] J. Rodness, A. Mihic, Y. Miyagi, J. Wu, R.D. Weisel, R.-K. Li, VEGF-loaded microsphere patch for local protein delivery to the ischemic heart, Acta Biomater. 45 (2016) 169–181. https://doi.org/10.1016/j.actbio.2016.09.009.

[90] B. Guo, P.X. Ma, Conducting Polymers for Tissue Engineering, Biomacromolecules. 19 (2018) 1764–1782. https://doi.org/10.1021/acs.biomac.8b00276.

[91] G. Liu, L. Li, D. Huo, Y. Li, Y. Wu, L. Zeng, P. Cheng, M. Xing, W. Zeng, C. Zhu, A VEGF delivery system targeting MI improves angiogenesis and cardiac function based on the tropism of MSCs and layer-by-layer self-assembly, Biomaterials. 127 (2017) 117–131. https://doi.org/10.1016/j.biomaterials.2017.03.001.

[92] N.E. Beltran-Vargas, E. Peña-Mercado, C. Sánchez-Gómez, M. Garcia-Lorenzana, J.-C. Ruiz, I. Arroyo-Maya, S. Huerta-Yepez, J. Campos-Terán, Sodium Alginate/Chitosan Scaffolds for Cardiac Tissue Engineering: The Influence of Its Three-Dimensional Material Preparation and the Use of Gold Nanoparticles, Polymers. 14 (2022) 3233. https://doi.org/10.3390/polym14163233.

[93] M. Tamimi, S. Rajabi, M. Pezeshki-Modaress, Cardiac ECM/chitosan/alginate ternary scaffolds for cardiac tissue engineering application, Int. J. Biol. Macromol. 164 (2020) 389–402. https://doi.org/10.1016/j.ijbiomac.2020.07.134.

[94] A. Mousavi, S. Mashayekhan, N. Baheiraei, A. Pourjavadi, Biohybrid oxidized alginate/myocardial extracellular matrix injectable hydrogels with improved electromechanical properties for cardiac tissue engineering, Int. J. Biol. Macromol. 180 (2021) 692–708. https://doi.org/10.1016/j.ijbiomac.2021.03.097.

[95] J. Zhou, W. Liu, X. Zhao, Y. Xian, W. Wu, X. Zhang, N. Zhao, F.-J. Xu, C. Wang, Natural Melanin/Alginate Hydrogels Achieve Cardiac Repair through ROS Scavenging and Macrophage Polarization, Adv. Sci. 8 (2021) 2100505. https://doi.org/10.1002/advs.202100505.

[96] M.I. Neves, L. Moroni, C.C. Barrias, Modulating Alginate Hydrogels for Improved Biological Performance as Cellular 3D Microenvironments, Front. Bioeng. Biotechnol. 8 (2020). https://www.frontiersin.org/articles/10.3389/fbioe.2020.00665 (accessed February 24, 2023).

[97] T. Hao, J. Li, F. Yao, D. Dong, Y. Wang, B. Yang, C. Wang, Injectable Fullerenol/Alginate Hydrogel for Suppression of Oxidative Stress Damage in Brown Adipose-Derived Stem Cells and Cardiac Repair, ACS Nano. 11 (2017) 5474–5488. https://doi.org/10.1021/acsnano.7b00221.

[98] K. Lv, Q. Li, L. Zhang, Y. Wang, Z. Zhong, J. Zhao, X. Lin, J. Wang, K. Zhu, C. Xiao, C. Ke, S. Zhong, X. Wu, J. Chen, H. Yu, W. Zhu, X. Li, B. Wang, R. Tang, J. Wang, J. Huang, X. Hu, Incorporation of small extracellular vesicles in sodium alginate hydrogel as a novel therapeutic strategy for myocardial infarction, Theranostics. 9 (2019) 7403–7416. https://doi.org/10.7150/thno.32637.

[99] G. Cattelan, A. Guerrero Gerbolés, R. Foresti, P.P. Pramstaller, A. Rossini, M. Miragoli, C. Caffarra Malvezzi, Alginate Formulations: Current Developments in the Race for Hydrogel-Based Cardiac Regeneration, Front. Bioeng. Biotechnol. 8 (2020). https://www.frontiersin.org/articles/10.3389/fbioe.2020.00414 (accessed February 28, 2023).

[100] J. Namkaew, P. Laowpanitchakorn, N. Sawaddee, S. Jirajessada, S. Honsawek, S. Yodmuang, Carboxymethyl Cellulose Entrapped in a Poly(vinyl) Alcohol Network: Plant-Based Scaffolds for Cartilage Tissue Engineering, Molecules. 26 (2021) 578. https://doi.org/10.3390/molecules26030578.

[101] C. Phan, H. Walther, D. Riederer, C. Lau, K.O. Lorenz, L.N. Subbaraman, L. Jones, Analysis of polyvinyl alcohol release from commercially available daily disposable contact lenses using an in vitro eye model, J. Biomed. Mater. Res. B Appl. Biomater. 107 (2019) 1662–1668. https://doi.org/10.1002/jbm.b.34259.

[102] S. Sakai, M. Tsumura, M. Inoue, Y. Koga, K. Fukano, M. Taya, Polyvinyl alcohol-based hydrogel dressing gellable on-wound via a co-enzymatic reaction triggered by glucose in the wound exudate, J. Mater. Chem. B. 1 (2013) 5067. https://doi.org/10.1039/c3tb20780c.

[103] S. Sedighim, Y. Chen, C. Xu, R. Mohindra, H. Liu, D.K. Agrawal, F.G. Thankam, Carboxymethyl cellulose–alginate interpenetrating hydroxy ethyl methacrylate crosslinked polyvinyl alcohol reinforced hybrid hydrogel templates with improved biological performance for cardiac tissue engineering, Biotechnol. Bioeng. 120 (2023) 819–835. https://doi.org/10.1002/bit.28291.

[104] Y. He, H. Hou, S. Wang, R. Lin, L. Wang, L. Yu, X. Qiu, From waste of marine culture to natural patch in cardiac tissue engineering, Bioact. Mater. 6 (2021) 2000–2010. https://doi.org/10.1016/j.bioactmat.2020.12.011.

[105] R.B. Simeoni, B.F. Mogharbel, J.C. Francisco, N.I. Miyague, A.C. Irioda, C.M.C.O. Souza, D. Souza, P.E.F. Stricker, N.N. da Rosa, C.F. Souza, C.R.C. Franco, M.-R. Sierakowski, E. Abdelwaid, L.C. Guarita-Souza, K.A.T. Carvalho, Beneficial Roles of Cellulose Patch-Mediated Cell Therapy in Myocardial Infarction: A Preclinical Study, Cells. 10 (2021) 424. https://doi.org/10.3390/cells10020424.

[106] E. Entcheva, H. Bien, L. Yin, C.-Y. Chung, M. Farrell, Y. Kostov, Functional cardiac cell constructs on cellulose-based scaffolding, Biomaterials. 25 (2004) 5753–5762. https://doi.org/10.1016/j.biomaterials.2004.01.024.

[107] P.-H. Chen, H.-C. Liao, S.-H. Hsu, R.-S. Chen, M.-C. Wu, Y.-F. Yang, C.-C. Wu, M.-H. Chen, W.-F. Su, A novel polyurethane/cellulose fibrous scaffold for cardiac tissue engineering, RSC Adv. 5 (2015) 6932–6939. https://doi.org/10.1039/C4RA12486C.

[108] An origami 3D patterned cellulose-based scaffold for bioengineering cardiovascular applications, (2022). https://doi.org/10.21203/rs.3.rs-2186204/v1.

[109] E. Chainoglou, V. Karagkiozaki, T. Choli-Papadopoulou, C. Mavromanolis, A. Laskarakis, S. Logothetidis, Development of Biofunctionalized Cellulose Acetate Nanoscaffolds for Heart Valve Tissue Engineering, World J. Nano Sci. Eng. 06 (2016) 129–152. https://doi.org/10.4236/wjnse.2016.64013.

[110] S. Iravani, R.S. Varma, Cellulose-Based Composites as Scaffolds for Tissue Engineering: Recent Advances, Molecules. 27 (2022) 8830. https://doi.org/10.3390/molecules27248830.

[111] F.K. Andrade, R. Costa, L. Domingues, R. Soares, M. Gama, Improving bacterial cellulose for blood vessel replacement: Functionalization with a chimeric protein containing a cellulose-binding module and an adhesion peptide, Acta Biomater. 6 (2010) 4034–4041. https://doi.org/10.1016/j.actbio.2010.04.023.

[112] D. Fusco, F. Meissner, B.K. Podesser, A. Marsano, M. Grapow, F. Eckstein, B. Winkler, Small-diameter bacterial cellulose-based vascular grafts for coronary artery bypass grafting in a pig model, Front. Cardiovasc. Med. 9 (2022) 881557. https://doi.org/10.3389/fcvm.2022.881557.

[113] L. Liu, X. Ji, L. Mao, L. Wang, K. Chen, Z. Shi, A.A.Q. Ahmed, S. Thomas, R.V. Vasilievich, L. Xiao, X. Li, G. Yang, Hierarchical-structured bacterial cellulose/potato starch tubes as potential small-diameter vascular grafts, Carbohydr. Polym. 281 (2022) 119034. https://doi.org/10.1016/j.carbpol.2021.119034.

[114] K. Novotna, P. Havelka, T. Sopuch, K. Kolarova, V. Vosmanska, V. Lisa, V. Svorcik, L. Bacakova, Cellulose-based materials as scaffolds for tissue engineering, Cellulose. 20 (2013) 2263–2278. https://doi.org/10.1007/s10570-013-0006-4.

[115] W.-F. Su, C.-C. Ho, T.-H. Shih, C.-H. Wang, C.-H. Yeh, Exceptional biocompatibility of 3D fibrous scaffold for cardiac tissue engineering fabricated from biodegradable polyurethane blended with cellulose, Int. J. Polym. Mater. Polym. Biomater. 65 (2016) 703–711. https://doi.org/10.1080/00914037.2016.1157802.

[116] L. Jongpaiboonkit, W.J. King, G.E. Lyons, A.L. Paguirigan, J.W. Warrick, D.J. Beebe, W.L. Murphy, An adaptable hydrogel array format for 3-dimensional cell culture and analysis, Biomaterials. 29 (2008) 3346–3356. https://doi.org/10.1016/j.biomaterials.2008.04.040.

[117] J.L. Young, A.J. Engler, Hydrogels with time-dependent material properties enhance cardiomyocyte differentiation in vitro, Biomaterials. 32 (2011) 1002–1009. https://doi.org/10.1016/j.biomaterials.2010.10.020.

[118] G.N. Grover, N. Rao, K.L. Christman, Myocardial Matrix-Polyethylene Glycol Hybrid Hydrogels for Tissue Engineering, Nanotechnology. 25 (2014) 014011. https://doi.org/10.1088/0957-4484/25/1/014011.

[119] Z. Li, J. Guan, Hydrogels for Cardiac Tissue Engineering, Polymers. 3 (2011) 740–761. https://doi.org/10.3390/polym3020740.

[120] X. Zhang, B. Xu, D.S. Puperi, A.L. Yonezawa, Y. Wu, H. Tseng, M.L. Cuchiara, J.L. West, K.J. Grande-Allen, Integrating valve-inspired design features into poly(ethylene glycol) hydrogel scaffolds for heart valve tissue engineering, Acta Biomater. 14 (2015) 11–21. https://doi.org/10.1016/j.actbio.2014.11.042.

[121] D.-H. Kim, P. Kim, I. Song, J.M. Cha, S.H. Lee, B. Kim, K.Y. Suh, Guided three-dimensional growth of functional cardiomyocytes on polyethylene glycol nanostructures, Langmuir ACS J. Surf. Colloids. 22 (2006) 5419–5426. https://doi.org/10.1021/la060283u.

[122] S. Somekawa, A. Mahara, K. Masutani, Y. Kimura, H. Urakawa, T. Yamaoka, Effect of Thermoresponsive Poly(L-lactic acid)-poly(ethylene glycol) Gel Injection on Left Ventricular Remodeling in a Rat Myocardial Infarction Model, Tissue Eng. Regen. Med. 14 (2017) 507–516. https://doi.org/10.1007/s13770-017-0067-9.

[123] L. Gómez-Cid, M.L. López-Donaire, D. Velasco, V. Marín, M.I. González, B. Salinas, L. Cussó, Á. García, S.B. Bravo, M.E. Fernández-Santos, C. Elvira, J. Sierra, E. Arroba, R. Bañares, L. Grigorian-Shamagian, F. Fernández-Avilés, Cardiac Extracellular Matrix Hydrogel Enriched with Polyethylene Glycol Presents Improved Gelation Time and Increased On-Target Site Retention of Extracellular Vesicles, Int. J. Mol. Sci. 22 (2021) 9226. https://doi.org/10.3390/ijms22179226.

[124] E. Dattola, E.I. Parrotta, S. Scalise, G. Perozziello, T. Limongi, P. Candeloro, M.L. Coluccio, C. Maletta, L. Bruno, M.T.D. Angelis, G. Santamaria, V. Mollace, E. Lamanna, E.D. Fabrizio, G. Cuda, Development of 3D PVA scaffolds for cardiac tissue engineering and cell screening applications, RSC Adv. 9 (2019) 4246–4257. https://doi.org/10.1039/C8RA08187E.

[125] M.M. Sayed, H.M. Mousa, M.R. El-Aassar, N.M. El-Deeb, N.M. Ghazaly, M.M. Dewidar, A. Abdal-hay, Enhancing mechanical and biodegradation properties of polyvinyl alcohol/silk fibroin nanofibers composite patches for Cardiac Tissue Engineering, Mater. Lett. 255 (2019) 126510. https://doi.org/10.1016/j.matlet.2019.126510.

[126] S. Mombini, J. Mohammadnejad, B. Bakhshandeh, A. Narmani, J. Nourmohammadi, S. Vahdat, S. Zirak, Chitosan-PVA-CNT nanofibers as electrically conductive scaffolds for cardiovascular tissue engineering, Int. J. Biol. Macromol. 140 (2019) 278–287. https://doi.org/10.1016/j.ijbiomac.2019.08.046.

[127] P. Pushp, R. Bhaskar, S. Kelkar, N. Sharma, D. Pathak, M.K. Gupta, Plasticized poly(vinylalcohol) and poly(vinylpyrrolidone) based patches with tunable mechanical properties for cardiac tissue engineering applications, Biotechnol. Bioeng. 118 (2021) 2312–2325. https://doi.org/10.1002/bit.27743.

[128] C. Hu, F. Tang, Q. Wu, B. Guo, W.A. Long, Y. Ruan, L. Li, Novel Trilaminar Polymeric Antiadhesion Membrane Prevents Postoperative Pericardial Adhesion, Ann. Thorac. Surg. 111 (2021) 184–189. https://doi.org/10.1016/j.athoracsur.2020.03.011.

[129] F. Gnanaprakasam Thankam, J. Muthu, V. Sankar, R. Kozhiparambil Gopal, Growth and survival of cells in biosynthetic poly vinyl alcohol–alginate IPN hydrogels for cardiac applications, Colloids Surf. B Biointerfaces. 107 (2013) 137–145. https://doi.org/10.1016/j.colsurfb.2013.01.069.

[130] H.M. Mousa, K.H. Hussein, M.M. Sayed, M.R. El-Aassar, I.M.A. Mohamed, H.-H. Kwak, H.-M. Woo, A. Abdal-hay, Development of biocompatible tri-layered nanofibers patches with endothelial cells for cardiac tissue engineering, Eur. Polym. J. 129 (2020) 109630. https://doi.org/10.1016/j.eurpolymj.2020.109630.

[131] R. Ravichandran, R. Sridhar, J.R. Venugopal, S. Sundarrajan, S. Mukherjee, S. Ramakrishna, Gold Nanoparticle Loaded Hybrid Nanofibers for Cardiogenic Differentiation of Stem Cells for Infarcted Myocardium Regeneration, Macromol. Biosci. 14 (2014) 515–525. https://doi.org/10.1002/mabi.201300407.

[132] M. Zuluaga, G. Gregnanin, C. Cencetti, C.D. Meo, V. Gueguen, D. Letourneur, A. Meddahi-Pellé, G. Pavon-Djavid, P. Matricardi, PVA/Dextran hydrogel patches as delivery system of antioxidant astaxanthin: a cardiovascular approach, Biomed. Mater. 13 (2017) 015020. https://doi.org/10.1088/1748-605X/aa8a86.

[133] I. Frisman, D. Seliktar, H. Bianco-Peled, Nanostructuring biosynthetic hydrogels for tissue engineering: a cellular and structural analysis, Acta Biomater. 8 (2012) 51–60. https://doi.org/10.1016/j.actbio.2011.07.030.

[134] J.B. Leach, C.E. Schmidt, Characterization of protein release from photocrosslinkable hyaluronic acid-polyethylene glycol hydrogel tissue engineering scaffolds, Biomaterials. 26 (2005) 125–135. https://doi.org/10.1016/j.biomaterials.2004.02.018.

[135] P.B. Welzel, S. Prokoph, A. Zieris, M. Grimmer, S. Zschoche, U. Freudenberg, C. Werner, Modulating Biofunctional starPEG Heparin Hydrogels by Varying Size and Ratio of the Constituents, Polymers. 3 (2011) 602–620. https://doi.org/10.3390/polym3010602.

[136] G.T. Finosh, M. Jayabalan, S. Vandana, K.G. Raghu, Hybrid alginate-polyester bimodal network hydrogel for tissue engineering - Influence of structured water on long-term cellular growth, Colloids Surf. B Biointerfaces. (2015). https://doi.org/10.1016/j.colsurfb.2015.03.020.

[137] M.G. Cascone, L. Lazzeri, E. Sparvoli, M. Scatena, L.P. Serino, S. Danti, Morphological evaluation of bioartificial hydrogels as potential tissue engineering scaffolds, J. Mater. Sci. Mater. Med. 15 (2004) 1309–1313. https://doi.org/10.1007/s10856-004-5739-z.

[138] J.C. Gayet, G. Fortier, Drug release from new bioartificial hydrogel, Artif. Cells. Blood Substit. Immobil. Biotechnol. 23 (1995) 605–611.

[139] X.J. Loh, J. Li, Biodegradable thermosensitive copolymer hydrogels for drug delivery, Expert Opin. Ther. Pat. 17 (2007) 965–977. https://doi.org/10.1517/13543776.17.8.965.

[140] B. Balakrishnan, A. Jayakrishnan, Self-cross-linking biopolymers as injectable in situ forming biodegradable scaffolds, Biomaterials. 26 (2005) 3941–3951. https://doi.org/10.1016/j.biomaterials.2004.10.005.

[141] J. Sun, H. Tan, Alginate-Based Biomaterials for Regenerative Medicine Applications, Materials. 6 (2013) 1285–1309. https://doi.org/10.3390/ma6041285.

[142] H. Jin Lee, G.H. Kim, Cryogenically direct-plotted alginate scaffolds consisting of micro/nano-architecture for bone tissue regeneration, RSC Adv. 2 (2012) 7578. https://doi.org/10.1039/c2ra20836a.

[143] B.-M. Tofanica, D. Belosinschi, I. Volf, Gels, Aerogels and Hydrogels: A Challenge for the Cellulose-Based Product Industries, Gels. 8 (2022) 497. https://doi.org/10.3390/gels8080497.

[144] C. Chen, Y. Xi, Y. Weng, Recent Advances in Cellulose-Based Hydrogels for Tissue Engineering Applications, Polymers. 14 (2022) 3335. https://doi.org/10.3390/polym14163335.

[145] H. Ma, Z. Cheng, X. Li, B. Li, Y. Fu, J. Jiang, Advances and challenges of cellulose functional materials in sensors, J. Bioresour. Bioprod. 8 (2023) 15–32. https://doi.org/10.1016/j.jobab.2022.11.001.

[146] J. Zhu, Bioactive Modification of Poly(ethylene glycol) Hydrogels for Tissue Engineering, Biomaterials. 31 (2010) 4639–4656. https://doi.org/10.1016/j.biomaterials.2010.02.044.

[147] S. Sun, Y. Cui, B. Yuan, M. Dou, G. Wang, H. Xu, J. Wang, W. Yin, D. Wu, C. Peng, Drug delivery systems based on polyethylene glycol hydrogels for enhanced bone regeneration, Front. Bioeng. Biotechnol. 11 (2023). https://www.frontiersin.org/articles/10.3389/fbioe.2023.1117647 (accessed March 8, 2023).

[148] M. Wang, J. Bai, K. Shao, W. Tang, X. Zhao, D. Lin, S. Huang, C. Chen, Z. Ding, J. Ye, Poly(vinyl alcohol) Hydrogels: The Old and New Functional Materials, Int. J. Polym. Sci. 2021 (2021) e2225426. https://doi.org/10.1155/2021/2225426.

[149] A. Kumar, S.S. Han, PVA-based hydrogels for tissue engineering: A review, Int. J. Polym. Mater. Polym. Biomater. 66 (2017) 159–182. https://doi.org/10.1080/00914037.2016.1190930.

[150] Y. Chen, J. Li, J. Lu, M. Ding, Y. Chen, Synthesis and properties of Poly(vinyl alcohol) hydrogels with high strength and toughness, Polym. Test. 108 (2022) 107516. https://doi.org/10.1016/j.polymertesting.2022.107516.

[151] F. Gnanaprakasam Thankam, J. Muthu, V. Sankar, R. Kozhiparambil Gopal, Growth and survival of cells in biosynthetic poly vinyl alcohol–alginate IPN hydrogels for cardiac applications, Colloids Surf. B Biointerfaces. 107 (2013) 137–145. https://doi.org/10.1016/j.colsurfb.2013.01.069.

[152] F.G. Thankam, C. Diaz, I. Chandra, J. Link, J. Newton, M.F. Dilisio, D.K. Agrawal, Hybrid interpenetrating hydrogel network favoring the bidirectional migration of tenocytes for rotator cuff tendon regeneration, J. Biomed. Mater. Res. B Appl. Biomater. 110 (2022) 467–477. https://doi.org/10.1002/jbm.b.34924.

[153] F. Gnanaprakasam Thankam, J. Muthu, Alginate based hybrid copolymer hydrogels--influence of pore morphology on cell-material interaction, Carbohydr. Polym. 112 (2014) 235–244. https://doi.org/10.1016/j.carbpol.2014.05.083.

[154] G.T. Finosh, M. Jayabalan, S. Vandana, K.G. Raghu, Hybrid alginate-polyester bimodal network hydrogel for tissue engineering--Influence of structured water on long-term cellular growth, Colloids Surf. B Biointerfaces. 135 (2015) 855–864. https://doi.org/10.1016/j.colsurfb.2015.03.020.

[155] F.G. Thankam, C. Diaz, I. Chandra, J. Link, J. Newton, M.F. Dilisio, D.K. Agrawal, Hybrid interpenetrating hydrogel network favoring the bidirectional migration of tenocytes for rotator cuff tendon regeneration, J. Biomed. Mater. Res. B Appl. Biomater. 110 (2022) 467–477. https://doi.org/10.1002/jbm.b.34924.

[156] G.T. Finosh, M. Jayabalan, Reactive oxygen species—Control and management using amphiphilic biosynthetic hydrogels for cardiac applications, Adv. Biosci. Biotechnol. 2013 (2013). https://doi.org/10.4236/abb.2013.412150.

[157] B. Manochai, Y. Paisooksantivatana, H. Choi, J.H. Hong, Variation in DPPH scavenging activity and major volatile oil components of cassumunar ginger, Zingiber montanum (Koenig), in response to water deficit and light intensity, Sci. Hortic. 126 (2010) 462–466. https://doi.org/10.1016/j.scienta.2010.07.011.

[158] S. Shukla, A. Mehta, P. Mehta, V.K. Bajpai, Antioxidant ability and total phenolic content of aqueous leaf extract of Stevia rebaudiana Bert, Exp. Toxicol. Pathol. Off. J. Ges. Für Toxikol. Pathol. 64 (2012) 807–811. https://doi.org/10.1016/j.etp.2011.02.002.

[159] W. Fang, S. Sekhon, D. Teramoto, C. Fung, V. La, C. Duong, C. Doescher, A. Thai, F.G. Thankam, D.K. Agrawal, Pathological alterations in the expression status of rotator cuff tendon matrix components in hyperlipidemia, Mol. Cell. Biochem. (2022). https://doi.org/10.1007/s11010-022-04643-6.

[160] F.G. Thankam, C.S. Boosani, M.F. Dilisio, D.K. Agrawal, MicroRNAs associated with inflammation in shoulder tendinopathy and glenohumeral arthritis, Mol. Cell. Biochem. (2017). https://doi.org/10.1007/s11010-017-3097-7.

[161] F.G. Thankam, N.K. Larsen, A. Varghese, T.-N. Bui, M. Reilly, R.J. Fitzgibbons, D.K. Agrawal, Biomarkers and heterogeneous fibroblast phenotype associated with incisional hernia, Mol. Cell. Biochem. 476 (2021) 3353–3363. https://doi.org/10.1007/s11010-021-04166-6.

[162] F.G. Thankam, C.S. Boosani, M.F. Dilisio, N.E. Dietz, D.K. Agrawal, MicroRNAs Associated with Shoulder Tendon Matrisome Disorganization in Glenohumeral Arthritis, PloS One. 11 (2016) e0168077. https://doi.org/10.1371/journal.pone.0168077.

[163] J. Xia, E.E. Gill, R.E.W. Hancock, NetworkAnalyst for statistical, visual and network-based meta-analysis of gene expression data, Nat. Protoc. 10 (2015) 823–844. https://doi.org/10.1038/nprot.2015.052.

[164] J. Xia, M.J. Benner, R.E.W. Hancock, NetworkAnalyst - integrative approaches for protein-protein interaction network analysis and visual exploration, Nucleic Acids Res. 42 (2014) W167–W174. https://doi.org/10.1093/nar/gku443.

[165] M.R. Singh, S. Patel, D. Singh, Natural polymer-based hydrogels as scaffolds for tissue engineering, in: Nanobiomaterials Soft Tissue Eng., Elsevier, 2016: pp. 231–260. https://doi.org/10.1016/B978-0-323-42865-1.00009-X.

[166] B. Niemczyk-Soczynska, A. Gradys, P. Sajkiewicz, Hydrophilic Surface Functionalization of Electrospun Nanofibrous Scaffolds in Tissue Engineering, Polymers. 12 (2020) 2636. https://doi.org/10.3390/polym12112636.

[167] I.M. El-Sherbiny, M.H. Yacoub, Hydrogel scaffolds for tissue engineering: Progress and challenges, Glob. Cardiol. Sci. Pract. 2013 (2013) 316–342. https://doi.org/10.5339/gcsp.2013.38.

[168] A.M.J. Coenen, K.V. Bernaerts, J.A.W. Harings, S. Jockenhoevel, S. Ghazanfari, Elastic materials for tissue engineering applications: Natural, synthetic and hybrid polymers, Acta Biomater. 79 (2018) 60–82. https://doi.org/10.1016/j.actbio.2018.08.027.

[169] S. Saravanan, A. Chawla, M. Vairamani, T.P. Sastry, K.S. Subramanian, N. Selvamurugan, Scaffolds containing chitosan, gelatin and graphene oxide for bone tissue regeneration in vitro and in vivo, Int. J. Biol. Macromol. 104 (2017) 1975–1985. https://doi.org/10.1016/j.ijbiomac.2017.01.034.

[170] F.G. Thankam, C. Diaz, I. Chandra, J. Link, J. Newton, M.F. Dilisio, D.K. Agrawal, Hybrid interpenetrating hydrogel network favoring the bidirectional migration of tenocytes for rotator cuff tendon regeneration, J. Biomed. Mater. Res. B Appl. Biomater. (2021). https://doi.org/10.1002/jbm.b.34924.

[171] G.T. Finosh, M. Jayabalan, Regenerative therapy and tissue engineering for the treatment of end-stage cardiac failure: new developments and challenges, Biomatter. 2 (2012) 1–14. https://doi.org/10.4161/biom.19429.

[172] B. Vagaská, L. Bacáková, E. Filová, K. Balík, Osteogenic cells on bio-inspired materials for bone tissue engineering, Physiol. Res. 59 (2010) 309–322. https://doi.org/10.33549/physiolres.931776.

[173] I. Bružauskaitė, D. Bironaitė, E. Bagdonas, E. Bernotienė, Scaffolds and cells for tissue regeneration: different scaffold pore sizes-different cell effects, Cytotechnology. 68 (2016) 355–369. https://doi.org/10.1007/s10616-015-9895-4.

[174] F.G. Thankam, J. Muthu, Influence of physical and mechanical properties of amphiphilic biosynthetic hydrogels on long-term cell viability, J. Mech. Behav. Biomed. Mater. 35 (2014) 111–122. https://doi.org/10.1016/j.jmbbm.2014.03.010.

[175] S. Kim, S.E. Ahn, J.H. Lee, D.-S. Lim, K.-S. Kim, H.-M. Chung, S.-H. Lee, A novel culture technique for human embryonic stem cells using porous membranes, Stem Cells Dayt. Ohio. 25 (2007) 2601–2609. https://doi.org/10.1634/stemcells.2006-0814.

[176] S.R. Peyton, Z.I. Kalcioglu, J.C. Cohen, A.P. Runkle, K.J. Van Vliet, D.A. Lauffenburger, L.G. Griffith, Marrow-Derived stem cell motility in 3D synthetic scaffold is governed by geometry along with adhesivity and stiffness, Biotechnol. Bioeng. 108 (2011) 1181–1193. https://doi.org/10.1002/bit.23027.

[177] G. Camci-Unal, N. Annabi, M.R. Dokmeci, R. Liao, A. Khademhosseini, Hydrogels for cardiac tissue engineering, NPG Asia Mater. 6 (2014) e99. https://doi.org/10.1038/am.2014.19.

[178] I. Allijn, M. Ribeiro, A. Poot, R. Passier, D. Stamatialis, Membranes for Modelling Cardiac Tissue Stiffness In Vitro Based on Poly(trimethylene carbonate) and Poly(ethylene glycol) Polymers, Membranes. 10 (2020) 274. https://doi.org/10.3390/membranes10100274.

[179] X. Gu, Y. Matsumura, Y. Tang, S. Roy, R. Hoff, B. Wang, W.R. Wagner, Sustained viral gene delivery from a micro-fibrous, elastomeric cardiac patch to the ischemic rat heart, Biomaterials. 133 (2017) 132–143. https://doi.org/10.1016/j.biomaterials.2017.04.015.

[180] F. Ghorbani, M. Sahranavard, Z. Mousavi Nejad, D. Li, A. Zamanian, B. Yu, Surface Functionalization of Three Dimensional-Printed Polycaprolactone-Bioactive Glass Scaffolds by Grafting GelMA Under UV Irradiation, Front. Mater. 7 (2020) 528590. https://doi.org/10.3389/fmats.2020.528590.

[181] G. Lin, X. Zhang, S.R. Kumar, J.E. Mark, Improved Hydrophilicity from Poly(ethylene glycol) in Amphiphilic Conetworks with Poly(dimethylsiloxane), Silicon. 1 (2009) 173–181. https://doi.org/10.1007/s12633-009-9011-5.

[182] P.B. van Wachem, A.H. Hogt, T. Beugeling, J. Feijen, A. Bantjes, J.P. Detmers, W.G. van Aken, Adhesion of cultured human endothelial cells onto methacrylate polymers with varying surface wettability and charge, Biomaterials. 8 (1987) 323–328. https://doi.org/10.1016/0142-9612(87)90001-9.

[183] P.B. van Wachem, T. Beugeling, J. Feijen, A. Bantjes, J.P. Detmers, W.G. van Aken, Interaction of cultured human endothelial cells with polymeric surfaces of different wettabilities, Biomaterials. 6 (1985) 403–408. https://doi.org/10.1016/0142-9612(85)90101-2.

[184] J. Kurowiak, A. Kaczmarek-Pawelska, A.G. Mackiewicz, R. Bedzinski, Analysis of the Degradation Process of Alginate-Based Hydrogels in Artificial Urine for Use as a Bioresorbable Material in the Treatment of Urethral Injuries, Processes. 8 (2020) 304. https://doi.org/10.3390/pr8030304.

[185] Q. Yu, H. Chen, Interaction of switchable biomaterials surfaces with proteins, in: Switch. Responsive Surf. Mater. Biomed. Appl., Elsevier, 2015: pp. 167–188. https://doi.org/10.1016/B978-0-85709-713-2.00007-9.

[186] N. Recek, M. Mozetic, M. Jaganjac, L. Milkovic, N. Zarkovic, A. Vesel, Adsorption of Proteins and Cell Adhesion to Plasma Treated Polymer Substrates, Int. J. Polym. Mater. Polym. Biomater. 63 (2014) 685–691. https://doi.org/10.1080/00914037.2013.854243.

[187] O. Maruyama, M. Nishida, T. Yamane, I. Oshima, Y. Adachi, T. Masuzawa, Hemolysis resulting from surface roughness under shear flow conditions using a rotational shear stressor, Artif. Organs. 30 (2006) 365–370. https://doi.org/10.1111/j.1525-1594.2006.00227.x.

[188] F. Gnanaprakasam Thankam, J. Muthu, Influence of plasma protein–hydrogel interaction moderated by absorption of water on long-term cell viability in amphiphilic biosynthetic hydrogels, RSC Adv. 3 (2013) 24509. https://doi.org/10.1039/c3ra43710h.

[189] A. Radhakrishnan, G.M. Jose, M. Kurup, PEG-penetrated chitosan–alginate co-polysaccharide-based partially and fully cross-linked hydrogels as ECM mimic for tissue engineering applications, Prog. Biomater. 4 (2015) 101–112. https://doi.org/10.1007/s40204-015-0041-3.

[190] P.-S. Li, I. -Liang Lee, W.-L. Yu, J.-S. Sun, W.-N. Jane, H.-H. Shen, A Novel Albumin-Based Tissue Scaffold for Autogenic Tissue Engineering Applications, Sci. Rep. 4 (2015) 5600. https://doi.org/10.1038/srep05600.

[191] K. Zhang, Y. Fan, N. Dunne, X. Li, Effect of microporosity on scaffolds for bone tissue engineering, Regen. Biomater. 5 (2018) 115–124. https://doi.org/10.1093/rb/rby001.

[192] F. Gnanaprakasam Thankam, J. Muthu, Alginate based hybrid copolymer hydrogels—Influence of pore morphology on cell–material interaction, Carbohydr. Polym. 112 (2014) 235–244. https://doi.org/10.1016/j.carbpol.2014.05.083.

[193] K. Ishihara, H. Nomura, T. Mihara, K. Kurita, Y. Iwasaki, N. Nakabayashi, Why do phospholipid polymers reduce protein adsorption?, J. Biomed. Mater. Res. 39 (1998) 323–330. https://doi.org/10.1002/(sici)1097-4636(199802)39:2<323::aid-jbm21>3.0.co;2-c.

[194] V. Kandi, S. Vadakedath, Implant-Associated Infections: A Review of the Safety of Cardiac Implants, Cureus. 12 (n.d.) e12267. https://doi.org/10.7759/cureus.12267.

[195] J. Li, W. Fang, T. Hao, D. Dong, B. Yang, F. Yao, C. Wang, An anti-oxidative and conductive composite scaffold for cardiac tissue engineering, Compos. Part B Eng. 199 (2020) 108285. https://doi.org/10.1016/j.compositesb.2020.108285.

[196] M.B. Morelli, J. Gambardella, V. Castellanos, V. Trimarco, G. Santulli, Vitamin C and Cardiovascular Disease: An Update, Antioxidants. 9 (2020) 1227. https://doi.org/10.3390/antiox9121227.

[197] M.A. Moser, O.K. Chun, Vitamin C and Heart Health: A Review Based on Findings from Epidemiologic Studies, Int. J. Mol. Sci. 17 (2016) 1328. https://doi.org/10.3390/ijms17081328.

[198] N. Zhu, B. Huang, W. Jiang, Targets of Vitamin C With Therapeutic Potential for Cardiovascular Disease and Underlying Mechanisms: A Study of Network Pharmacology, Front. Pharmacol. 11 (2021). https://www.frontiersin.org/articles/10.3389/fphar.2020.591337 (accessed September 13, 2023).

[199] B.R. Dollinger, M.K. Gupta, J.R. Martin, Craig.L. Duvall, Reactive Oxygen Species Shielding Hydrogel for the Delivery of Adherent and Nonadherent Therapeutic Cell Types, Tissue Eng. Part A. 23 (2017) 1120–1131. https://doi.org/10.1089/ten.tea.2016.0495.

[200] P.L. Thi, Y. Lee, D.L. Tran, T.T.H. Thi, J.I. Kang, K.M. Park, K.D. Park, In situ forming and reactive oxygen species-scavenging gelatin hydrogels for enhancing wound healing efficacy, Acta Biomater. 103 (2020) 142–152. https://doi.org/10.1016/j.actbio.2019.12.009.

[201] A. Jha, E. Moore, Collagen-derived peptide, DGEA, inhibits pro-inflammatory macrophages in biofunctional hydrogels, J. Mater. Res. 37 (2022) 77–87. https://doi.org/10.1557/s43578-021-00423-y.

[202] W. Bu, Y. Wu, A.M. Ghaemmaghami, H. Sun, A. Mata, Rational design of hydrogels for immunomodulation, Regen. Biomater. 9 (2022) rbac009. https://doi.org/10.1093/rb/rbac009.

[203] S. Hauck, P. Zager, N. Halfter, E. Wandel, M. Torregrossa, A. Kakpenova, S. Rother, M. Ordieres, S. Räthel, A. Berg, S. Möller, M. Schnabelrauch, J.C. Simon, V. Hintze, S. Franz, Collagen/hyaluronan based hydrogels releasing sulfated hyaluronan improve dermal wound healing in diabetic mice via reducing inflammatory macrophage activity, Bioact. Mater. 6 (2021) 4342–4359. https://doi.org/10.1016/j.bioactmat.2021.04.026.

[204] M.J. George, O. Kleveland, J. Garcia-Hernandez, J. Palmen, R. Lovering, R. Wiseth, P. Aukrust, J. Engmann, J.K. Damås, A.D. Hingorani, L. Gullestad, J.P. Casas, T. Ueland, Novel Insights Into the Effects of Interleukin 6 Antagonism in Non–ST-Segment–Elevation Myocardial Infarction Employing the SOMAscan Proteomics Platform, J. Am. Heart Assoc. 9 (2020) e015628. https://doi.org/10.1161/JAHA.119.015628.

[205] C. Alter, A.-S. Henseler, C. Owenier, J. Hesse, Z. Ding, T. Lautwein, J. Bahr, S. Hayat, R. Kramann, E. Kostenis, J. Scheller, J. Schrader, IL-6 in the infarcted heart is preferentially formed by fibroblasts and modulated by purinergic signaling, J. Clin. Invest. 133 (2023). https://doi.org/10.1172/JCI163799.

[206] I.M. Tøllefsen, C. Shetelig, I. Seljeflot, J. Eritsland, P. Hoffmann, G.Ø. Andersen, High levels of interleukin-6 are associated with final infarct size and adverse clinical events in patients with STEMI, Open Heart. 8 (2021) e001869. https://doi.org/10.1136/openhrt-2021-001869.

[207] H.E. Groot, L. Al Ali, I.C.C. van der Horst, R.A.J. Schurer, H.W. van der Werf, E. Lipsic, D.J. van Veldhuisen, J.C. Karper, P. van der Harst, Plasma interleukin 6 levels are associated with cardiac function after ST-elevation myocardial infarction, Clin. Res. Cardiol. 108 (2019) 612–621. https://doi.org/10.1007/s00392-018-1387-z.

[208] S.M. Schumacher, S.V. Naga Prasad, Tumor Necrosis Factor-α in Heart Failure: An updated review, Curr. Cardiol. Rep. 20 (2018) 117. https://doi.org/10.1007/s11886-018-1067-7.

[209] R. Schulz, G. Heusch, Tumor Necrosis Factor-α and Its Receptors 1 and 2, Circulation. 119 (2009) 1355–1357. https://doi.org/10.1161/CIRCULATIONAHA.108.846105.

[210] M. Tian, Y.-C. Yuan, J.-Y. Li, M.R. Gionfriddo, R.-C. Huang, Tumor necrosis factor-α and its role as a mediator in myocardial infarction: A brief review, Chronic Dis. Transl. Med. 1 (2015) 18–26. https://doi.org/10.1016/j.cdtm.2015.02.002.

[211] J.W. Gordon, J.A. Shaw, L.A. Kirshenbaum, Multiple Facets of NF-κB in the Heart, Circ. Res. 108 (2011) 1122–1132. https://doi.org/10.1161/CIRCRESAHA.110.226928.

[212] A. Kis, D.M. Yellon, G.F. Baxter, Role of nuclear factor-κB activation in acute ischaemia-reperfusion injury in myocardium, Br. J. Pharmacol. 138 (2003) 894–900. https://doi.org/10.1038/sj.bjp.0705108.

[213] G. Hall, J.D. Hasday, T.B. Rogers, Regulating the regulator: NF-κB signaling in heart, J. Mol. Cell. Cardiol. 41 (2006) 580–591. https://doi.org/10.1016/j.yjmcc.2006.07.006.

[214] Y. Yao, F. Li, M. Zhang, L. Jin, P. Xie, D. Liu, J. Zhang, X. Hu, F. Lv, H. Shang, W. Zheng, X. Sun, J. Duanmu, F. Wu, F. Lan, R.-P. Xiao, Y. Zhang, Targeting CaMKII-δ9 Ameliorates Cardiac Ischemia/Reperfusion Injury by Inhibiting Myocardial Inflammation, Circ. Res. 130 (2022) 887–903. https://doi.org/10.1161/CIRCRESAHA.121.319478.

[215] P. Krishnamurthy, J. Rajasingh, E. Lambers, G. Qin, D.W. Losordo, R. Kishore, IL-10 inhibits inflammation and attenuates left ventricular remodeling after myocardial infarction via activation of STAT-3 and suppression of HuR, Circ. Res. 104 (2009) e9-18. https://doi.org/10.1161/CIRCRESAHA.108.188243.

[216] Z. Yang, B. Zingarelli, C. Szabó, Crucial Role of Endogenous Interleukin-10 Production in Myocardial Ischemia/Reperfusion Injury, Circulation. 101 (2000) 1019–1026. https://doi.org/10.1161/01.CIR.101.9.1019.

[217] R. Gupta, L. Liu, X. Zhang, X. Fan, P. Krishnamurthy, S. Verma, J. Tongers, S. Misener, N. Ashcherkin, H. Sun, J. Tian, R. Kishore, IL-10 provides cardioprotection in diabetic myocardial infarction via upregulation of Heme clearance pathways, JCI Insight. 5 (2020). https://doi.org/10.1172/jci.insight.133050.

[218] A. Hanna, N.G. Frangogiannis, The Role of the TGF-β Superfamily in Myocardial Infarction, Front. Cardiovasc. Med. 6 (2019) 140. https://doi.org/10.3389/fcvm.2019.00140.

[219] M. Bujak, N.G. Frangogiannis, The role of TGF-β Signaling in Myocardial Infarction and Cardiac Remodeling, Cardiovasc. Res. 74 (2007) 184–195. https://doi.org/10.1016/j.cardiores.2006.10.002.

[220] N.G. Frangogiannis, The role of transforming growth factor (TGF)-β in the infarcted myocardium, J. Thorac. Dis. 9 (2017). https://doi.org/10.21037/jtd.2016.11.19.

[221] M.-J. Goumans, P. ten Dijke, TGF-β Signaling in Control of Cardiovascular Function, Cold Spring Harb. Perspect. Biol. 10 (2018) a022210. https://doi.org/10.1101/cshperspect.a022210.

[222] B.V. Sridhar, N.R. Doyle, M.A. Randolph, K.S. Anseth, Covalently tethered TGF-β1 with encapsulated chondrocytes in a PEG hydrogel system enhances extracellular matrix production, J. Biomed. Mater. Res. A. 102 (2014) 4464–4472. https://doi.org/10.1002/jbm.a.35115.

[223] J. Kim, B. Lin, S. Kim, B. Choi, D. Evseenko, M. Lee, TGF-β1 conjugated chitosan collagen hydrogels induce chondrogenic differentiation of human synovium-derived stem cells, J. Biol. Eng. 9 (2015) 1. https://doi.org/10.1186/1754-1611-9-1.

[224] J.M. Kyriakis, J. Avruch, Protein kinase cascades activated by stress and inflammatory cytokines, BioEssays. 18 (1996) 567–577. https://doi.org/10.1002/bies.950180708.

[225] A. Viola, F. Munari, R. Sánchez-Rodríguez, T. Scolaro, A. Castegna, The Metabolic Signature of Macrophage Responses, Front. Immunol. 10 (2019) 1462. https://doi.org/10.3389/fimmu.2019.01462.

[226] S.K. Wculek, G. Dunphy, I. Heras-Murillo, A. Mastrangelo, D. Sancho, Metabolism of tissue macrophages in homeostasis and pathology, Cell. Mol. Immunol. 19 (2022) 384–408. https://doi.org/10.1038/s41423-021-00791-9.

[227] T. Seimon, I. Tabas, Mechanisms and consequences of macrophage apoptosis in atherosclerosis, J. Lipid Res. 50 (2009) S382–S387. https://doi.org/10.1194/jlr.R800032-JLR200.

[228] Q.A. Majid, A.T.R. Fricker, D.A. Gregory, N. Davidenko, O. Hernandez Cruz, R.J. Jabbour, T.J. Owen, P. Basnett, B. Lukasiewicz, M. Stevens, S. Best, R. Cameron, S. Sinha, S.E. Harding, I. Roy, Natural Biomaterials for Cardiac Tissue Engineering: A Highly Biocompatible Solution, Front. Cardiovasc. Med. 7 (2020) 554597. https://doi.org/10.3389/fcvm.2020.554597.

[229] S.S. Virani, A. Alonso, H.J. Aparicio, E.J. Benjamin, M.S. Bittencourt, C.W. Callaway, A.P. Carson, A.M. Chamberlain, S. Cheng, F.N. Delling, M.S.V. Elkind, K.R. Evenson, J.F. Ferguson, D.K. Gupta, S.S. Khan, B.M. Kissela, K.L. Knutson, C.D. Lee, T.T. Lewis, J. Liu, M.S. Loop, P.L. Lutsey, J. Ma, J. Mackey, S.S. Martin, D.B. Matchar, M.E. Mussolino, S.D. Navaneethan, A.M. Perak, G.A. Roth, Z. Samad, G.M. Satou, E.B. Schroeder, S.H. Shah, C.M. Shay, A. Stokes, L.B. VanWagner, N.-Y. Wang, C.W. Tsao, American Heart Association Council on Epidemiology and Prevention Statistics Committee and Stroke Statistics Subcommittee, Heart Disease and Stroke Statistics-2021 Update: A Report From the American Heart Association, Circulation. 143 (2021) e254–e743. https://doi.org/10.1161/CIR.0000000000000950.

[230] B. Arjmand, M. Abedi, M. Arabi, S. Alavi-Moghadam, M. Rezaei-Tavirani, M. Hadavandkhani, A. Tayanloo-Beik, R. Kordi, P.P. Roudsari, B. Larijani, Regenerative Medicine for the Treatment of Ischemic Heart Disease; Status and Future Perspectives, Front. Cell Dev. Biol. 9 (2021) 704903. https://doi.org/10.3389/fcell.2021.704903.

[231] T.G. Neltner, N.R. Kulkarni, H.M. Alger, M.V. Maffini, E.D. Bongard, N.D. Fortin, E.D. Olson, Navigating the U.S. Food Additive Regulatory Program, Compr. Rev. Food Sci. Food Saf. 10 (2011) 342–368. https://doi.org/10.1111/j.1541-4337.2011.00166.x.

[232] F.J. Giordano, Oxygen, oxidative stress, hypoxia and heart failure, J. Clin. Invest. 115 (2005) 500–508. https://doi.org/10.1172/JCI24408.

[233] A.A.M. Truffa, C.B. Granger, K.R. White, L.K. Newby, R.H. Mehta, J.S. Hochman, M.R. Patel, K.S. Pieper, H.R. Al-Khalidi, P.W. Armstrong, R.D. Lopes, Serious Infection Following Acute Myocardial Infarction: Incidence, Clinical Features, and Outcomes, JACC Cardiovasc. Interv. 5 (2012) 10.1016/j.jcin.2012.03.018. https://doi.org/10.1016/j.jcin.2012.03.018.

PUBLICATIONS

PUBLICATIONS

ORIGINAL ARTICLE

- Polysaccharide-PVA/PEG blended Crosslinked Hybrid Hydrogels for Cardiac Tissue Engineering, Joshi C. O, Soumya K. Chandrasekhar, Trends in Biomaterials and Artificial Organs 37 (1), 27-35

BOOK CHAPTERS

- Interface biology of stem cell–driven tissue engineering: concepts, concerns, and approaches, SK Chandrasekhar, FG Thankam, DK Agrawal, JC Ouseph, Biointegration of Medical Implant Materials, 19-44,6, 2020
- Engineered cardiac tissue: Concepts and future, SK Chandrasekhar, FG Thankam, JC Ouseph, DK Agrawal, Regenerated Organs, 133-151, 2021
- Myocardial tissue engineering: Fundamentals and future, SK Chandrasekhar, FG Thankam, JC Ouseph, DK Agrawal, Tissue Engineering, 33-51,2022

PRESENTATIONS

Sl No.	Title of the Paper	Title and Date of the Seminar	Organizers	Type of the Seminar
1	A study on the expression of inflammatory mediators in RAW 264.7 cells cocultured with hybrid hydrogels for cardiac tissue engineering.	Nanotechnology and Phytochemistry: Exploring the Interface of Science and Nature (7th Dec, 2023)	Dept. of Botany, Govt. Arts and Science Collee for Women, Malappuram	National
2.	Immunocompatibility of Alginate-PEG-Starch inspired hydrogel templates for regenerative cardiology.	Biodiversity for sustainable future (14th -16th Nov, 2023)	Dept. of Zoology, SNGS College, Pattambi.	National
3	Alginate-PVA-CMC based hybrid hydrogel as template for cardiac tissue engineering"	Modern Trends in Biological Research (9th January, 2021)	Dept. of Zoology, Vimala College, Thrissur.	National Virtual Paper presentation Competition.
4	Alginate-PEG-Starch based semi-interpenetrating hybrid hydrogel scaffold for guided cardiac tissue engineering	Conservation of Nature and Siddha Medicine (14th -15th Dec, 2020)	William Research Centre, Nagercoil.	International Webinar
5	Polyol-polysaccharide interpenetrating network hydrogels for cardiac tissue engineering applications.	From Health to Well Being: An Interdisciplinary Approach. (9th - 11th January, 2019)	St. Xaviers College, Mumbai.	International